CHEMICAL REVIEWS

Review

pubs.acs.org/CR

Terms of Use

Microbial and Animal Rhodopsins: Structures, Functions, and Molecular Mechanisms

Oliver P. Ernst,*[,†] David T. Lodowski,[‡] Marcus Elstner,[§] Peter Hegemann,[∥] Leonid S. Brown,[⊥] and Hideki Kandori[#]

[†]Departments of Biochemistry and Molecular Genetics, University of Toronto, 1 King's College Circle, Medical Sciences Building, Toronto, Ontario M5S 1A8, Canada

[‡]Center for Proteomics and Bioinformatics, Case Western Reserve University School of Medicine, 10900 Euclid Avenue, Cleveland, Ohio 44106, United States

[§]Institute for Physical Chemistry, Karlsruhe Institute of Technology, Kaiserstrasse 12, 76131 Karlsruhe, Germany

[∥]Institute of Biology, Experimental Biophysics, Humboldt-Universität zu Berlin, Invalidenstrasse 42, 10115 Berlin, Germany

[⊥]Department of Physics and Biophysics Interdepartmental Group, University of Guelph, 50 Stone Road East, Guelph, Ontario N1G 2W1, Canada

[#]Department of Frontier Materials, Nagoya Institute of Technology, Showa-ku, Nagoya 466-8555, Japan

Supporting Information

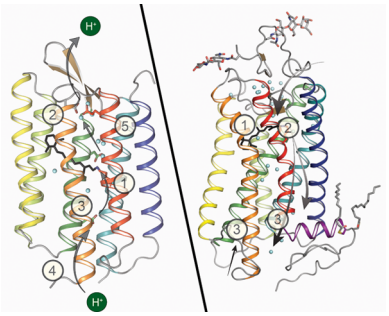

CONTENTS

1. INTRODUCTION

Organisms of all domains of life use photoreceptor proteins to sense and respond to light. The light-sensitivity of photoreceptor proteins arises from bound chromophores such as retinal in retinylidene proteins, bilin in biliproteins, and flavin in flavoproteins. Rhodopsins found in *Eukaryotes*, *Bacteria*, and *Archaea* consist of opsin apoproteins and a covalently linked

Special Issue: Chemistry and Biology of Retinoids and Carotenoids

Received: July 14, 2013
Published: December 23, 2013

 © 2013 American Chemical Society dx.doi.org/10.1021/cr4003769 | *Chem. Rev.* 2014, 114, 126−163

retinal which is employed to absorb photons for energy conversion or the initiation of intra- or intercellular signaling.[1] Both functions are important for organisms to survive and to adapt to the environment. While lower organisms utilize the family of microbial rhodopsins for both purposes, animals solely use a different family of rhodopsins, a specialized subset of G-protein-coupled receptors (GPCRs).[1,2] Animal rhodopsins, for example, are employed in visual and nonvisual phototransduction, in the maintenance of the circadian clock and as photoisomerases.[3,4] While sharing practically no sequence similarity, microbial and animal rhodopsins, also termed type-I and type-II rhodopsins, respectively, share a common architecture of seven transmembrane α-helices (TM) with the N- and C-terminus facing out- and inside of the cell, respectively (Figure 1).[1,5] Retinal is attached by a Schiff base

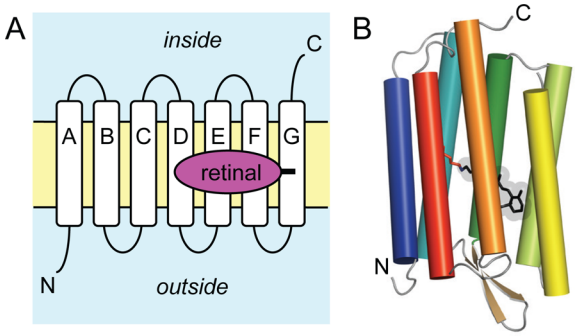

Figure 1. Topology of the retinal proteins. (A) These membrane proteins contain seven α-helices (typically denoted helix A to G in microbial opsins and TM1 to 7 in the animal opsins) spanning the lipid bilayer. The N-terminus faces the outside of the cell and the C-terminus the inside. Retinal is covalently attached to a lysine side chain on helix G or TM7, respectively. (B) Cartoon representation of the helical arrangement of a microbial rhodopsin with attached all-*trans*-retinal (bacteriorhodopsin, PDB ID: 1C3W).

linkage to the ε-amino group of a lysine side chain in the middle of TM7 (Figures 1 and 2). The retinal Schiff base (RSB) is protonated ($RSBH^+$) in most cases, and changes in protonation state are integral to the signaling or transport activity of rhodopsins.

Retinal, the aldehyde of vitamin A, is derived from β-carotene and is utilized in the all-*trans*/13-*cis* configurations in microbial rhodopsins and the 11-*cis*/all-*trans* configurations in animal rhodopsins (Figure 2).[1,6] For optimal light to energy or light to signal conversion, defined chromophore−protein interactions in rhodopsins direct the unique photophysical and photochemical processes, which start with specific retinal isomerization and culminate with distinct protein conformational changes. The protein environment is typically optimized for light-induced retinal isomerization from all-*trans* → 13-*cis* in microbial rhodopsins and for 11-*cis* → all-*trans* in animal rhodopsins. Variations in this isomerization pattern are discussed in sections 3 and 4.

The 7TM protein scaffold of microbial rhodopsins is designed for light-driven ion pumps, light-gated ion channels, and light sensors which couple to transducer proteins (Figure 3).[7] Microbial rhodopsins were first found in the *Archaea* (*Halobacterium salinarum*, historically referred to as *Halobacterium halobium*)[8] and were therefore initially termed archaeal rhodopsins. *H. salinarum* contains bacteriorhodopsin (BR)[8] and halorhodopsin (HR)[9] that act as a light-driven outward proton

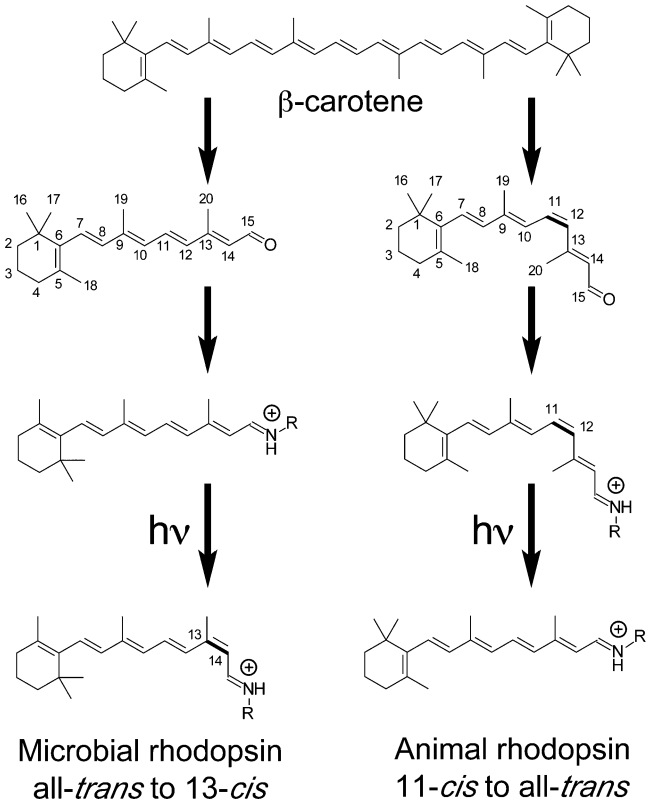

Figure 2. Genesis of the chromophore of microbial and animal rhodopsins. Cleavage of β-carotene is the source of the chromophore. The ground state of microbial and animal rhodopsins possesses all-*trans*- and 11-*cis*-retinal as its chromophore, respectively, bound to a Lys residue via a Schiff base, which is normally protonated and exists in the 15-*anti* configuration. It should be noted that microbial rhodopsins depend exclusively on all-*trans*-retinal, while some animal rhodopsins possess vitamin A2 (C3═C4 double bond for fish visual pigments) and hydroxyl (C3—OH for insect visual pigments) forms of 11-*cis*-retinal. Usually, photoactivation isomerizes microbial rhodopsin selectively at the C13═C14 double bond and animal rhodopsin at the C11═C12 double bond.

pump and inward chloride pump, respectively. As ion pumps, they contribute to the formation of a membrane potential and thus have their function in light−energy conversion. The other two *H. salinarum* rhodopsins are sensory rhodopsin I and II (SRI and SRII),[10] which act as positive and negative phototaxis sensors, respectively. Since the original discovery of BR in *H. salinarum*, similar rhodopsins have been found in *Eubacteria* and lower *Eukaryota*, leading to the name microbial rhodopsins. For example, *Anabaena* sensory rhodopsin (ASR), the first sensory rhodopsin observed in the *Eubacteria*,[11] is a sensor that activates a soluble transducer (Figure 3).

Channelrhodopsins (ChRs), another group of microbial rhodopsins, were discovered in green algae where they function as light-gated cation channels within the algal eye to depolarize the plasma membrane upon light absorption.[12,13] The primary depolarization of the eyespot membrane is transferred to the flagellar membrane and results in a reorientation of the alga toward a light source (photophobic responses and phototaxis). Thus, ChRs naturally function as signaling photoreceptors as well. Discovery of ChR led to an emergence of a new field, optogenetics,[14] in which light-gated ion channels and light-driven ion pumps are used to depolarize and hyperpolarize selected cells of neuronal networks, e.g., for therapeutic

dx.doi.org/10.1021/cr4003769 | *Chem. Rev.* 2014, 114, 126−163

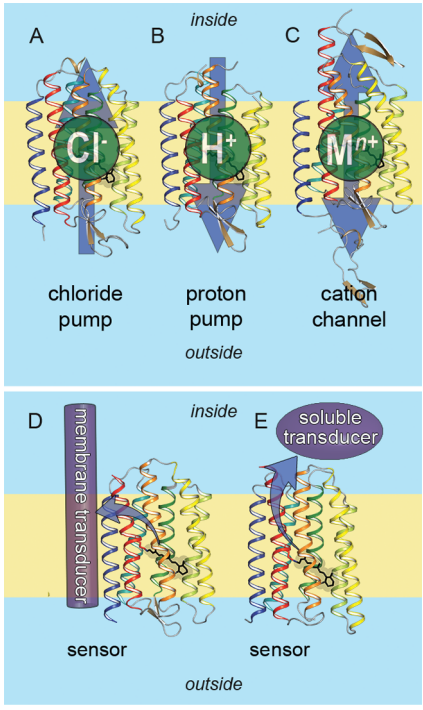

Figure 3. Microbial rhodopsins can function as pumps, channels, and light-sensors. Arrows indicate the direction of transport or flow of signal: (A) light-driven inward chloride pump (halorhodopsin (HR), PDB ID: 1E12), (B) light-driven outward proton pump (bacteriorhodopsin (BR), PDB ID: 1C3W), (C) light-gated cation channel (channelrhodopsin (ChR), PDB ID: 3UG9), (D) light-sensor activating transmembrane transducer protein (sensory rhodopsin II (SRII), PDB ID: 1JGJ), (E) light-sensor activating soluble transducer protein (*Anabaena* sensory rhodopsin (ASR), PDB ID: 1XIO).

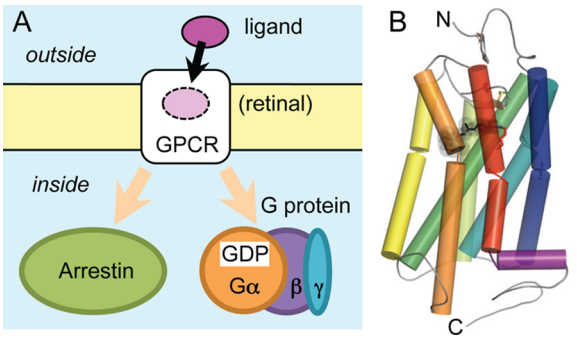

Figure 4. Animal rhodopsins are specialized G-protein-coupled receptors (GPCRs). (A) Binding of extracellular ligands stabilizes certain GPCR conformations which enable the GPCR to catalyze GDP/GTP exchange in heterotrimeric G proteins ($G\alpha\beta\gamma$) and/or to induce G-protein-independent, arrestin-mediated signaling. (B) Typical GPCR fold shown in cartoon representation for bovine rhodopsin (PDB ID: 1U19). Structures of animal and microbial rhodopsins differ largely (cf. Figure 1B) and are drawn in opposite orientations with respect to the membrane. As model for the GPCR family, animal rhodopsin is shown in the orientation commonly used for GPCRs. In a large number of publications, animal rhodopsins are shown for historical reasons in the orientation of microbial rhodopsins (C-terminus up).

reasons[15] or in order to understand the circuitry of the brain.[16,17] Thus, studies on microbial rhodopsins are beneficial not only for our basic understanding of retinal proteins, but also for providing a toolset to study neuronal signaling through optogenetics.

Animal rhodopsins belong to the superfamily of GPCRs which detect extracellular signals, typically by binding small molecule ligands like hormones and neurotransmitters.[18,19] By a ligand-induced conformational change, GPCRs become activated and capable of transducing the activation signal by catalyzing GDP/GTP exchange on membrane-bound heterotrimeric G proteins within the cell, thus initiating G protein-mediated signaling cascades (Figure 4).[19] After activation-dependent phosphorylation by a G-protein-coupled receptor kinase, active GPCRs can also interact with arrestin to effect G protein-independent signaling and attenuation of the ligand-mediated activation signal.[20] Animal rhodopsins are typically specialized GPCRs, capable of detecting single photons as a physical stimulus.[21] Because the 11-*cis*-retinal ligand is covalently bound within the retinal-binding pocket of the receptor, photon absorption and the ensuing retinal *cis* → *trans* isomerization convert an inactivating ligand (the inverse agonist 11-*cis*-retinal) into an activating ligand (the agonist all-*trans*-retinal) *in situ*. Vertebrate rhodopsin was discovered more than 130 years ago and has long been used as a prototypical GPCR.[22] Due to the relative ease of purification from native material, it has been studied extensively.[2]

The goal of this review is to provide mechanistic insights from biophysical and structural studies into the function of microbial and animal rhodopsins, with the latter as representatives of GPCRs. After a general description of retinal photoisomerization in section 2, the functional mechanisms of various basic types of microbial rhodopsins will be discussed in section 3. In section 4, animal rhodopsins will be reviewed with a focus on bovine visual rhodopsin (abbreviated as Rho in some cases), the photoreceptor in retinal rod cells, followed by some extension to color visual rhodopsins and invertebrate rhodopsins.

2. LIGHT ABSORPTION AND PHOTOISOMERIZATION

2.1. Color Tuning

Light absorption initiates functions of both microbial and animal rhodopsins,[23,24] and the wavelength dependence of the absorption efficiency determines the colors of the proteins (Figure 5). The length of the π-conjugated polyene chain in the retinal chromophore as well as the protonation of the RSB linkage determine the energy gap of the $\pi-\pi^*$ transition,[25] so that the absorption of most rhodopsins is within the visible region (400−700 nm). Humans have a single photoreceptor for dim light vision (rhodopsin, λ_{max} ∼500 nm) and three receptors for color vision (blue, λ_{max} ∼425 nm; green, λ_{max} ∼530 nm; red, λ_{max} ∼560 nm),[26,27] whereas some shrimp species contain up to 16 rhodopsins covering the spectral range from 300 to 700 nm.[28] While the chromophore molecule is usually the same in all pigments (retinal bound via a (protonated) Schiff base), the absorption maxima differ significantly, implying an active protein control of the energy gap between the ground and excited states of the retinal chromophore. The mechanism of color tuning has fascinated researchers for a long time, and several factors have been determined to be responsible for it.

The protonation state of the chromophore plays a crucial role in color tuning; the unprotonated RSB absorbs in the UV region (λ_{max} ∼360−380 nm), and this absorption is quite insensitive to the environment in contrast to the $RSBH^+$, which exhibits a large variation in absorption covering the entire visible light spectrum. Other factors defining the spectral tuning

dx.doi.org/10.1021/cr4003769 | *Chem. Rev.* 2014, 114, 126−163

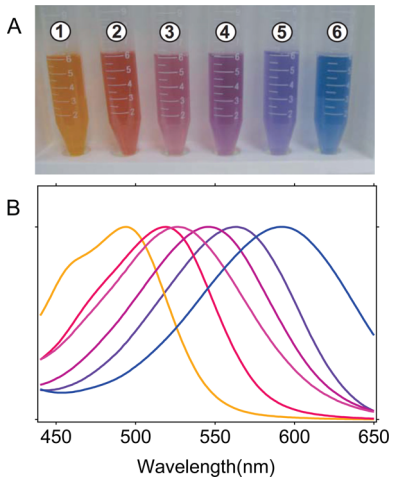

Figure 5. Microbial rhodopsins exhibit a wide range of absorption maxima. Colors of microbial rhodopsins (A) and their absorption spectra (B). The following rhodopsins are shown: (1) a blue-proteorhodopsin (LC1-200, pH 7), (2) Q105L mutant of LC1-200 (pH 7), (3) a green-proteorhodopsin (EBAC31A08, pH 7), (4) A178R mutant of green-proteorhodopsin (pH 7), (5) bacteriorhodopsin (pH 7), (6) *H. salinarum* sensory rhodopsin I (pH 4).

of individual rhodopsins are given by chromophore−protein interactions such as electrostatic interactions with charged and polar amino acids, termed electrostatic tuning and extensively studied, first using retinal analogues,[29−32] and, later, site-directed mutagenesis.[33−35] Electrostatic tuning was elegantly demonstrated in a model system based on cellular retinol-binding protein II. This system was engineered to covalently bind all-*trans*-retinal and its absorption maximum was changed from 425 to 644 nm via mutations that changed the electrostatic potential within the retinal-binding pocket.[36] Interactions of retinal with charged, polar, and aromatic amino acids play a role in changing the electronic energy levels, as do hydrogen-bonding interactions and steric contact effects. Strong hydrogen bonds can lead to charge transfer, and steric contacts can lead to a twist of retinal. All these tuning processes in concert shape the absorbance maxima of retinal in microbial and animal rhodopsins.

One of the most prominent factors in color tuning is the interaction of retinal with the counterion(s) (Figure 6). In the ground state, the retinal chromophore is positively charged due to $RSBH^+$ ($C{=}NH^+$). The excited state has strong charge transfer character where the positive charge is displaced toward the β-ionone ring, leading to a neutralization of the $RSBH^+$ (Figure 6B).[37,38] Interaction of the $RSBH^+$ with the negatively charged counterion(s) in microbial and animal rhodopsins leads to an electrostatic stabilization in the electronic ground state of retinal accompanied by an increase of the RSB p*K*a (Figure 6A). The resulting larger energy gap between ground and excited states causes a blue-shift of the absorption (Figure 6D, compare cases [A] and [B]).[39,40] If a negative charge is located near the β-ionone ring, the excited state is energetically stabilized compared to the ground state (Figure 6C,D), which leads to a smaller energy gap and therefore to a red-shift of the wavelength of electronic excitation. As the absorption maximum of isolated all-*trans* $RSBH^+$ in gas phase is 610 nm (Figure 6B,D, case [B]),[40] in principle, absorption in the deep red range (λ_{max} > 600 nm) should be possible for case [C] in Figure 6, while λ_{max} < 600 nm is expected for case [A]. However, microbial and animal rhodopsins only exhibit λ_{max} < 600 nm, with some exceptions in *Crustaceae* that absorb beyond 600 nm, indicating that case [C] is less favorable, and indeed, a negative charge near the $RSBH^+$ (case [A]) is found in the crystal structures of microbial and animal rhodopsins, where water-containing hydrogen-bonding networks constitute complex counterions.

It should be noted that, historically, the protein-induced spectral shift of retinal absorption (so-called opsin shift) has been considered bathochromic (i.e., red), because the absorption maximum of $RSBH^+$ in organic solvents (~440 nm),[41] rather than the more recently measured absorption in the gas phase (~610 nm),[40] served as a reference point. The interaction with individual polar and polarizable residues exerts a much smaller influence, on the order of several nanometers. The overall effect of the opsin is, in most cases, to counteract the blue-shift induced by the counterion. The delicate interplay of these electrostatic effects can now be understood in detail.[42−45]

Further spectral tuning can be achieved by other factors. Figure 2 shows that the retinal chromophore in microbial and animal rhodopsins differs not only in configuration of the C11=C12 double bond, but also in the conformation of the C6−C7 single bond. For bovine rhodopsin it is known that the

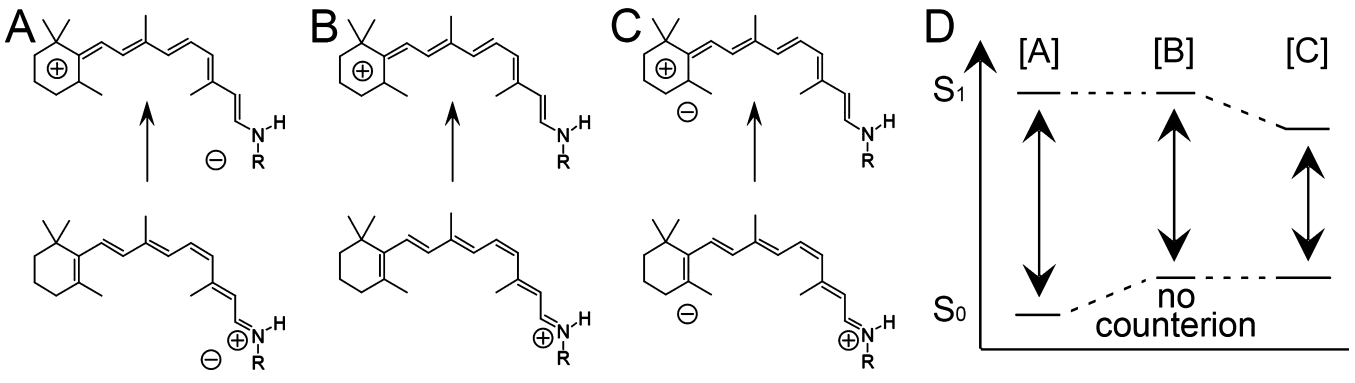

Figure 6. Color tuning exemplified by visual rhodopsins (containing 11-*cis*-retinal and $RSBH^+$). Photoexcitation causes bond alteration, which leads in the electronically excited state to the movement of the positive charge from the $RSBH^+$ to the β-ionone ring. (A) Excitation when a negatively charged counterion is close to the positively charged $RSBH^+$. (B) Excitation in the absence of a negatively charged counterion. (C) Excitation when the chromophore counterion is located near the β-ionone ring. (D) Electrostatic interactions with the counterion lower the energy level of the ground state (case [A]) or excited state (case [C]), yielding a spectral blue- or red-shift, respectively.

dx.doi.org/10.1021/cr4003769 | *Chem. Rev.* 2014, 114, 126−163

C6−C7 bond is in a 6-s-*cis* conformation,[46,47] making the polyene chain and β-ionone ring not planar due to steric hindrance between the C8-hydrogen and the C5-methyl group. As a result, the conjugation of π-electrons does not extend to the β-ionone ring efficiently. For microbial rhodopsins, however, the C6−C7 bond is 6-s-*trans*,[1] although the C6−C7 6-s-*cis* conformer is more stable in solution.[48] As a consequence, an extended conjugation of π-electrons becomes possible from the polyene chain to the β-ionone ring, which presumably contributes to the considerable spectral red-shift observed in microbial rhodopsins. In fact, while absorbance spectra of protonated Schiff bases of all-*trans*- and 11-*cis*-retinal in solution are similar (λ_{max} ~450 nm),[49] most microbial and animal rhodopsins typically possess λ_{max} in 520−580 nm and 480−525 nm ranges, respectively,[50] which can in part be explained by the differences in the C6−C7 bond conformation. In the 480−525 nm range, a C6−C7 6-s-*cis*-retinal conformer is found predominantly. However, it should be noted that SRII and ChR absorb maximally at 470−500 nm, even though these microbial rhodopsins possess the C6−C7 6-s-*trans* conformation,[51−53] while some visual pigments are substantially red-shifted.[45] The presence of a different chromophore (11-*cis*-3,4-didehydroretinal, e.g., in some fish species) or a different counterion (e.g., where Glu181 (in bovine Rho) is replaced by a His residue to form a chloride binding site in green and red color pigments) can contribute to this. These facts reveal the complexity of color tuning mechanism in microbial and animal rhodopsins, and the importance of structural information in understanding the mechanistic basis of color tuning in rhodopsins.

Pioneering calculations by Birge, Schulten, Tavan, and Warshel gave interesting qualitative insights into the electronic structure of retinal and basic mechanisms of color tuning.[54−56] However, only the combination of high-resolution structural data for many rhodopsins with more accurate computational methods has allowed estimating the contributions of the different mechanisms of color tuning. Retinal proteins are highly challenging for study by quantum chemical methods,[57] necessitating QM/MM approaches where the retinal and a few surrounding amino acids are included in the quantum mechanical (QM) description and the remainder of the system is treated by molecular mechanics (MM). This coupled analysis leads to a description of steric effects, but most importantly, the electrostatic environment of retinal is provided by fixed point charges on the atoms treated by MM. For very accurate predictions, the fixed point charge representation of MM may even become too simplistic, and a more complicated model is required.[58−60]

QM/MM calculations have been applied to many microbial rhodopsins such as BR,[61−64] HR,[58,65] SRII,[66,67] and ASR.[68] The color tuning mechanism has been examined for both bovine Rho[44,64,69−73] and squid rhodopsin.[74] In the case of color visual pigments, computational studies based on the homology models with bovine Rho have been reported,[75−77] and a similar approach was applied to green- and blue-absorbing proteorhodopsins.[43,78] These QM/MM studies gave detailed insight into the mechanisms of color tuning, since the calculations allow the different mechanistic factors to be separated. The environment tunes the absorption wavelength of retinal, but there are limits to color tuning, as other properties of retinal are affected by the environment, as well. The pK_a of the $RSBH^+$ is affected by steric and electrostatic factors,[57] as is the isomerization efficiency of retinal, which are both crucial for retinal protein activation.[73] Therefore, extensive color tuning can be in conflict with other functions of rhodopsins, limiting the possible protein modifications for efficient color tuning.

2.2. Primary Photochemical Reactions

The initial photochemical reaction in microbial and animal rhodopsins is known to be one of the fastest and most efficient chemical events in biology. The fate of the photoexcited molecules is determined within several hundreds of femtoseconds, and to avoid nonproductive de-excitation back to the ground state, microbial and animal rhodopsins have optimized the primary photochemical reaction in a specific manner.[79−82] The quantum yield of the photoreaction of bovine Rho is very high and is essentially independent of temperature and excitation wavelength,[83−85] while the fluorescence quantum yield is quite low ($\Phi \sim 10^{-5}$).[86] Since the radiative lifetime of nearly all rhodopsins is expected to be within the range 1−10 ns (from the Strickler−Berg equation),[87] these extremely low fluorescence quantum efficiencies led to the conclusion that the ultrafast reaction occurs through a barrierless excited-state potential surface.[88] Because the formation of the primary photoproduct takes place for rhodopsins even at liquid nitrogen (77 K) and liquid helium (4 K) temperatures, where molecular motions are essentially arrested,[89,90] the *cis*→*trans* isomerization as the primary event in vision was initially questioned.[91,92]

Figure 7 shows the pathways of photochemical reactions in microbial and animal rhodopsins, represented as a combination

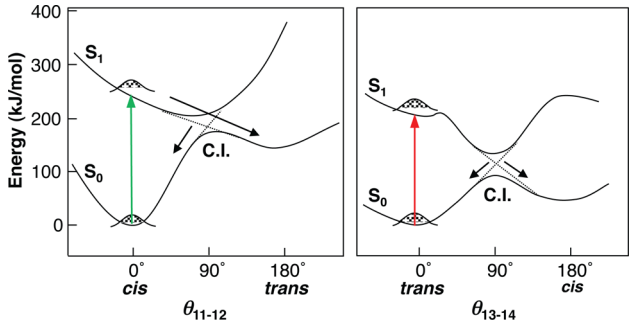

Figure 7. Suggested mechanism of retinal photoisomerization in rhodopsins. Potential energy profiles along the reaction coordinate (the dihedral angle of C11═C12 and C13═C14 bonds of animal (left) and microbial (right) rhodopsins): S_0, ground state; S_1, the first electronic excited state. Colored arrows represent excitation by visible light. C.I. represents conical intersection, the point of the closest approach of the energy surfaces of the ground and the excited states, through which transitions are the most probable.

of transitions between the ground and excited electronic states and evolution along the isomerization reaction coordinate (dihedral angle of the respective bond). As the energy barrier for the rotation around the double C═C bond is prohibitively high, isomerization becomes possible only in the excited state, where the chromophore becomes twisted before relaxing into the ground state through the so-called conical intersection (CI), the point of the closest approach of the energy surfaces. In microbial rhodopsins, all-*trans*-retinal is typically isomerized into the 13-*cis* form, even though the reverse reaction is possible for 13-*cis*-forms of several rhodopsins. The selectivity of isomerization is 100%, and the quantum yield was found to be 0.64 for BR.[93,94] In animal rhodopsins, such as bovine

dx.doi.org/10.1021/cr4003769 | *Chem. Rev.* 2014, 114, 126−163

rhodopsin, the isomerization of 11-*cis*-retinal to all-*trans*-retinal occurs with 100% selectivity and a quantum yield of 0.67.[95] It should be noted that some photoisomerases, such as retinochromes, and circadian and visual bistable pigments, such as melanopsin and squid rhodopsin, can perform photoisomerization in the opposite direction.[96−98] Photoisomerization in both microbial and animal rhodopsins has much higher efficiency (4−5 times) and selectivity than in solution, suggesting that rhodopsins developed highly efficient isomerization pathways which favor their respective photoproducts.

In the case of animal rhodopsins, low-temperature spectroscopy of bovine Rho at 87 K detected a trapped, red-shifted photointermediate, now called bathorhodopsin.[89] Bathorhodopsin converts to lumirhodopsin upon warming and ultimately decomposes through several intermediates to all-*trans*-retinal and opsin. It was therefore proposed that bathorhodopsin has a higher potential energy than dark state bovine Rho and subsequent intermediates and contains a "highly constrained and distorted" all-*trans* form of the chromophore.[90] According to this assumption, the process of converting dark state Rho to bathorhodopsin would be a *cis*→*trans* isomerization of retinal (Figure 7). When the first experiment with picosecond resolution was performed on bovine Rho in 1972,[91] it revealed that bathorhodopsin forms within 6 ps after excitation at room temperature, and the interpretation was that its formation was too fast to arise solely from a conformational change as large as the *cis*→*trans* isomerization of the retinal chromophore,[92] but this perspective has been entirely revised by more recent experiments.

Time-resolved studies on bovine Rho containing 11-*cis*-ring-locked retinal analogues provided the experimental evidence for 11-*cis* to all-*trans* isomerization as the primary reaction.[99] The *cis*→*trans* isomerization process has also been observed in real time by femtosecond transient absorption spectroscopy of bovine Rho. These experiments revealed that within 200 fs the all-*trans* photoproduct formation is complete, suggesting that isomerization is a femtosecond time scale event.[100] Further, oscillatory features with a period of 550 fs (60 cm^{-1}) were observed in the kinetics of the primary photoproduct of bovine Rho, whose phase and amplitude demonstrated that they are the result of nonstationary vibrational motions in the ground state of photorhodopsin, the precursor of bathorhodopsin.[101] Coherent vibrational motions in the isomerized product support the idea that the primary step in vision is a vibrationally coherent process and that the high reaction quantum yield in bovine Rho is a result of the extremely fast excited-state torsional motion.[101] Ultrafast photoisomerization in bovine Rho was also confirmed by other experimental techniques, such as femtosecond fluorescence spectroscopy[102] and femtosecond stimulated Raman spectroscopy.[103]

In the case of microbial rhodopsins, light absorption by BR at 77 K causes formation of a red-shifted primary intermediate, the K intermediate (λ_{max} ∼590 nm). The presence of a red-shifted K precursor termed the J intermediate (λ_{max} ∼625 nm) was revealed by time-resolved visible spectroscopy.[104] The excited state of BR possesses a blue-shifted absorption, which decays in two components of about 200 and 500 fs.[105] As expected from the formation of the J intermediate within 500 fs, photoisomerization must take place on the femtosecond time scale.[105,106] Although the results obtained from BR containing all-*trans*-ring-locked 5-membered retinal were not as easy to interpret as those for bovine Rho,[107,108] the common principle of retinal isomerization for animal and microbial rhodopsins has been established, namely, that photoisomerization takes place in the excited state (Figure 7). Using femtosecond visible-pump and infrared-probe spectroscopy enabling higher temporal resolution, the 13-*cis* characteristic vibrational band at 1190 cm^{-1} was observed with a time constant of 500 fs.[109] Thus, isomerization of all-*trans* to 13-*cis* occurs on the femtosecond time scale, which is coincident with the formation of the J intermediate. The appearance of the 13-*cis* form in less than 1 ps was also shown through the Fourier-transform of the transient absorption data with less than 5-fs resolution, supporting that the all-*trans* → 13-*cis* isomerization takes place within femtoseconds.[110,111] Additionally, previous anti-Stokes resonance Raman spectroscopy data suggested that the J intermediate is a vibrationally hot state of the K intermediate, showing that its chromophore is highly twisted and thermally excited.[112] Thus, isomerization in the excited state is supported by experimental data for microbial rhodopsins, too (Figure 7). More recently, the role of vibrational coherence in the efficient excited-state photoisomerization suggested for bovine Rho (see above) has been demonstrated for BR via coherent control experiments.[113]

While Rho and BR share a light-driven isomerization event in the excited state, they may utilize different relaxation pathways from the Franck−Condon state (Figure 7). In Rho, the excited wavepacket slides down a barrierless potential surface. For BR, however, several experiments favor a 3-state model that postulates a small potential barrier along the isomerization coordinate.[110,114−116] Isomerization does not occur instantly as shown by real-time spectroscopy of BR with sub-5-fs pulse, but involves the transient formation of a tumbling state,[110] consistent with this 3-state model. Interestingly, recent spectroscopic measurements performed on the 13-*cis* forms of microbial rhodopsins BR and ASR show an ultrafast ballistic barrierless wavepacket movement on the excited state surface, similar to that observed in bovine Rho, suggesting that the isomeric state of retinal may define the dynamics of the excited state.[117]

By ultrafast spectroscopy, reduced rates and efficiency of photoisomerization were measured for various BR mutants where charged counterion residues had been replaced with neutral residues.[37] Thus, the efficient primary photoisomerization mechanism involves a charged counterion complex. In addition to electrostatic interactions, steric interactions with the methyl groups at the C9 and C13 positions seem to be of importance. For example, upon photoisomerization in bovine Rho, the C13-methyl group moves whereas the C9-methyl group does not. Furthermore, to avoid collision of retinal's C13-methyl group and the C10-hydrogen, the C11═C12 and C12—C13 bonds are pretwisted even in the dark state. Experimental and theoretical evidence has been provided that the C13-methyl is important for efficient isomerization.[118,119] The C9-methyl group appears to function as a scaffold for the primary isomerization event,[120] while its motion is important for G protein activation in the late photointermediates.[121,122]

The isomerization reaction mechanism has been further detailed with the help of quantum chemical simulations, first of retinal in gas phase, then with QM/MM methods that include the surrounding protein. In both animal and microbial rhodopsins, after the photoexcitation, retinal leaves the Franck−Condon region by relaxing the stretching and torsional vibrations and moving into the S_1 potential minimum (Figure 7). The evolution follows two reaction coordinates: first, the

dx.doi.org/10.1021/cr4003769 | Chem. Rev. 2014, 114, 126−163

bond length alternation along the retinal chain changes, and then, the motion follows the torsional coordinate at C11=C12 in animal rhodopsins and C13=C14 in microbial rhodopsins leading to a conical intersection funnel (C.I. in Figure 7), where the chromophore displays an approximately 90° twisted double bond, and very efficient decay to the ground state of the primary photointermediate or to the parent state occurs.[56,123−125]

Most of the earlier studies used energy minimization techniques, i.e., basically following the molecular forces acting on the chromophore structure after excitation, moving down the excited states surface toward the conical intersection as shown in Figure 7. Using Molecular Dynamics (MD) techniques in combination with QM/MM methods, the fast femtosecond dynamics of the excited chromophore can also be directly studied.[126−136] With the help of these computational models an atomistic understanding of the primary events in different rhodopsins can be achieved.[137] In particular, the role of the hydrogen-out-of-plane (HOOP) vibrations of retinal, the isomerization pathway, the nature of the fast photointermediate, and the isomerization efficiency can be understood in greater detail for different rhodopsins.

2.3. Primary Energy Storage and Relaxation

Functions of microbial and animal rhodopsins are initiated by light absorption, followed by the efficient isomerization of retinal (see above). Since the photoisomerization occurs on a femtosecond time scale (Figure 8), the protein environment

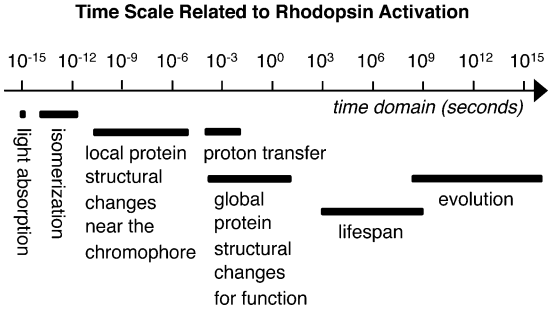

Figure 8. Time scale related to activation of microbial and animal rhodopsins. Light absorption, retinal isomerization, proton transfer, and local and global protein structural changes take place hierarchically, leading to functional activity.

does not have time to show a large structural response, which means that the chromophore pocket does not change on this time scale, even though the neighboring amino acids were shown to respond to the charge motions inside the retinal.[138,139] Restricting the degrees of freedom of the retinal promotes the fast isomerization reaction and assures that part of the energy of light is stored through structural changes of the chromophore and its hydrogen bonding interactions.

Most (rhodopsin-like) GPCRs exist in equilibrium between inactive and active states, where thermal fluctuations are sufficient for transitions and ligand binding shifts the equilibrium. Unlike other GPCRs (with the exception of a handful of protease-activated receptors), animal rhodopsins are covalently bound to an inverse agonist, 11-*cis*-retinal, such that the equilibrium is essentially irreversibly shifted to the inactive state until the photoisomerization of the chromophore occurs. Contrary to what could be expected from a simple rotation around the individual C=C bond, the RSB does not actually rotate upon photoisomerization. Experimentally this has been shown by resonance Raman spectroscopy of bovine Rho,[140] which revealed no change of the RSB hydrogen bond upon retinal isomerization. This view is also consistent with the X-ray structure of bathorhodopsin at 105 K,[120] where the displacement of the retinal chromophore is very small at both ends, (i.e., at the RSB and the β-ionone ring). In contrast, isomerization is clearly indicated by the change of the dihedral angle around the C11=C12 bond from −40° to −155°. Thus, a large local distortion of the polyene chain must be produced to keep the minimally changed overall chromophore geometry, an idea which is supported by the results of femtosecond stimulated Raman spectroscopy[103] and quantum chemical calculations.[128,130,133]

In bathorhodopsin, about 60% of the photon energy (∼150 kJ/mol) is stored as revealed by low-temperature photocalorimetry,[141] and confirmed by a room-temperature transient grating method applied to octopus rhodopsin.[142] Energy is stored in the highly twisted retinal chromophore and the enhanced HOOP vibrational modes at 1000−800 cm^{-1} allow monitoring the structural deformation of the polyene chain.[140,143] It should be noted that, in the Rho → bathorhodopsin conversion, changes in hydrogen-bonding interactions of the retinal are small, as retinal isomerization does not affect the hydrogen-bonding strength of the RSB.[140] This trend seems to be general for animal rhodopsins, since similarly enhanced HOOP modes were observed for squid rhodopsin[144] and color visual pigments.[145] Relaxation of the distorted polyene chain leads to the formation of lumirhodopsin, signifying energy transfer to the opsin moiety, as was clearly observed by X-ray crystallography.[146] The bathointermediate is ∼150 kJ/mol higher in energy than the dark state of rhodopsin, and activation energy for the isomerization (Figure 7) is estimated to be larger than 180 kJ/mol. Such a high energy barrier is consistent with the rigid structure of the retinal binding site, leading to a low noise that is a prerequisite for highly sensitive dim light vision (see section 4).

The amount of photon energy stored in early photointermediates of microbial rhodopsins is smaller than in animal rhodopsins, as low-temperature photocalorimetric studies reported the energy stored to be ∼67 kJ/mol for the K state of BR,[147] which is only about 30% of the absorbed photon energy (about half of that stored in bovine Rho).[141] Despite a loss of 70% of photon energy upon formation of the K intermediate, the remaining energy is still sufficient for the pumping activity of BR (one proton per photon), assuming that pumping a proton normally requires a free energy of ∼25 kJ/mol.[148] Since the photoisomerization quantum yields are very similar for bovine Rho (0.67) and BR (0.64), the differences in energy storage efficiency must correlate with the structures of the primary intermediates, Batho and K, respectively. Interestingly, the trend of lower energy storage in the ion pumps compared to photosensors is supported by the finding that the K intermediate of sensory rhodopsin II in its proton-pumping transducer-free form stores less energy than in its transducer-bound signaling form (88 vs 134 kJ/mol).[149]

As expected, X-ray crystallographic studies of the K intermediate of BR show that the protein structure is not changed significantly upon isomerization.[150−152] According to vibrational spectroscopy, the enhanced HOOP vibration bands in the K intermediate mainly come from the H−D exchangeable groups, implicating that the chromophore is distorted at the RSB region.[153] The stretching vibration of the

dx.doi.org/10.1021/cr4003769 | *Chem. Rev.* 2014, 114, 126−163

$RSBH^+$ is largely up-shifted upon photoisomerization (350 cm^{-1} and ~500 cm^{-1} for the N−D and N−H stretches, respectively), indicating that the hydrogen bond has been weakened.[154] Thus, retinal isomerization induces rotational motion of the RSB dipole in the case of BR, so that its hydrogen bond is remarkably weakened.

The hydrogen-bonding acceptor of the $RSBH^+$ in BR is a water molecule, and this water bridges the $RSBH^+$ with the primary proton acceptor Asp85. Rotation of the NH^+ group of the $RSBH^+$ causes rearrangement of the water-containing hydrogen-bonding network in the RSB active site and weakens hydrogen bonds of water molecules upon K formation,[155,156] contributing to the high-energy state. The contribution of the weakened hydrogen bonds to the energy storage was estimated to be 46 kJ/mol,[157,158] which is more than half of the total energy storage (67 kJ/mol). While the idea of energy storage through the distortion of retinal has been well-accepted, energy storage through hydrogen-bonding destabilization was novel. Another computational study has analyzed this aspect in more detail, reporting that about half of the energy is stored in the twist of retinal while the other half results from changed interactions of retinal with the protein environment.[159] The importance of hydrogen-bonding alteration in the energy storage leads to an unexpected finding for microbial rhodopsins, i.e., positive correlation between strong hydrogen bond of water near the RSB and proton pumping activity (examined in depth in section 3).[153,160]

Figure 8 summarizes the events occurring in microbial and animal rhodopsins by placing them on a single time scale. Light absorption and photoisomerization take place in 10^{-15} and 10^{-14}−10^{-12} s, respectively, and converted light energy in each protein, as steric constraints in animal rhodopsins, or as hydrogen-bonding alterations and steric constraints in microbial rhodopsins, drive protein structural changes in later time domains. The primary stable photoproducts are red-shifted from the original absorption, being called "K intermediate" and "Batho intermediate" for microbial and animal rhodopsins, respectively. Relaxation of these high energy states of the chromophore and its immediate vicinity trigger global protein structural changes necessary for function. For many microbial and animal rhodopsins, such changes accompany deprotonation of the $RSBH^+$, forming the "M intermediate" and "Meta-II intermediate", respectively. These intermediates are the key states for function, which are described in detail in sections 3 and 4. Figure 8 also contains a time domain of evolution, the time of natural design of protein architecture, by which both microbial and animal rhodopsins have been functionally optimized.

Microbial and animal rhodopsins have further striking differences in the fate of their photoproducts (see the relevant sections below). In microbial rhodopsin, all-*trans* → 13-*cis* photoisomerization usually triggers a cyclic sequence of reactions linking a series of intermediates and including thermal reisomerization of retinal, which is not released from opsin during this photocycle. This is important for organisms in which the rhodopsins are not embedded within a specialized organelle and enzymatic reisomerization is not possible. In animal rhodopsins, retinal photoisomerization from the 11-*cis* to the all-*trans* configuration triggers a reaction pathway that also comprises a series of intermediates, whereas the reaction is not necessarily cyclic and often requires the retinal molecule to be released from the opsin apoprotein and reisomerized either enzymatically[161,162] or photochemically.[163] It appears that, depending on the biological function of a rhodopsin, the specific design of a protein/retinal combination determines whether the light-induced conformational changes in the RSB region are large enough for RSB hydrolysis to occur.

3. MICROBIAL RHODOPSINS

3.1. General Features of Microbial Rhodopsins

For about 25 years since the early 1970s, microbial rhodopsins were epitomized by haloarchaeal proteins, the first-discovered and best-studied light-driven proton pump bacteriorhodopsin (BR) and its close relatives halorhodopsin and sensory rhodopsin I and II (HR, SRI and SRII). But in the last 15 years, thousands of related photoactive proteins with similar or different functions have been identified in *Archaea*, in marine, freshwater, and terrestrial *Eubacteria* and *Eukaryota* (Figure 9).[1,7,164−166] Thus, a small group of proteins, believed to be

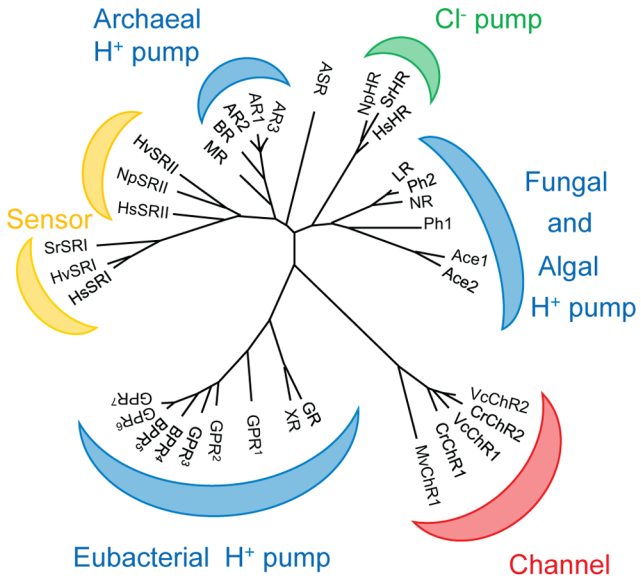

Figure 9. Phylogenetic tree of selected microbial rhodopsins. Four main functions of microbial rhodopsins are shown in different colors: blue, proton pumps; green, chloride ion pumps; red, light-gated cation channels; yellow, photosensors. Proton pumps are widely distributed among *Archaea*, *Eubacteria*, and *Eukaryota*. Two additional poorly studied functional groups (sodium ion pumps and enzymerhodopsins) are not included. See Supporting Information Figure 1 for additional information on genus and species of the microbial rhodopsins.

present only in halobacteria and having a limited number of functions (proton and chloride pumps and phototactic/photophobic receptors), grew into a confounding variety of species with versatile sequences, ecology, taxonomy, and functions. Among the new functions are light-gated cation channels (see the section on channelrhodopsins below), light-

dx.doi.org/10.1021/cr4003769 | *Chem. Rev.* 2014, 114, 126−163

switchable enzymes, light-driven sodium pumps, and novel photosensors distinct from the haloarchaeal SRs (Figures 3 and 9).[167−170]

Despite the variety of sequences and functions, the common structural and mechanistic principles of microbial rhodopsin architecture can be deduced on the basis of about a dozen of structures of unique proteins. X-ray and NMR structures are available for various proton and chloride pumps, as well as for photosensors and a light-gated channel. While all of the known structures of microbial rhodopsins show a common tight α-helical bundle of 7TM helices surrounding the retinal chromophore, there is substantial variation in the arrangement of side chains, the structure of the interfacial regions and loops, as well as in the positions of internal water molecules.[7,165,171,172] The retinal binding pocket is the most conserved common element of the structure. Figure 10

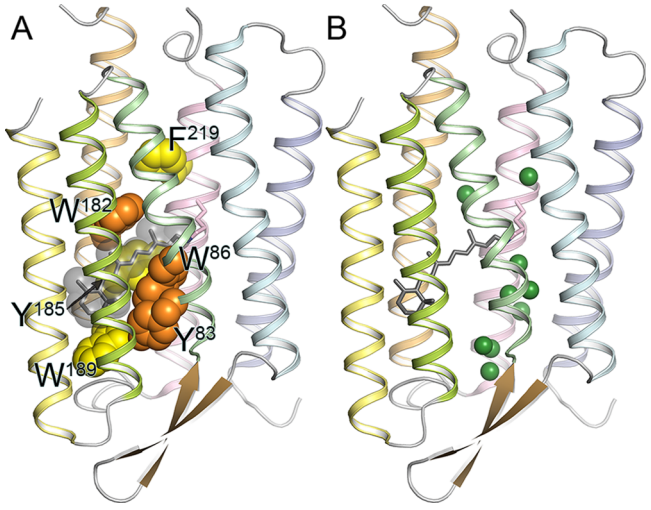

Figure 10. (A) Structure of bacteriorhodopsin (BR), with conserved aromatic residues highlighted (PDB ID: 1QM8). Tyr83, Trp86, and Trp182 are strongly conserved among microbial rhodopsins (orange). Aromatic amino acids are strongly conserved at the position of Tyr185, Trp189, and Phe219 (yellow). In BR, Trp86, Trp182, Tyr185, and Trp189 constitute the chromophore binding pocket for all-*trans*-retinal (gray). (B) Crystallographically observed internal water molecules of BR (shown as green spheres). Note much higher hydration of the extracellular half compared to the cytoplasmic one.

illustrates the overall structure of BR with the conserved aromatic amino acids important to function shown. Strongly conserved Trp86 and Trp182 constitute an important part of the chromophore binding site by sandwiching all-*trans*-retinal (Figure 10). The presence of these bulky groups possibly determines the isomerization pathway from the all-*trans* to 13-*cis* form, and the interaction of photoisomerized retinal with Trp182 may serve as the mechanical transducer for passing the energy stored in retinal deformation into the functionally important changes of the helical tilts necessary for function.[173] Another important position occupied by aromatic amino acids in the retinal binding pocket is that of Tyr185 in BR (Figure 10), which participates in hydrogen-bonding stabilization of the $RSBH^+$ counterion for many rhodopsins, but is replaced by a Phe in channelrhodopsins (Supporting Information Figure 1), suggesting that the lack of hydrogen-bonding interaction at this position is important for channel function. Interestingly, an aromatic pair similar to Trp182/Tyr185 is found in retinal binding pockets of many animal visual rhodopsins (Trp265/Tyr268 in bovine Rho), suggesting a conceptually similar mechanism of energy transfer between retinal and opsin.[174]

In addition to the retinal polyene chain−aromatic side chain rings interactions described above, electrostatic and hydrogen-bonding interactions in the proximal part of retinal are crucial in defining the functionality of microbial rhodopsins. The side chain of Lys216 of BR (or its equivalent in other microbial rhodopsins) forms a covalent bond with the retinal molecule through the Schiff base (Figures 2 and 11). Since the RSB is

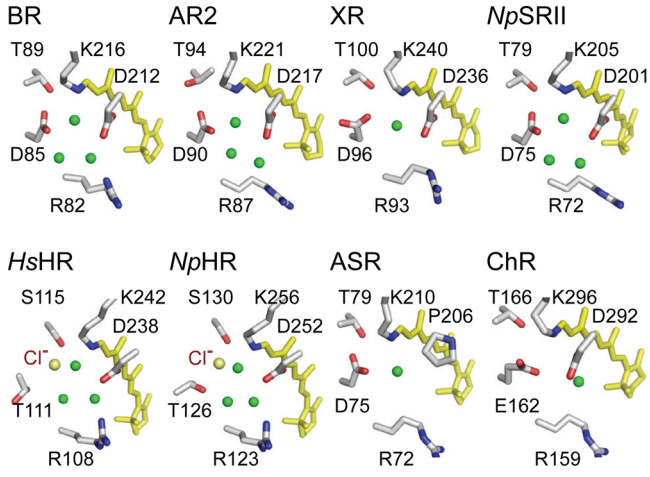

Figure 11. X-ray crystallographic structures of the RSB region for eight representative microbial rhodopsins with various transport/signaling functions. BR, AR2 (archaerhodopsin 2), and XR function as proton pumps. *Np*SRII is a phototaxis sensor, but pumps protons in the absence of its transmembrane transducer. *Hs*HR and *Np*HR are chloride pumps, ASR is a photochromic sensor, and ChR is a light-gated cation channel. Membrane normal is approximately in the vertical direction of the figure. Upper and lower regions correspond to the cytoplasmic and extracellular sides, respectively. Green spheres denote ordered water molecules observed crystallographically. For abbreviations of microbial rhodopsins, see Supporting Information Figure 1.

usually protonated, Lys216 and superconserved Arg of helix C (Arg82 in BR) provide two positive charges within the protein, which require two negative charges for electrostatic stabilization. This dictates the most common configuration of the $RSBH^+$ counterion, that with two carboxylic acids (Asp85 and Asp212 in BR), which are perfectly conserved for proton-pumping microbial rhodopsins (Figure 11). Any deviation from this arrangement has strong functional consequences (Supporting Information Figure 1). For example, in the chloride-pumping HR, the negatively charged Asp at position 85 (of BR) is replaced with Thr, and in the recently discovered sodium-pumping rhodopsins, it is replaced with an Asn.[168,175] Similarly, in *Anabaena* sensory rhodopsin (ASR), the negatively charged Asp at position 212 of BR is replaced with Pro, which prevents light-induced transfer of the $RSBH^+$ proton to the homologue of Asp85 of BR.[176,177] Importantly, all microbial rhodopsins contain protein-bound water molecules near the RSB, presumably contributing to the stabilization of the $RSBH^+$ in the hydrophobic protein interior (Figure 11). These water molecules play crucial roles in protein function, and have been extensively studied by X-ray crystallography of photointermediates, Fourier transform infrared spectroscopy (FTIR), and computational methods (see below).

dx.doi.org/10.1021/cr4003769 | *Chem. Rev.* 2014, 114, 126−163

As described in section 2, photoisomerization (which usually proceeds from the all-*trans*- to 13-*cis*-retinal in microbial rhodopsins) disrupts the finely tuned retinal−opsin interactions, inducing functionally important changes in the protein moiety. Most importantly, this results in changes in ion affinities and/or conformational changes of the backbone (e.g., helical tilts), that are required for ion transport and photosensory transduction (see the respective subsections below for a detailed description of these events). It should be noted that, in some microbial rhodopsins, most notably in BR, all-*trans*-retinal is not stable in the dark (Figure 2), and thermal compact isomerization from the all-*trans*- to 13-*cis*,15-*syn*-form takes place (so-called dark-adaptation).[178−181] The thermally stable 13-*cis*,15-*syn*-form is different from the metastable 13-*cis*,15-*anti*-form (C═N *trans*) that appears during the photocycle of microbial rhodopsins. The converse light-induced conversion from the 13-*cis*,15-*syn*- to all-*trans*-form is called light-adaptation and restores the functionally active state for most microbial rhodopsins.[182] There are some notable exceptions among sensory rhodopsins, as the direction of light- and dark-adaptation are reversed in ASR, which also presents an exception to the normally cyclic character of photoreactions of microbial rhodopsins.[183,184]

Most often, photoisomerization from the all-*trans*- to 13-*cis*-form of microbial rhodopsins triggers a cyclic series of reactions (the photocycle) comprising a series of photointermediates, which have been studied by various methods in a time-resolved manner. Figure 12 shows the typical photocycle for a microbial rhodopsin, exemplified by BR.[185−189] Spectroscopic properties of photointermediates reflect isomeric configuration, planarity, and protonation state of the retinal, as well as the position of surrounding protein and ion charges and water molecules. The primary red-shifted K intermediate with twisted retinal, introduced in detail in section 2, is usually followed by the blue-shifted L intermediate.[190] For proton-pumping (and some of the photosensory) rhodopsins, the L intermediate serves as the precursor of the proton transfer reaction from the $RSBH^+$ to its primary carboxylic proton acceptor, by which the M intermediate is formed, the key step in proton transport. Since the M intermediate has a deprotonated 13-*cis* chromophore,[191] it exhibits a characteristic strongly blue-shifted absorption (λ_{max} at 360−410 nm), well-isolated from that of other intermediates. In the case of chloride pumps, the $RSBH^+$ does not deprotonate during the photocycle and the L intermediate converts directly to the N intermediate,[192] which in proton-pumping rhodopsins arises as a result of reprotonation of the RSB from the cytoplasmic side (detected as the M intermediate decay). The N intermediate is often characterized by the largest changes in the protein backbone conformation, most notably, outward tilts of the cytoplasmic end of helix F, which are functionally significant both for ion transport and interactions with transducers of sensory rhodopsins.[193] The photocycle usually ends with another red-shifted intermediate, known as O, serving as a last step in resetting the original unphotolyzed conformation. A more detailed description of the individual photocycles for different classes of microbial rhodopsins can be found in the subsequent sections.

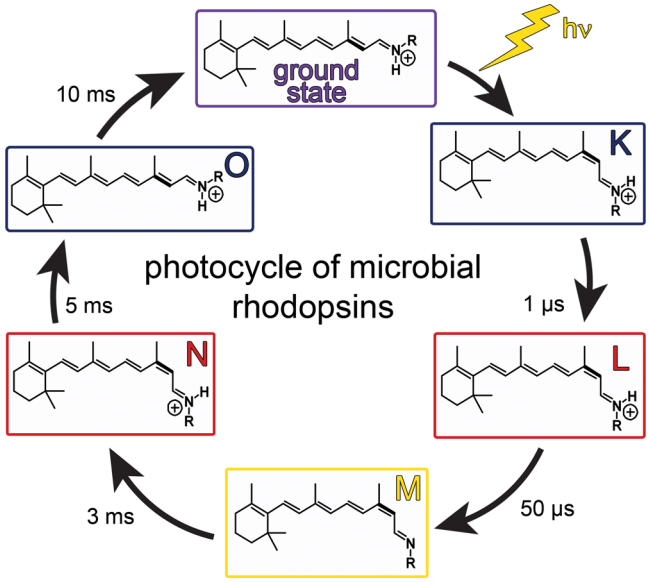

Figure 12. Typical photocycle of microbial rhodopsins showing isomeric and protonation state of the retinal. Names of the photocycle intermediates and their characteristics were originally established for BR. In the case of BR, K and O are the red-shifted intermediates, while L, M, and N are all blue-shifted intermediates. The primary photoreaction is the retinal isomerization from the all-*trans*,15-*anti*- to 13-*cis*,15-*anti*-isomer. The $RSBH^+$ deprotonates upon M formation and is reprotonated upon M decay. Thermal reisomerization occurs upon O formation from the 13-*cis*,15-*anti*- to reform the all-*trans*,15-*anti*-state.

3.2. Bacteriorhodopsin, the Prototypical Ion Pump

Bacteriorhodopsin from *Halobacterium salinarum*, the first discovered microbial rhodopsin,[194] was the first membrane protein whose structure was found to be composed of seven helices by electron microscopy,[195] and was also the first membrane protein to have its amino acid sequence determined.[196] As the best studied microbial rhodopsin, it serves as a paradigm of a light-driven retinal-binding ion pump and aids in studies of novel rhodopsins. The photocycle of BR, during which a proton is vectorially translocated across the membrane from the cytoplasmic to the extracellular side, is shown in Figure 12, and the main proton transfer steps with the respective transitions between photocycle intermediates are shown in Figure 13. These intermediate states were first identified by visible absorption spectroscopy, while the structure of the retinal chromophore in each photointermediate was revealed by resonance Raman and FTIR spectroscopy.[189,197−199] In the early days of BR research, it became clear that all-*trans* → 13-*cis* isomerization occurs upon photoexcitation of BR, and that the RSB is deprotonated in the M intermediate and reprotonates upon formation of the N intermediate.[191,200−202] In combination with site-directed mutagenesis and photoelectric measurements, this indicated that the $RSBH^+$ proton is transferred to the extracellular side upon M formation, and is taken up from the cytoplasmic side by the RSB upon M decay (Figure 13).[203−205] Since then, the intricate details of the proton transport mechanism and structure of proton-conducting pathways of BR have been elucidated by the concerted efforts of many research groups, with seminal contributions made by site-directed mutagenesis, vibrational spectroscopy, X-ray crystallography, solid-state NMR, and molecular dynamics simulations.

The molecular mechanism of vectorial transport by pumps has been a long-standing challenge in bioenergetics, and proton transport by BR is not an exception to this rule. An ion pump must be fundamentally different from a channel, where the ion

dx.doi.org/10.1021/cr4003769 | *Chem. Rev.* 2014, 114, 126−163

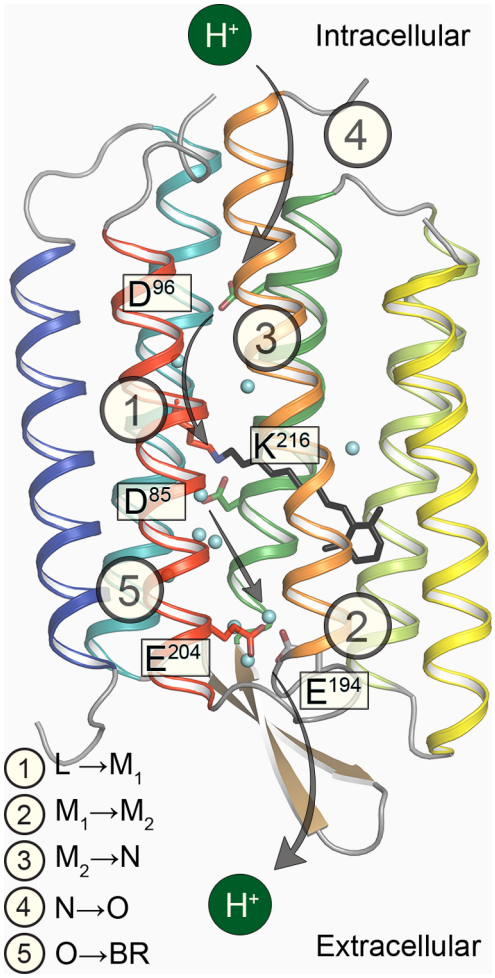

Figure 13. Main proton transfers in the bacteriorhodopsin photocycle. Protonatable groups and bound water molecules important for transport activity are shown as stick representation and blue spheres, respectively (PDB ID: 1C3W). Numbers with arrows represent the sequence of proton transfer reactions, the corresponding transitions between the photointermediates are indicated in the inset. The TM helices are shown in the following colors: A, blue; B, teal; C, green; D, lime green; E, yellow; F, orange; G, red; and the chromophore is depicted as black sticks. ① Proton transfer from the $RSBH^+$ to the primary proton acceptor Asp85; ② proton release to the extracellular medium from the proton-releasing complex; ③ reprotonation of the RSB from the primary proton donor Asp96; ④ reprotonation of Asp96 from the cytoplasmic medium; ⑤ proton transfer from Asp85 to the proton-releasing complex.

pathway is continuous between the cytoplasmic and extracellular aqueous phases, because a pump should be able to prevent ion backflow for transport against an electrochemical gradient. Therefore, the alternating access model has been developed for BR, wherein the RSB accessibility is switched between the cytoplasmic and extracellular sides (Figures 13 and 14). The nature of this so-called reprotonation switch has been disputed for many years, with models ranging from the pure structural accessibility (conformational changes of the retinal and/or opsin) to pure affinity (changes in the pK_a's of proton donors and acceptors) mechanisms, but is most likely a combination of both.[187,189,206−210] As can be seen in Figure 12, the isomeric states of the retinal chromophore are identical between the L and N intermediates, whereas the RSB accessibility must be switched between them, from the extracellular to the cytoplasmic side, to ensure vectorial transport. Thus, in addition to the two unidirectional steps in the photocycle (the primary isomerization reaction and the last step, the O-to-BR reaction), a third unidirectional step is often considered between the two M substates, M_1 and M_2, to account for the vectorial transport (Figure 14). The presence of multiple M states has been confirmed by several techniques and is consistent with this idea.[211−217] While M1 exists in equilibrium with the L intermediate whose accessibility is to the extracellular side, M2 is in equilibrium with the N intermediate whose accessibility is to the cytoplasmic side. Thus, the switch should occur between the M1 and M2 states, preceded by the proton release to the extracellular surface (Figure 13). It appears that the conformational changes associated with the switch must be very subtle, as there is no significant difference in the vibrational signals of retinal and protein between M1 and M2, with the only detectable difference being in the water FTIR signals (so-called IR continuum).[212,218]

Extensive studies by FTIR spectroscopy in combination with site-directed mutagenesis and other techniques revealed the capture and donation of protons by specific amino acids during the pumping process. For the analysis of proton pathways, the C═O stretching vibrations of protonated carboxylic acids in the 1800−1700 cm^{-1} spectral region provided much needed information on protonation and hydrogen-bonding changes of proton donors and acceptors during the photocycle.[198,199,219−222] Transient deprotonation of Asp96 in the N intermediate and transient protonation of Asp85 in the M, N, and O states have been observed, indicating that a proton is translocated via Asp96 (the donor), the RSB, and Asp85 (the

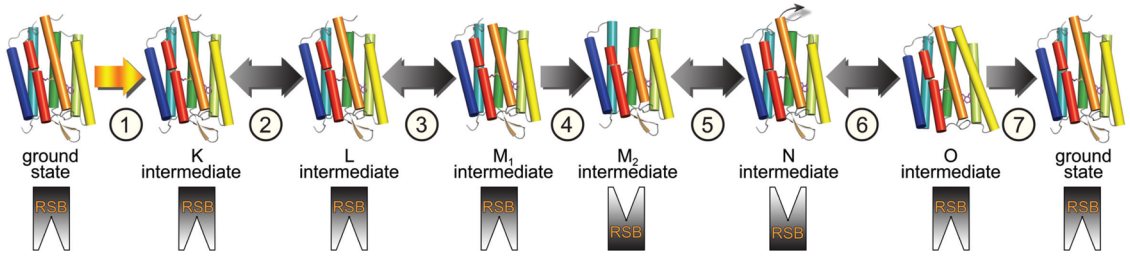

Figure 14. Sequence of the main molecular events in the bacteriorhodopsin photocycle and accessibility of RSB: ① absorption of a photon by all-*trans*-retinal, photoisomerization to twisted 13-*cis* form; ② relaxation of retinal twist, strengthening of water-mediated hydrogen-bonding between $RSBH^+$ and Asp85; ③ proton transfer from $RSBH^+$ to the primary proton acceptor Asp85; ④ proton release to the extracellular medium from the proton-releasing complex and switch of the accessibility of RSB to the cytoplasmic side; ⑤ conformational change of the backbone in the cytoplasmic half and reprotonation of RSB from the primary proton donor Asp96; ⑥ reprotonation of Asp96 from the cytoplasmic medium and thermal reisomerization of retinal to all-*trans*; ⑦ proton transfer from Asp85 to the proton-releasing complex and restoration of the initial conformation.

dx.doi.org/10.1021/cr4003769 | *Chem. Rev.* 2014, 114, 126−163

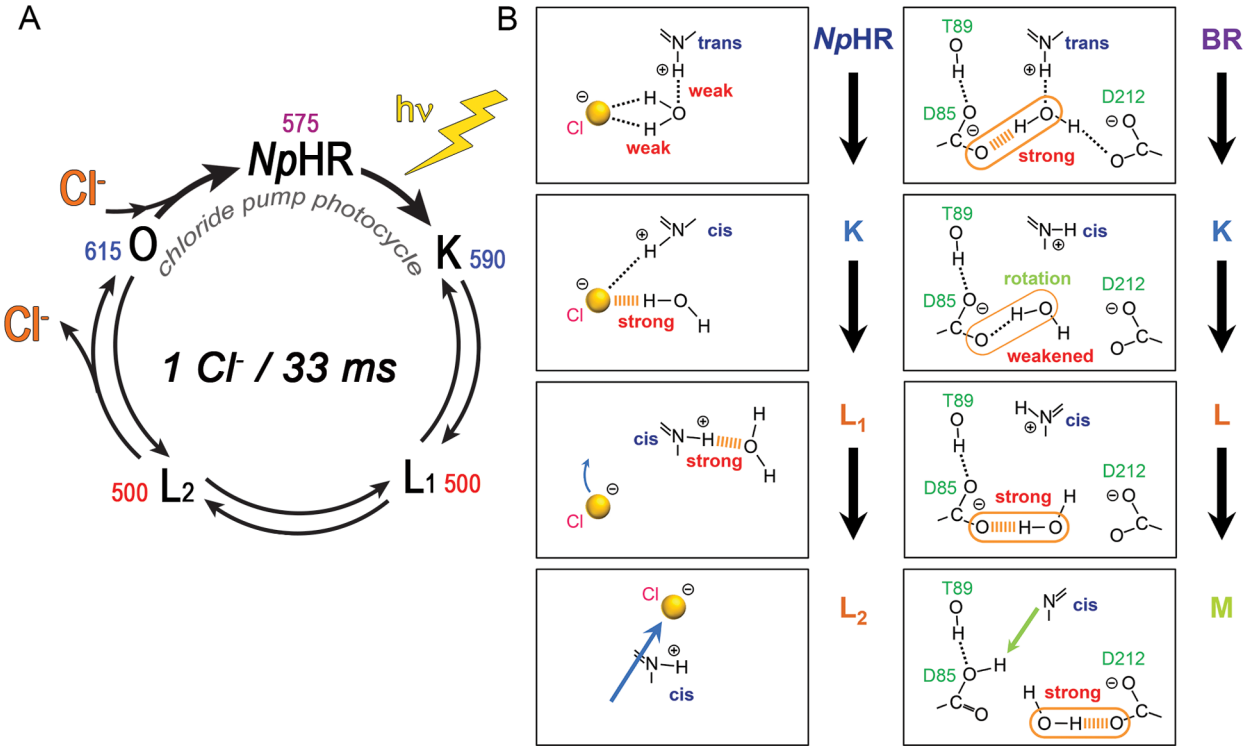

Figure 15. (A) Photocycle of *Natronomonas pharaonis* halorhodopsin (*Np*HR). (B) Light-induced hydrogen-bonding alteration in the RSB region of *Np*HR (left) and bacteriorhodopsin (BR, right), suggesting the mechanism of proton and chloride ion translocation (refs 306, 566, respectively).

acceptor) (Figure 13). The temporal coincidence between the deprotonation of the RSB and protonation of Asp85 directly demonstrated that the primary proton transfer occurs from the $RSBH^+$ to Asp85 (process 1 in Figure 13).[200,223] Similarly, the kinetic coincidence between the reprotonation of the RSB and deprotonation of Asp96 signifies proton transfer from Asp96 to the RSB (process 3 in Figure 13), and reprotonation of Asp96 upon decay of the N state coincides with proton uptake from the cytoplasmic bulk phase (process 4 in Figure 13).[205,220,224] The persistence of Asp85 in the protonated state even after proton release upon M formation suggests that there is another proton release group (or complex) located close to the extracellular surface of BR. While site-directed mutagenesis studies pointed to the involvement of several protein side chains in the proton-releasing mechanism (most notably, Glu204, Glu194, Arg82, and Tyr57), the exact identity of the proton-releasing group remained controversial for a long time, due to the lack of a clear deprotonation signal.[225−229] The observation of the infrared continuum band (presumably of a protonated water cluster) at 2000−1800 cm^{-1} by time-resolved FTIR provided the data needed to confirm the presence of a highly delocalized proton,[230] and the involvement of water vibrations in this continuum band was proven directly using ^{18}O water.[231] As the negative continuum band disappears in mutants deficient in proton release, it can serve as an experimental signature for this proton transfer.[232] A theoretical study proposed that a low-barrier hydrogen bond between Glu194 and Glu204 explains the presence of this continuum band, reflecting the existence of a delocalized excess proton in the water cluster stabilized by these residues, which may serve as the proton-releasing group.[233]

It should be noted that the essential character of the early proton release has not been proven, as BR retains its proton-pumping activity even when proton release occurs after uptake, as happens in a number of BR mutants, at low pH and in some close homologues of BR.[164,234] Nevertheless, it has been postulated that early release is important for the functionality of the reprotonation switch, as it ensures irreversibility of the M1 → M2 reaction by changing the proton affinity of Asp85.[235,236] FTIR spectroscopy in combination with mutagenesis showed that strongly hydrogen-bonded (as judged from the low O−D stretching frequency) water molecule in the RSB vicinity is a prerequisite for efficient proton pumping.[153,155] In the "hydration switch model", it was proposed that the light-induced shift of this water molecule from Asp85 to Asp212 ensures efficient deprotonation of the $RSBH^+$ (Figure 15), but a further increase in the proton affinity of Asp85 is required to make it unidirectional, and this is exactly where the early proton release may become important.[237] This might be achieved through the electrostatic coupling of Asp85 with the proton releasing complex, demonstrated by both mutagenesis and crystallography. When Asp85 becomes protonated, the positive charge of Arg82 is reoriented toward the proton-releasing water cluster and the destabilized proton is released to the extracellular bulk solvent.[238,239] Conversely, this stabilizes the proton on Asp85 and prevents the backflow of protons to the RSB, ensuring its eventual reprotonation from the cytoplasmic side.

The BR crystal structure exhibits an asymmetric pattern of hydration, where the extracellular half contains seven internal water molecules, but the cytoplasmic half contains only two (Figures 10 and 13).[165,240] Such asymmetry makes sense in view of BR function, as the water molecules build a hydrogen-bonding network on the extracellular side for fast proton release, while the cytoplasmic side should be inaccessible in the dark and allow proton uptake only after the light-induced accessibility switch. To make proton conduction in the cytoplasmic region possible, an additional conformational

dx.doi.org/10.1021/cr4003769 | *Chem. Rev.* 2014, 114, 126−163

change allowing the entrance of water into the vicinity of Asp96 should take place. Such a conformational alteration is realized mainly by changes in helical tilts (especially that of the cytoplasmic half of helix F) in the late M and early N intermediates (Figure 14), as was observed by neutron diffraction, X-ray diffraction, electron diffraction, and EPR spectroscopy, and most recently by high-speed atomic force microscopy.[216,241−246] Interestingly, the cytoplasmically open conformation of BR can be obtained via mutagenesis,[247,248] for example, by neutralizing the charge of Asp85 and/or by promoting deprotonation of Asp96, emulating the N intermediate.[249] It should be noted that a similar outward opening motion of the TM6 helix takes place for bovine Rho (see section 4 below), as well as for some of the sensory rhodopsins,[193] once again suggesting a common mechanism of energy transduction.

X-ray crystallography has been very successful in revealing the sequence of structural alterations in each of the photocycle intermediates through finding an appropriate illumination regime of BR crystals under suitable temperature and pH conditions or by using mutants which stabilize or emulate particular intermediate states.[185,250,251] The reader is referred to excellent and extensive crystallographic reviews, which give an atomistic level of detail of the conformational changes and mechanistic insights (many of which have been mentioned above).[165,188,252−254]

In conclusion, it should be mentioned that an alternative model of BR function has been proposed, postulating that BR works as an inward-directed hydroxide (OH^-) pump rather than the commonly accepted outward-directed proton (H^+) pump. The model was based on the presence of the strongly polarized water hydrogen-bonded to the RSB in the dark state of BR and its absence in M intermediate structures, and supported by the fact that in homologous halorhodopsins and some BR mutants other anions can also be transported.[187,255−257] While this is an interesting model, the Grotthus mechanism, a concerted proton transfer through hydrogen bonds, is sufficient to explain the proton transfer reactions in BR, but it should be however noted that there has been no strong experimental evidence to rule out this alternative hydroxide pump model either.

3.3. Other Light-Driven Proton Pumps: Variations on the Common Mechanism

During the past decade, it became clear that BR-like light-driven proton pumps exist not only in *Archaea*, but also are abundant among *Eubacteria* and lower *Eukaryota* (Figure 9).[7,164,166] Even though the molecular mechanism of proton pumping has been thoroughly investigated for BR, these additional rhodopsins present many interesting variations assisting in our understanding of the common principles of proton transport. While it would be impossible to survey all the details of the numerous (the count goes by thousands) species of proton-pumping rhodopsins in the framework of this review, we would like to outline the major classes of such rhodopsins and stress the interesting mechanistic and structural differences and commonalities with BR. Even though the number of taxonomic species bearing genes encoding proton-pumping rhodopsins is large, these rhodopsins can be conveniently classified into a small number of subtypes with substantial sequence similarity within each class. The main subtypes are bacteriorhodopsins (mostly haloarchaeal), proteorhodopsins (mainly eubacterial but also found in some *Archaea*), xanthorhodopsins (and related actinorhodopsins), and fungal/algal proton pumps.

Green-absorbing proteorhodopsin (PR) was the first eubacterial proton pump identified by metagenomic analysis of marine proteobacteria.[258] Since this groundbreaking discovery in 2000, it became clear that proteorhodopsins are likely to be the most abundant and widely distributed of the microbial rhodopsins, now found in many different bacterial taxa and not only in marine organisms.[259−263] Spectrally, PRs can be classified into green-absorbing PRs (GPR, $\lambda_{max} \sim 525$ nm) and blue-absorbing PRs (BPR, $\lambda_{max} \sim 490$ nm), thought to be characteristic for marine bacteria living near the surface and in the deep sea, respectively.[264,265] It was found that a single amino acid at position 105 (equivalent to Leu93 in BR) is the determinant of the specific color (Leu in GPR and Gln in BPR). Although the proton-pumping function was clearly demonstrated for GPR heterologously expressed in *E. coli*,[258,266,267] its native physiological significance was not clear until recently. Initially, it was reported that several PR-harboring species exhibited no differences between the growth rates of cultures grown in the dark or under illumination, but it eventually became clear that PR expression can give significant advantages to some bacteria under the conditions of carbon starvation.[268−271] Additionally, many PR variants (especially BPRs) possess very slow photocycles and weak photoelectric signals, making it unlikely that they function as proton pumps. Alternative physiological functions (e.g. photosensory) have been suggested.[266,272−274] Another group of related (but distinct from PR) eubacterial pumps is represented by xanthorhodopsin (XR) from *Salinibacter ruber* and its homologues, including the cyanobacterial rhodopsin from *Gloeobacter* (GR) and numerous actinorhodopsins.[172,275,276] Actinorhodopsins were originally identified as numerous metagenomic PR-like sequences in predominantly freshwater habitats, but further analysis revealed that they represent a separate subgroup along with XR.[261,276,277] The most novel and distinctive feature of XR is its second chromophore, a carotenoid salinixanthin, which serves as a light-harvesting antenna that transfers the absorbed light energy to retinal with a quantum efficiency of ~40%.[278,279] GR can bind carotenoids as well, and it has been suggested that the structural prerequisite of such binding is the replacement of Trp near the β-ionone ring of retinal (Trp138 of BR) with Gly.[280]

The crystal structure of XR provides many structural insights into the mechanism as well as unique features of eubacterial proton pumps.[172,279] On the extracellular side of the RSB, one observes at least four important differences from BR. First, there is only a single water molecule observed in the RSB region (Figure 11), considerably different from the pentagonal water cluster (comprising three water molecules and two aspartates) and adjacent extended hydrogen-bonding network (seven water molecules in total) of the archaeal rhodopsins (Figures 10 and 11).[155] Second, the carboxylic counterion exists as a His-Asp complex in XR and most other eubacterial pumps. As a result, the carboxylic counterion is no longer electrostatically coupled to the conserved equivalent of Arg82, in contrast to BR.[279,281−284] The higher pK_a of the RSB counterion is characteristic for GPR and other eubacterial rhodopsins, and interactions with a conserved His may modulate this.[281,285−287] Third, the proton-releasing complex of BR (the glutamate dyad with intercalating water) is not present in eubacterial proton pumps, and early proton release is not observed, at least under physiological conditions.[275,285,288] This may imply that early

dx.doi.org/10.1021/cr4003769 | Chem. Rev. 2014, 114, 126−163

proton release is not essential for a proton-pumping mechanism in general.[164] Finally, the β-stranded BC loop is displaced, opening a hydrophilic cavity on the extracellular side, which may account for the alternative proton release mechanism.[279] On the cytoplasmic side, the proton donating Asp96 of BR, which is usually paired with a conserved Thr residue (Thr46 of BR), is replaced by a Glu paired with Ser (Supporting Information Figure 1). It appears that this Glu residue is more tightly coupled with the $RSBH^+$ in the dark state of XR than in BR and that the proton transfer pathway between them is partially prebuilt.[275,279,289] One important exception to this rule is a unique rhodopsin from *Exiguobacterium* (ESR), in which the carboxylic proton donor is replaced by a Lys residue, suggesting a completely different mechanism of RSB reprotonation.[290]

While a few proton-pumping microbial rhodopsins in lower eukaryotes (mainly dinoflagellates) are homologous to XR or PR,[166,291] many rhodopsin-bearing eukaryotes, such as fungi and green algae, have BR-like pumps. Fungi demonstrate many different forms of rhodopsins, some of which have been shown to be proton pumps, starting with rhodopsin from *Leptosphaeria* (LR).[292−294] Fungal proton-pumping rhodopsins are similar to BR in many respects, but their exact physiological role is unclear.[295] The marine green algae *Acetabularia acetabulum* contains a proton-pumping microbial rhodopsin (Ace2), and recently its crystal structure was determined to 3.2 Å resolution, providing the first glimpse of a eukaryotic retinal-binding proton pump.[296,297] Similar to fungal proton pumps, proton uptake in Ace2 occurs earlier than release, which was expected as it lacks the proton-releasing complex of BR (Supporting Information Figure 1). While its overall structure is similar to that of BR, the most distinct feature of this rhodopsin is the unique interaction of the carboxylic cytoplasmic proton donor with a Cys residue on helix G, replacing typical pairing with Thr or Ser on helix B found in other microbial rhodopsins.

Despite the unique features and differences described above, all of the eubacterial and eukaryotic proton pumps conserve the carboxylic primary proton acceptor (homologous to Asp85 of BR). Importantly, they also seem to preserve the strongly hydrogen-bonded water molecule between the $RSBH^+$ and this counterion, further confirming the importance of hydrogen-bonding strength of protein-bound waters for proton pumps.[153] In fact, strongly hydrogen-bonded water molecules were found in proton-pumping fungal rhodopsins from *Leptosphaeria* and *Phaeosphaeria*, but not in their nonpumping homologues from *Neurospora* (NR),[298] and also found for GPR at high pH (proton-pumping active), but not at low pH.[299]

3.4. Changing the Ion Specificity: Light-Driven Chloride and Sodium Pumps

It appears that, by changing the finely tuned structural template of BR-like proton pumps a little further, one can produce ion pumps with different ion specificities, namely, chloride and sodium pumps.[168,300] Sometimes, these function-altering changes of the template can be achieved not only by evolution but simply by applying a few mutations to key residues *in vitro*.[301,302] A good example of such functional conversion is HR, initially identified in *Halobacterium salinarum* and shown to transport chloride ions in the cytoplasmic direction. While the overall architecture of HRs is BR-like, the crystal structures of two chloride pumps (*Hs*HR and *Np*HR) clearly show the presence of a chloride ion in the RSB region (Figure 11), where it occupies the position of Asp85 carboxylate in BR.[303,304] In HR, this unprotonated carboxylate is replaced by Thr (Supporting Information Figure 1), suggesting that the electric quadrupole of the $RSBH^+$ with its counterion complex (Asp85, Asp212, and Arg82 in BR) lacks a negative charge and the charge balance is compensated for by the binding of the negatively charged chloride ion. Hydrogen bonds of the RSB and of protein-bound water molecules in HR are weak, suggesting that the transported chloride ion is not involved in strong hydrogen-bonding (Figure 15), in stark contrast to the case for proton transport in BR.[305,306]

The photocycle of HR has no M intermediate reflecting the absence of $RSBH^+$ deprotonation (Figure 15), which might, however, occur as a side reaction.[307,308] Instead, the existence of two L intermediates (L_1 and L_2, sometimes called L and N) was observed by various methods, suggesting an extracellular to intracellular accessibility change during their interconversion, analogous to the M_1 and M_2 intermediates of BR.[192,309−311] The photoisomerization induces changes in the electric and hydrogen-bonding environment of the Cl^- ion, driving its movement to the cytoplasmic side of the $RSBH^+$. The hydrogen bond of the RSB is strengthened in the L intermediate, but the hydrogen-bonding acceptor is not the chloride ion, but most likely a water molecule (Figure 15).[306,312] Rearrangement of the water-containing hydrogen-bonding network most likely opens the valve to the cytoplasmic region, and the chloride ion is released to the cytoplasmic side during the transition to the O intermediate.[313,314]

Surprisingly, BR can be converted into an HR-like chloride pump (albeit, a very inefficient one) *in vitro* by replacing Asp85 with Thr, suggesting that the amino acid at position 85 is a determinant for ion specificity.[301,302] In contrast, the reverse Thr-to-Asp mutations of HR, such as Thr108Asp of *Hs*HR and Thr126Asp of *Np*HR, fail to convert HR into a BR-like outward proton pump.[315,316] This may imply that the molecular determinants of a proton pump are more demanding than those of a chloride pump, and indeed, an *Np*HR mutated to contain 10 key BR-like amino acids still fails to pump protons (Supporting Information Figure 3), consistent with its lack of a strongly hydrogen-bonded water.[160] Nevertheless, the conversion of HR into a proton pump can be achieved by the simple addition of sodium azide, which most likely serves as an artificial proton shuttle, suggesting common elements in the transport mechanism of proton and chloride pumps.[316] The restoration of a strongly hydrogen-bonded water for the azide-bound HR is completely consistent with these results.[317]

The recent discovery of a new group of rhodopsins homologous to XR, but with different ion specificities, gives very strong confirmation for the ideas gleaned from the comparisons of HR to BR.[168,318] In this new group of eubacterial rhodopsins the main carboxylic proton acceptor and donor (Asp and Glu homologous to Asp 85 and Asp 96 of BR, respectively) are replaced by Asn and Gln (Supporting Information Figure 1), giving them a name of NQ rhodopsins. A subgroup of these rhodopsins introduces a new proton acceptor for the $RSBH^+$, at the position homologous to Thr89 of BR (Figure 11), creating the so-called NDQ motif. It appears that the NDQ rhodopsins can selectively transport sodium in the extracellular direction and that $RSBH^+$ deprotonation is a required step for such transport. This once again demonstrates that new functions can be generated on the BR template through a limited number of amino acid substitutions, and that the energy stored during photoisomerization can be channeled into various processes.

dx.doi.org/10.1021/cr4003769 | *Chem. Rev.* 2014, 114, 126−163

3.5. Light-Signal Transduction by Microbial Rhodopsins

Originally, it was believed that the photosensory functional class of microbial rhodopsins was typified by SRI and SRII, signaling via the classical two-component transduction pathway.[1,319] In the past decade, it became clear that there are several more types of sensory rhodopsins present in *Eubacteria* and lower *Eukaryota*, which employ dramatically different signaling mechanisms.[11,167,171,274] While in halobacterial SRs, primary signal transduction occurs via interaction with a membrane-embedded transducer, other novel types of signaling employ soluble transducers or fused signaling domains, or are performed via changes in membrane potential by light-gated channels (see section 3.6 on channelrhodopsins).

SRI and SRII were the third and fourth species of microbial rhodopsins found in *Halobacterium salinarum*, and their homologues have been discovered in *Eubacteria*, such as *Salinibacter*.[320−322] They function as phototactic (and photophobic) receptors controlling the cell's swimming behavior in response to changes in light intensity and color. SRI and SRII form 2:2 complexes with their cognate transducers, HtrI and HtrII (Figure 16).[274,319,323] These transducers share homology

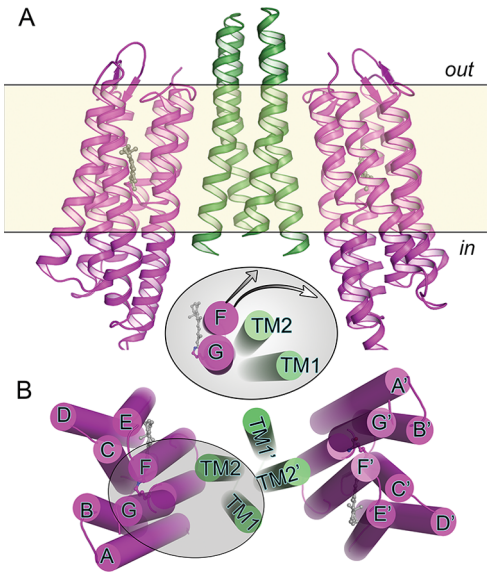

Figure 16. X-ray crystallographic structure of the transmembrane part of the *Np*SRII−*Np*HtrII complex (PDB ID: 1H2S). *Np*SRII helices are shown in purple, and *Np*HtrII helices are shown in green. (A) Side view of the complex. (B) Complex viewed from the cytoplasmic side. Inset: Illustration of the light-induced conformational changes of helix F of SRII and TM2 of HtrII. Because of the tight interaction between helix F and TM2, the outward movement of helix F in the receptor (arrow) causes a clockwise rotary motion of TM2 in the transducer.

with bacterial chemotaxis receptors, and comprise two transmembrane helices and a large cytoplasmic domain that binds to the histidine kinase CheA. CheA kinase activity is modulated by these SR−Htr complexes, culminating in control of the flagellar-motor switch. SRI and SRII exhibit no proton pumping activity in the SR−Htr complex, whereas they pump protons in the absence of transducer, suggesting their close structural relationship to BR.[324−326] Indeed, both transducer-free SRI and SRII show photocycles similar to that of BR, but with long-lived M intermediates. The conserved cytoplasmic carboxylic proton donor of proton pumps (Asp96 in BR, Supporting Information Figure 1) is replaced by aromatic amino acids in SRI and SRII. Consequently, the photocycles of SRs are long-lived, as would be expected for a sensory photoreceptor to allow time for the signal to move from receptor to transducer.

Dependent on the wavelength of stimulating light, SRI is a dual function attractant−repellent phototaxis receptor.[10,327] SRI uses an intrinsic mechanism to discriminate between colors, thus allowing the cells to be attracted by orange light or be repelled by UV light. SRI absorbs maximally at 587 nm, and absorbance of a photon at 587 nm results in the formation of the M intermediate, triggering the attractant signal. However, if the M intermediate itself is photoexcited (by near UV light), a repellent-signaling intermediate is generated. Therefore, excitation with orange light attracts cells, whereas subsequent excitation with a second photon of near-UV light repels the cells. The molecular mechanism of this dual attractant−repellent function is intriguing, and it was suggested that the direction of the behavioral response directly correlates with the state of the RSB accessibility switch (see above).[328] SRII (also called phoborhodopsin) absorbs in the midvisible range (λ_{max} = 490−500 nm) and only performs repellent signaling.

Structural studies are much more advanced for SRII than for SRI owing to the determination of crystal structures of SRII from *Natronomonas pharaonis* (*Np*SRII) for both the receptor alone and the receptor−transducer complex (Figure 16).[52,53,329] The structure of *Np*SRII is largely the same regardless of the presence of its transducer, *Np*HtrII, consistent with the lack of significant changes in color, the RSBH$^+$ pK_a, or photocycle upon transducer binding.[326,330] The M intermediate structure of the receptor−transducer complex revealed several light-induced structural alterations of both proteins, most notably, in TM2 of the transducer, which interacts with the receptor closely.[331] It should be noted that EPR studies suggest much larger conformational changes in the activated receptor than those observed in the crystal structure.[193,332,333] In particular, significant outward tilting of the cytoplasmic half of helix F was detected (Figure 16), similar to other microbial and animal rhodopsins. The mechanism of signal transduction was also extensively studied by FTIR spectroscopy, which revealed that steric interaction between the retinal chromophore and conserved Thr204 (Ala215 in BR; Supporting Information Figure 1) is a prerequisite for light-signal transduction in SRII.[334,335] The common pattern of structural changes upon the light activation of both haloarchaeal photosensors and proton pumps was elegantly demonstrated by introducing three strategically placed hydrogen-bonding residues of *Np*SRII into BR, inducing a functional interaction with *Np*HtrII.[336]

The first identified eubacterial sensory rhodopsin (ASR) was from the freshwater cyanobacterium, *Anabaena*.[11] In contrast to SRI and SRII, ASR activates a soluble transducer protein (ASRT), possibly leading to transcriptional control of several genes.[169,337] Even though ASRT was shown to interact with DNA *in vitro*, the exact mechanism of photosensory transduction is not clear, especially in view of the existence of many close homologues of ASR which do not coexist with ASRT-like transducers.[338] In addition, a direct interaction of the C-terminus of ASR with DNA has been reported, suggesting that ASR itself may function as a transcription factor as well.[339] The X-ray structure of ASR has been determined, and it reveals an unusually polar water-filled cytoplasmic half, distinct from that of BR and other proton pumps.[184] Unique to ASR, the highly conserved Asp of the RSBH$^+$ counterion (Asp212 position in

dx.doi.org/10.1021/cr4003769 | *Chem. Rev.* 2014, 114, 126−163

BR; Supporting Information Figure 1) is replaced by Pro, dramatically modifying the hydrogen-bonding pattern in the SB region.[340] One of the most unique aspects of ASR is its photochromism. Its chromophore binding site accommodates both all-*trans*- and 13-*cis*,15-*syn*-retinal in the dark, which can be interconverted by choosing an appropriate wavelength of illumination due to the difference in the spectral maxima of these two isomeric forms.[183,184,341] The working (and very preliminary) model of ASRT activation includes release of the transducer from the cytoplasmic side of the receptor during the formation of the M intermediate arising from the excitation of all-*trans*-ASR.[177,342]

Green algae, such as *Chlamydomonas*, give us another example of the versatility of sensory mechanisms in microbial rhodopsins.[167,343] In addition to channelrhodopsins (see below), the unusual histidine kinase rhodopsins (HKR) have been recently identified. HKRs are modular proteins consisting of a rhodopsin domain, a histidine kinase domain, a response regulator domain, and in some cases an effector domain such as an adenylyl or guanylyl cyclase, reminiscent of signaling by LOV (light−oxygen−voltage) domain-bearing proteins. Surprisingly, the heterologously expressed rhodopsin fragment acts as a bistable UVA receptor which can be switched by UV and blue light between 380 and 490 nm absorbing forms.[344] The chromophore of the former was found to be in the 13-*cis*,15-*anti* configuration, which is normally observed only during the photocycle of other rhodopsins. It was suggested that the photochromic HKR1 plays a role in the adaptation of behavioral responses in the presence of UVA light.

3.6. Channelrhodopsin, a Light-Gated Cation Channel

3.6.1. Basic Discoveries. The work of many scientists studying the light responses and swimming behavior of the motile microalgae *Euglena gracilis* and *Chlamydomonas reinhardtii* provided the basis for the discovery of channelrhodopsin.[345] The unicellular *Chlamydomonas* has an equatorial diameter of about 8 μm, two flagella, and a 1 μm orange eye. About 100 years ago, it was discovered that the eye senses light to modulate the flagellar beating for helical swimming of the alga.[346] In the 1950s it was found that behavioral responses depend on Mg^{2+} and Ca^{2+}.[347] Next, a correlation between Ca^{2+} influx and changes of the flagellar beat frequency was observed.[348] The function of rhodopsin as the sensory photoreceptor in microalgae was interpreted from published action spectra for phototactic movement,[349] and was further supported by the capability of retinal and retinal analogues to restore behavioral light responses in blind *Chlamydomonas* mutants.[350] Detailed retinal complementation studies revealed an all-*trans* configuration as characteristic for microbial rhodopsins, rather than the 11-*cis* configuration characteristic of the animal (visual) rhodopsins.[351,352]

Several years later, electric responses were measured from single *Chlamydomonas* cells and action spectra were recorded which led to the proposal that the photocurrents were mediated by the photoreceptor rhodopsin to control phototaxis and phobic responses.[353] On the basis of the appearance of the photoreceptor current in *Chlamydomonas reinhardtii and Volvox carteri* within 50 μs after a brief light flash, it was postulated that their photoreceptors and ion channel(s) are closely linked, forming a tight complex.[353,354] In 2001, three groups identified novel DNA sequences that encode microbial type rhodopsins in *Chlamydomonas*.[12,355−357] By *in vivo* analysis of photoreceptor electrical current and RNA interference technology in *Chlamydomonas*, two rhodopsin genes were found to mediate phototaxis.[356] The concept of a light-gated ion channel was finally demonstrated through the expression of ChR in *Xenopus* oocytes and in HEK cells by voltage clamp measurements.[12] Further experiments showed that both rhodopsin DNAs from *Chlamydomonas* directly encode light-gated ion channels, henceforth termed channel-rhodopsin-1 (ChR1) and channel-rhodopsin-2 (ChR2).[12,13] In the alga, ChR1 is more dominant than ChR2 but the amount of ChR1 strongly varies with environmental conditions,[358] whereas ChR2 is more or less constitutively expressed, albeit at a lower level. ChR2 absorbs maximally at 460 nm whereas for ChR1 the absorption shifts from 465 nm at high pH to 505 nm at low pH with a pK_a of 7.5.[359] ChR2 inactivates (reduction of the conductance) more strongly in continuous light compared to ChR1, and its selectivity for sodium is 2-fold higher than that of ChR1.

3.6.2. Transfer to Neuroscience, Birth of Optogenetics. On the basis of the ability to express light-gated ChR2 in HEK293 and BHK cells, it was also proposed for neuronal cells that expression of ChR2 might allow depolarization of the cells by illumination.[13] Several groups began to apply ChRs in neuroscience, mainly using a truncated version of ChR2, due to an expression level twice as high as the full-length protein and more than 10 times better than ChR1. With a set of seminal publications, five groups almost in parallel demonstrated the applicability of ChR in hippocampal neurons, PC12 cells, the spine of living chicken embryos, mouse brain slices, the retina of blind mice and transgenic *C. elegans*.[360−364] These publications marked the genesis of what we term today, optogenetics. In optogenetics, researchers target well-defined neuronal cell subpopulations by using cell-specific promoters to express light-activatable proteins and thus are able to selectively activate or silence (depolarize or hyperpolarize) cells through the application of short light pulses. Most surprisingly, the mammalian brain contains sufficient retinoid levels to allow wild-type ChR2 to function without addition of exogenous retinal. The affinity of the apoprotein for retinal is in the nanomolar range but varies widely in ChR isotypes and mutants, partially explaining why some variants work better than others in neurons, even though expression and membrane targeting is equivalent.[365] More recently, channelrhodopsins from algal species other than *Chlamydomonas*, most notably, from *Volvox*, have been similarly adopted for use in optogenetics.[170,366,367]

3.6.3. Channelrhodopsin Architecture. ChRs are microbial rhodopsins with long C-terminal extensions. These extensions, unusual for a rhodopsin, appear to be important for targeting the channel to the algal eyespot overlaying part of the plasma membrane but are not required for ion channel function. Despite remarkable achievements in protein engineering, a mechanistic understanding of activation and ion transport in channelrhodopsins has been hampered due to a lack of accurate structural data. Although ChR1 is the dominant photoreceptor in the alga, our knowledge about ChR1 and its relatives in other algae is scarce since the heterologous expression in host cells is difficult.[356,359] ChR2 expresses reasonably well in mammalian COS-1 and HEK293 cells as well as in the yeast *Pichia pastoris*, allowing purification and spectroscopic characterization.[368−370]

Recently, two new structural models have been proposed independently, in addition to the earlier model built using low-resolution electron crystallography data.[371] The first one was based on a 2.3 Å X-ray crystal structure (PDB ID: 3UG9),

dx.doi.org/10.1021/cr4003769 | *Chem. Rev.* 2014, 114, 126−163

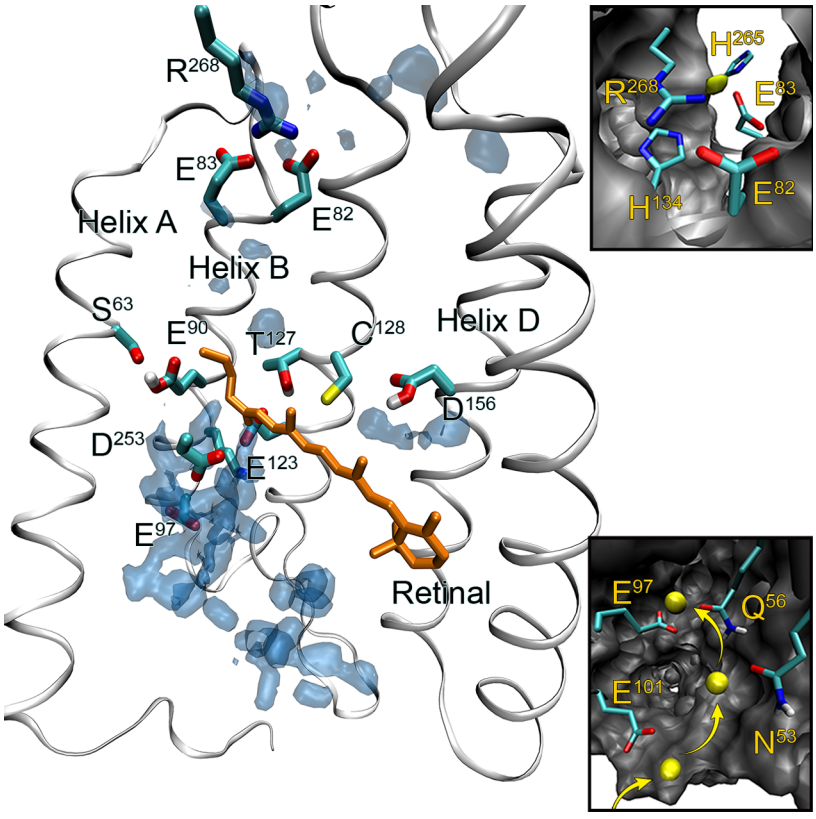

Figure 17. Structural model of ChR2 based on the C1C2 chimera crystal structure as derived from extensive MD simulations.[376] Shown are the relevant amino acids as discussed in the text and the calculated water (blue) and sodium ion (yellow) distributions averaged over the course of MD simulations. Insets: cation binding site (top) and cation uptake pathway observed in MD simulations with sodium trajectory (bottom). Cytoplasmic side of ChR2 is facing up.

which revealed the dark state of C1C2, a ChR1/ChR2 chimera variant mainly consisting of ChR1 with the last two helices derived from ChR2.[51] The C1C2 hybrid[372] (also termed ChrGR[373] and ChEF[374] in the literature) has not been well-characterized spectroscopically, but as judged from electrical studies its properties are close to those of ChR1. The other model was built for ChR2 using homology modeling on the ASR template, global sampling with classical force-field MD simulations, and structural refinement by combined QM/MM methods.[375] These models agree in many aspects such as orientations of common charged residues, hydrogen-bonding patterns, and the active site. From the seven TM helices, helices C−G of ChR1 and ChR2 have sufficient homology to other microbial rhodopsins (Supporting Information Figure 1) so that a homology model is readily built; however, ambiguities in the model arise from helices A and B which both contain a large number of unique charged residues, unlike BR or ASR.

Figure 17 shows the structure of ChR2 as derived from homology modeling based on the C1C2 crystal structure.[376] The model was embedded into the membrane and aqueous solution including sodium and chloride ions. The computational model displays a larger water density in the protein core compared to the crystal structure, probably because many of these waters are highly mobile and may not contribute to a defined electron density in the X-ray structure. The water is mainly distributed along helix B, where a large number of charged amino acids are lined up, and a continuous water distribution can also be observed at the cytoplasmic side, stabilized by a cluster of hydrophilic residues consisting of Glu82, Glu83, His134, His265, and Arg268. The two continuous water densities are separated by the residues Ser63 and Glu90, which are highly conserved among the ChRs, and may define constriction sites as discussed previously.[51] Glu90 deprotonates during the photocycle; however, the functional importance and exact timing of this event in the photocycle is controversial.[377,378]

The active site in ChR2 is defined by Glu123 (Asp85 in BR) and Asp253 (Asp212 in BR). The hydrogen-bonded network as observed in the C1C2 crystal structure differs from that of BR, with fewer water molecules and a direct salt-bridge between retinal and the counterion (Figure 17). Classical MD simulations predict water molecules entering the active site. In the case of the ChR2 dark-adapted state, this could lead to the formation of a hydrogen-bonding network similar to the pentagonal cluster found in BR, since the ultrafast reaction dynamics after photoexcitation is similar for these proteins,[379] but with faster energy transfer from retinal to protein and water molecules in ChR2.[139] However, due to imperfections in present classical force field methods,[375,376,380] the precise active site water arrangement could not be determined until now. In the C1C2 X-ray structure, Asp253 (ChR2 numbering) is in close proximity with the $RSBH^+$ compared to Glu123, and the electrical studies on various ChR2 mutants revealed that Glu123 (but not Asp253) is dispensable for function.[51,381] This suggests that either Asp253 is the preferred primary proton acceptor or it takes over this function in the absence of Glu123. Interestingly, Glu123 serves as the voltage sensor that regulates the photocycle speed at different membrane voltages,[382] as replacement of Glu123 with Gln, Thr, or Ala completely eliminates the voltage sensitivity of the reaction cycle thus

dx.doi.org/10.1021/cr4003769 | Chem. Rev. 2014, 114, 126−163

allowing ultrafast action potential firing when expressed in neurons.[382]

3.6.4. Channel Function, Gating, and Selectivity. Electrical studies in combination with structural data identified two gates as key elements of the channel, the central gate defined by Ser63, Glu90, Asn258, and, second, the inner gate built by Glu82, Glu83, His134, and His265. Density attributed to a sodium ion has been found by computer modeling in a cavity defined by these residues (Figure 17, inset). Conformational changes open both gates and mediate pore formation and ion conductance, but our knowledge of the conducting state is still vague since the structural information about the conducting state(s) is lacking. The key residue of the central gate, Glu90, is in close proximity to the $RSBH^+$, but the mechanistic rationale for this connection is unclear. Both the central gate and inner gate serve as selectivity filters, and mutagenesis of the participating residues changes the selectivity quite substantially. For example, both H134R (inner gate) and E90Q mutants (central gate) conduct more Na^+ than the wild-type and give larger currents, especially under alkaline conditions.[374,383] The two gates are the objectives of intensive research in expectation that modification of the gates will reveal novel and useful ChR properties. Despite the large volume of extant electrophysiological data, in the future, X-ray crystallography, NMR, theoretical modeling, and time-resolved vibrational spectroscopy must be employed to fully understand the gating process.

The ultrafast retinal isomerization, similar to other rhodopsins, activates the protein and leads, ~1 ms later, to an opening of the ion pore. The structural rearrangement of the chromophore is expected to be very minor, but the NH^+ dipole of the RSB is switched upon isomerization, leading to a rearrangement of the H-bond network surrounding the RSB. The induced rearrangement of the protein structure is a multistep process, and at present, only a few intermediate states can be identified as defined by their optical spectra. The on-kinetics of the photocurrents (on-gating) are defined by this sequence of reactions. So far, two early reaction intermediates, P500 and P380 (corresponding to the L and M states of bacteriorhodopsin), have been assigned, preceding the conducting state P520 which relates to the N state of BR (Figure 18).[368,369,379] The structural changes involved in the opening are reversed for a closure of the conducting pore, completing the photocycle by leading back to the dark state. Opening and closure of the ion pore follow different reaction pathways because the kinetics of channel opening and dark state recovery differ by many orders of magnitudes. By electron paramagnetic resonance spectroscopy, a light-induced movement of helix B was identified as an important step in this process.[384,385] Strictly speaking, the ion selectivity of the channel immediately after the onset of illumination and under steady-state conditions differs significantly suggesting the existence of two conducting states, O1 and O2. These states are populated differently depending on the light intensity, wavelength, and duration. At the moment there are no spectroscopic criteria available to discriminate O1 from O2, and they are both subsumed under the photocyle intermediate P520 in Figure 18.

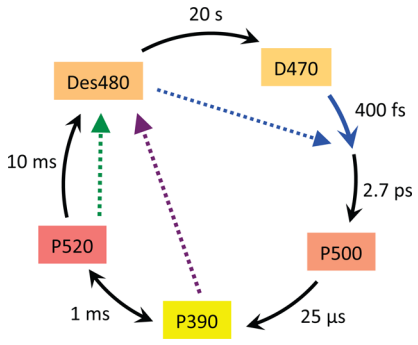

Figure 18. Simplified scheme of the ChR2 photocycle with D470 as dark-adapted state and P520 as conducting state based on data from refs 369, 370, 379, 386. It is worth noting that during bright continuous illumination or repetitive flashing the photocycle is fed by photoconversion of the late photocycle intermediate Des480, the so-called desensitized or light-adapted state (blue dotted arrow). Green and UV light photoconverts the conducting state P520 and the early state P390, respectively, back to the light-adapted state (green and purple dotted arrows).

The residues Cys128 and Asp156, which are in contact with each other via a water molecule (Figure 17),[51,376] play a fundamental role in on- and off-gating as evidenced by the fact that mutation of either Cys128 or Asp156 causes a dramatic slowdown of reaction kinetics and results in a great increase of the lifetime of the open state(s).[386,387] Illumination of the open state (P520) with longer wavelength light results in photochemical conversion back to the dark state and closes the channel. Since these ChR variants are bimodal and switchable with light they were named "Step Function Rhodopsins" or simply SFRs.[386−388] Asp156 deprotonates during the photocycle with kinetics that closely correlate with the reprotonation of the RSB nitrogen suggesting that this Asp156 is the proton donor.[378] Cys128 is hydrogen-bonded via Thr127 to the side chain of the active site residue Glu123, a feature that has been considered to be crucial for the structural changes occurring during the photocycle. Simulations suggest that this hydrogen bond in the dark state switches to a backbone oxygen of Glu123 (intrahelical hydrogen bond) after its protonation.[376] This finding suggests a mechanism where the protonation change of Glu123 is propagated via Thr127 to Cys128 and Asp156, which change conformations accordingly. This event is believed to cause breakage of the water-mediated hydrogen bond between them, the central event for channel opening according to spectroscopic measurements.[389−391] However, this model is challenged by the fact that Glu123 is dispensable for ChR2 activation,[382,392] and in E123T or E123A mutants Asp253 functions as the negative $RSBH^+$ counterion. Certainly, additional residues are involved in the activation process.[375,393]

During the lifetime of the light-induced conducting state, P520, up to 100 ions are conducted in wild-type ChR2 with a unitary conductance of 40−100 fs.[374,394,395] Ions approach the inner gate via the access channel that is mainly defined by the charged residues of helix B (Figure 17). The individual mutations of up to three glutamates on helix B (Glu101, Glu97, and Glu90) reduced the cation conductance gradually, but did not abolish transport completely.[383,396−398] MD simulations predict the access channel entrance to be defined by Asn53, Gln56, Glu97, and Glu101, due to the high ion density found in this region.[376]

3.6.5. Perspectives for Optogenetics Development. The hopes for future applications of optogenetics are high, but ChR is not the optogenetic prodigy as some advertise it, as it shows clear limitations for optogenetic use: (i) Nature employs ChR for gradual membrane depolarization, resulting in small conductance and not in the all or none responses required for efficient optogenetic use. (ii) Molecular engineering may lead

dx.doi.org/10.1021/cr4003769 | Chem. Rev. 2014, 114, 126−163

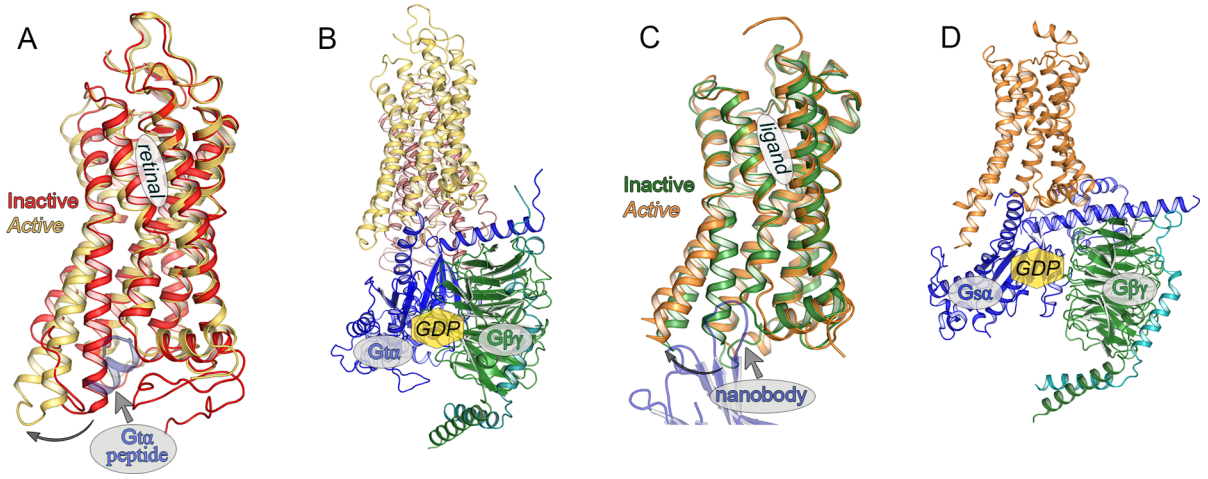

Figure 19. Global changes in the structure of rhodopsin and other GPCRs upon attainment of the active state. (A) Structural superposition of inactive and active G-protein-interacting state of bovine Rho reveals structural rearrangement of TM5 and TM6 to accommodate binding of the C-terminus of the α-subunit of transducin (Gt_α peptide, shown in gray). Inactive rhodopsin (dark state; PDB ID: 1U19) is denoted in red, and active rhodopsin (Meta II; PDB ID: 3PQR) is denoted in yellow. (B) Model of the complex between a rhodopsin dimer and transducin built into electron microscopy map derived from native source purified bovine rhodopsin/transducin complex. GDP/GTP binding site is denoted by a yellow hexagon in parts B and D although both structures are solved in the nucleotide-free state. (C) Structural superposition of antagonist bound (inactive state, denoted in green) and agonist bound (active state, denoted in orange) β_2-adrenergic receptors (β_2AR). Structural displacement of TM5 and TM6 is similar to that seen in the comparison shown in part A. A nanobody (shown in gray) was utilized to stabilize the agonist bound state, and a nanobody loop protrudes into a similar position as seen for the Gt_α peptide which stabilizes the Meta II state in part A. A T4 lysozyme (T4L) domain used to facilitate crystallization is not shown for clarity. The antagonist bound structure is the carazolol bound β_2AR-T4L fusion (PDB ID: 2RH1), and the agonist bound structure is the nanobody stabilized, BI-167107 high affinity agonist bound structure (PDB ID: 3POG). (D) Crystal structure of an agonist bound β_2AR-T4L fusion (T4L not shown) in complex with its cognate heterotrimeric G protein, $Gs_{\alpha\beta\gamma}$, and a stabilizing nanobody (not shown) reveals the mode of Gs binding to monomeric β_2AR (PDB ID: 3SN6). In this complex, the Gs_α C-terminus also binds in the cleft formed by the outward movement of TM5 and TM6. All representations are in approximately the same orientations, and all superpositions were performed with TM1 to TM4, TM7, and cytoplasmic helix H8 to accurately portray the differences in the positions of TM5 and TM6.

to wider pores (and thus greater depolarization), but only at the risk of destabilization and thermal activation in the dark. (iii) Although the ion selectivity can be changed toward higher or even exclusive H^+ conductance (as, e.g., found naturally for ChR of the halotolerant alga *Dunaliella salina*)[170] or tuned toward higher selectivity for monovalent or divalent cations, it will be an enormous challenge to reach the high selectivity ratio for K^+ over Na^+ necessary for light-controlled hyperpolarization of host cells. (iv) The upper limit for possible shift of the absorption maximum will be reached at approximately 630 nm due to an increase of thermal activation with longer wavelengths.[399]

Nevertheless, engineering of ChR and other microbial rhodopsins will continue and the ongoing sequencing of hundreds of algal genomes will provide countless new ChR variants with more advantageous characteristics.[400] Furthermore, development of improved techniques to target ChRs to organelles and specific membrane subareas, to make ChR bimodally switchable, to control expression more accurately, and to guarantee a better turnover of the protein when used as retinal prostheses in bright light vision will continue. Several ChRs with blue- and red-shifted absorption were described recently and await further characterization.[366,401,402] A set of ChRs that covers a spectral range similar to that of rhodopsins of animal eyes is within reach. Also, ChRs will be further optimized for two-photon microscopy.[403] Nevertheless, ChRs are basically analytical tools and will only be used for treatment of diseases in patients in a few very special cases, such as deep brain stimulation or retinal prosthesis.[404−406]

From our perspective, the greatest potential for optogenetic application lies unexploited in a smart combination of light-gated channels or light-driven pumps with endogenous channels of host cells in the sense that both primary outward or inward directed transport of Ca^{2+} or H^+ can be used to activate Ca^{2+}- or H^+-sensitive endogenous channels of high selectivity and high conductance (two-component optogenetics). The question will be how to connect these two units to ensure that the on-gating of the endogenous channel is fast enough for the specific needs. Such constructs will move the field a great step forward. Similarly, gene-fusion strategies for combining excitatory ChR2 and various inhibitory ion pumps or bovine Rho and a G protein-activated potassium channel have been explored.[407,408]

4. ANIMAL RHODOPSINS

4.1. Animal Rhodopsins are Prototypical GPCRs

In the previous sections we have seen how microbial (or type I) rhodopsins are employed in microorganisms in light-dependent functions as ion pumps, channels, and sensors. Animals employ in their eyes and other organs a different type of rhodopsin, which was optimized during evolution to perform a variety of roles pertaining to vision, sensation of light for nonvisual reasons (e.g., circadian rhythms, sensing dawn/dusk, determining the horizon, pupillary constriction, body color change, and seasonal reproduction), and direct utilization for the isomerization of retinal.[3,4,409−412] These animal (or type II) rhodopsins are GPCRs which are activated by light to catalyze GDP → GTP nucleotide exchange in heterotrimeric G proteins. Opsins belong to the largest GPCR family (the family of rhodopsin-like GPCRs with ~700 members in humans)[413] and can be roughly subdivided into ciliary and rhabdomeric opsins, which are further diversified by their G

dx.doi.org/10.1021/cr4003769 | *Chem. Rev.* 2014, 114, 126−163

protein subtypes, and photoisomerases.[3,410,414] Typically, expression of the ciliary rhodopsins occurs in vertebrate ciliary photoreceptor cells with cyclic nucleotide signaling cascades or in invertebrate rhabdomeric photoreceptor cells with phosphoinositol signaling cascade. However, this is a simplified view, as ciliary and rhabdomeric opsins are present in both vertebrates and invertebrates, and expression is also known for other cell types, such as intrinsically photosensitive retinal ganglion cells and human epidermal melanocytes.[3,4,409,414−416]

Although the 7TM architecture appears at first glance to be similar for microbial and animal rhodopsins (Figures 1 and 4), the primary and tertiary structures of microbial and animal rhodopsins differ largely.[252,413,417−419] As GPCRs, animal rhodopsins feature kinked TM helices, a strongly tilted TM3, longer cytoplasmic loops connecting TMs, a cytoplasmic helix 8 (H8) with palmitoylated Cys residue at its end, a disulfide bridge linking TM3 with the extracellular loop 2 connecting TM4 and TM5, as revealed by the crystal structures of bovine Rho,[46,420,421] and squid rhodopsin (Figures 19 and 20 and Supporting Information Figure 4).[422,423] Unique to rhodopsin is a compact extracellular domain that is formed by the N-terminus and extracellular loops connecting TMs, with a β-sheet in extracellular loop 2 forming a plug to cover the hydrophobic retinal and the RSB. This "retinal plug" occludes the chromophore-binding site,[424,425] whereas retinal binds in microbial rhodopsins closer to the center of the protein such that a plug is not needed (cf. Figures 1 and 4). Due to limited data, it is not clear whether microbial rhodopsins and animal rhodopsins (as GPCRs) have a common ancestry or acquired their photosensitivity and topology independently. Although the sequence similarity between microbial and animal rhodopsins is low, they share in TM7 a specific Lys residue for retinal attachment, and in TM6 they share homology for two aromatic residues that serve to interact with the retinal (Trp265 and Tyr268 in bovine Rho). It has therefore been proposed that animal rhodopsins may have developed via exon shuffling caused by recombination of microbial rhodopsins and GPCRs. Exons for TM6 and 7 would have been provided by microbial rhodopsins and for TM1−5 by GPCRs.[415]

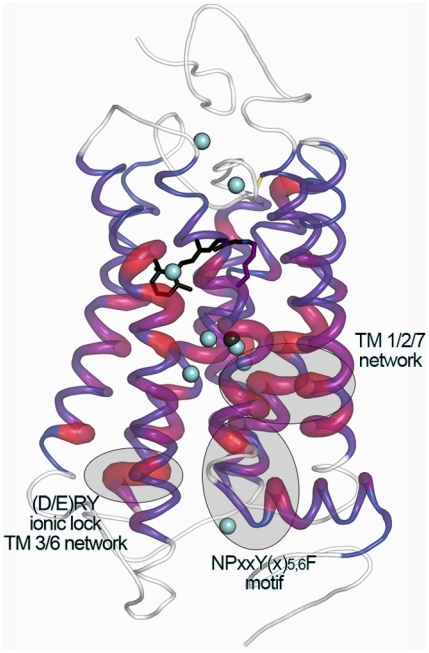

Figure 20. Sequence and motif conservation in GPCRs extends to ordered bound water molecules. Sequence conservation among rhodopsin-like (class A) GPCR sequences was mapped onto the backbone of rhodopsin as reported in ref 463; greater "tube" thickness and ramping from blue to red indicate greater residue conservation at that position. Because of considerably lower sequence conservation outside of the TM region, these regions were not included in the analysis and are denoted in white. Structural superposition of all antagonist bound structures of GPCRs with a resolution 2.7 Å or higher reveals a subset of ordered water molecules that are found within the transmembrane bundle (shown in light blue). As indicated by the color and thickness of the cartoon representation, these waters are found in close proximity to positions within the TM region that have high homology throughout all class A GPCRs. Water molecules shared among four or more different receptor structures are shown here. In addition, density best represented by a bound octahedrally coordinated sodium ion has been found within the TM bundle of A_{2A}-adenosine and PAR1 receptor structures (PDB ID: 4EIY, 3VW7; shown as a black sphere) in a similar position to a water observed in the bovine Rho structure (PDB ID: 1U19). Three motifs important for GPCR activation are denoted by shaded ovals.

The GPCR 7TM scaffold allows animal rhodopsins to undergo conformational changes upon activation by light which are larger than the light-induced changes in microbial rhodopsins. Key for G protein coupling to active rhodopsin is a 2−3 Å motion of TM5 and a 6−7 Å motion of TM6 which open up the cytoplasmic surface for G protein binding and catalysis of GDP/GTP exchange in the G protein.[426] A summary of the current knowledge of the structural basis of GPCR/G protein coupling is shown in Figure 19. Movement of TM5 and TM6 was shown first in the crystal structure of bovine opsin, the apoprotein of Rho.[427,428] This crystal structure is consistent with TM movements upon transition from the resting state to the active receptor state as concluded from electron paramagnetic resonance (EPR) spectroscopy[429,430] and biochemical cross-linking experiments.[430,431] On the basis of these results, it was proposed that the opsin conformation (Ops*) observed in these crystals and subsequent crystallographic studies of opsin bound to G-protein-derived peptides was analogous to that of the active state.[428,432] Indeed, the protein backbone conformation found in the opsin crystal is almost perfectly superposable with the structure of the active Meta II photoproduct (Figure 19A),[426] as well as with the structures of constitutively active rhodopsin mutants.[433−435]

The presence of a G-protein-interacting conformation in Ops* or Meta II structures was established by cocrystallization experiments with synthetic peptides representing one of the key interaction sites on rhodopsin's cognate heterotrimeric G protein, transducin (Gt).[426,428,433] Similar to these peptides derived from the distal C-terminus of the Gt_α-subunit, suitable nanobodies can stabilize the active conformation of GPCRs as was demonstrated for the human β_2-adrenergic receptor (β_2AR) in an active agonist-bound form, crystallized in complex with a nanobody binding in the cytoplasmic cleft opened for the G protein (Figure 19C).[436,437] In the subsequently solved crystal structure of the nucleotide-free complex between the β_2AR and the G protein Gs, the binding mode for the Gs_α C-terminus was revealed to be similar to that of the Gt_α-derived peptide bound to Meta II.[438] The β_2AR−Gs complex structure provided important insight into the interface and the relative orientation of the receptor and G protein and confirmed the role of the G_α C-terminal helix in coupling the G_α nucleotide binding site to the GPCR. GPCR-catalyzed nucleotide exchange in heterotrimeric G proteins is a complex multistep

dx.doi.org/10.1021/cr4003769 | Chem. Rev. 2014, 114, 126−163

process which is not fully understood yet; the reader is referred to the literature for greater detail.[438−441] For the Rho/Gt pair, a high-resolution structure of the nucleotide-free complex remains elusive, but a model similar to the β_2AR-Gs complex was built into the 3-D envelope calculated from single particle analysis of negative-stained electron microscopy images of bovine Rho−Gt complexes purified directly from native source (Figure 19B).[442] The proposed Rho−Gt complex model, however, differs from the β_2AR−Gs complex crystal structure by comprising one G protein and two Rho molecules, with one protomer interacting with the active Rho* conformation, although binding to Gt occurs in a similar orientation.[442−444] Dimerization of rhodopsin and opsin as well as of other GPCRs (for review see ref 445) can occur and affect receptor function and signaling allosterically.[446−448]

Animal rhodopsins thus can be seen as both prototypic and highly specialized GPCRs which differ from diffusible ligand-activated GPCRs by their unique photoactivation mechanism. On one hand, the GPCR 7TM scaffold of animal rhodopsins has been optimized by evolution, for fast and selective retinal isomerization with the high quantum yield (section 2) necessary for fast millisecond time scale receptor activation. Also, on the other hand, visual rhodopsins couple to specific G proteins, transducins, specific to rod or cone cells, which were co-optimized for high fidelity and fast nucleotide exchange. For bovine Rho in native membranes, a nucleotide exchange rate of several hundred Gt turnovers per single light-activated rhodopsin molecule has been determined.[449] This value is much higher than that computed for other G protein signaling systems.[450] It is likely related to the fact that vertebrate photoreceptor cells are responsive to a large range of photons, spanning 8 orders of magnitude,[451] starting from single photons, where fast nucleotide exchange is mandatory for sufficient signal amplification. Due to the common architecture found for all GPCR structures determined to date and common gross conformational changes observed in bovine Rho and other GPCR structures upon activation,[452] knowledge of the activation steps in Rho's photochemical core and signal propagation from the retinal binding site to the G protein coupling cytoplasmic surface is likely to be directly applicable to understanding of the activation of other GPCRs.

4.2. Bovine Visual Rhodopsin as a Model System

A wealth of information on the structure and function of rhodopsin has been gained from the bovine visual signal transduction system.[2] Rhodopsin is the most abundant membrane protein in the outer segment of retinal rod photoreceptor cells. Because of the high sensititvity of these photoreceptors, single photons are sufficient to couple retinal *cis* → *trans* isomerization via rhodopsin conformational changes and GDP−GTP exchange catalysis to Gt activation. Activated (GTP-bound) Gt further amplifies the signal via activation of a cGMP-specific phosphodiesterase and the resulting closure of cGMP-gated cation channels in the plasma membrane to generate an electrical signal (see, e.g., ref 453). Visual signal transduction in rod cells has been studied extensively by biochemical and biophysical means, because of the relative ease of obtaining pure preparations of protein from bovine eye tissue. This enabled bovine rhodopsin to be the first GPCR to be conventionally sequenced[454,455] and cloned.[456] Its sequence homology to the β_2AR was observed in 1986,[457] making rhodopsin the eponym of the largest class of GPCRs which comprises much of the ~800 GPCRs in the human genome.[413] Rhodopsin was also chosen for the first chemical synthesis of a eukaryotic GPCR gene for expression in mammalian cells allowing extensive structure/function studies.[458−461]

A milestone in both rhodopsin and GPCR research was the elucidation of the crystal structure of bovine rhodopsin by Palczewski and colleagues in 2000.[421] This first GPCR structure served and continues to serve as a framework to interpret much of the biochemical and biophysical studies on GPCRs. The structure also revealed constraints which stabilize the inactive dark state of rhodopsin. Among these constraints are hydrogen-bonding networks involving the RSB region and conserved residues in the cytoplasmic part of TMs (Figures 20 and 25, and Supporting Information Figure 4). Comparison of inactive and active Rho and GPCR structures indicate general functional roles for microdomains comprising residues of motifs conserved among rhodopsin-like GPCRs (Figure 25). The TM3/6 network comprises four residues with a central salt bridge between Arg135 of the (D/E)RY motif in TM3 and Glu247 on TM6 known as the "ionic lock", and was initially proposed for the β_2AR as a feature that stabilized the inactive receptor conformation.[462] The NPxxY(x)$_{5,6}$F motif constrains the end of TM7 with H8 by electrostatic interaction between

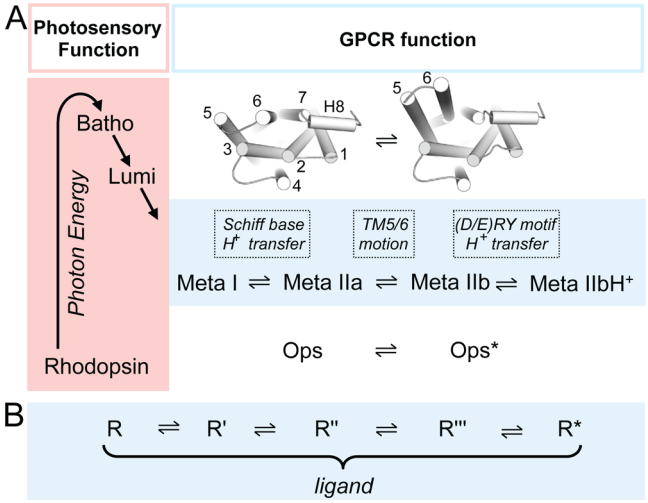

Figure 21. Activation states of rhodopsin and GPCRs. (A) In the photochemical core process, photon energy is used to convert the inverse agonist 11-*cis*-retinal into the full agonist all-*trans*-retinal. Energy stored in the initially twisted all-*trans*-retinylidene-Lys296 chromophore is gradually released via local protein (side chain) conformational changes in the Batho and Lumi photoproducts. Conformational changes in more distant parts of the protein begin within microseconds of when Meta I forms, the first intermediate of several Meta states in equilibrium, which as GPCR funtional states interact with G protein, GRK1 (rhodopsin kinase), and arrestin. Deprotonation of the RSBH$^+$ and protonation of its counterion Glu113 lead to the formation of Meta II substates which develop sequentially. The largest conformational changes (inset and Figure 19A) are observed in the transition from Meta IIa to Meta IIb; the latter intermediate is further stabilized by proton uptake to Glu134 of the (D/E)RY motif at the cytoplasmic end of TM3. The retinal-free apoprotein opsin exists also in an equilibrium between inactive (rhodopsin-like) and active (Meta-II-like) conformations,[426,427,530] termed Ops and Ops*. (B) Diffusible ligand activated GPCRs similarly exist in equilibrium between inactive and active conformations in which similar activating conformational changes as in the Meta states are thought to occur.[503] Ligand binding shifts the equilibrium toward ligand type specific energetic states.[567,568]

dx.doi.org/10.1021/cr4003769 | *Chem. Rev.* 2014, 114, 126−163

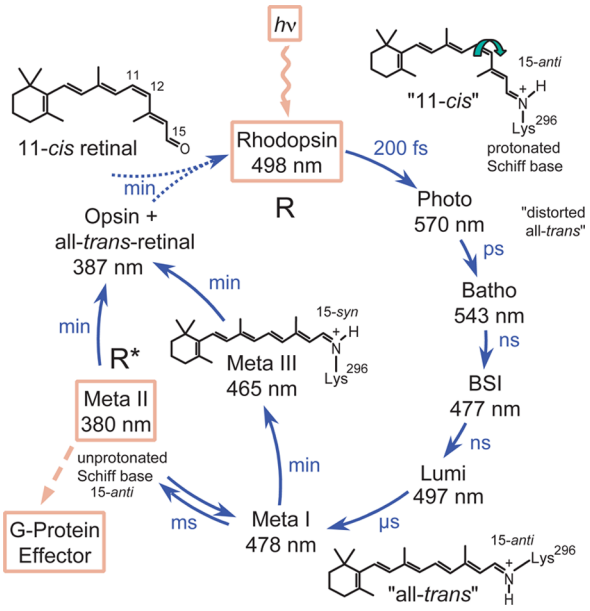

Figure 22. Spectroscopically detected intermediates of photoactivated bovine rhodopsin. Photoisomerization of the retinal 11-*cis* double bond leads within femtoseconds to photorhodopsin with a highly distorted 11-*trans* bond. Via thermal relaxation, several intermediates form with distinct λ_{max} values, distinguishable by low-temperature or time-resolved spectroscopy.[476,569] Gradual release of the strain in the chromophore leads through Batho and Lumi to Meta I, as seen by the different absorption maxima that arise from changes in chromophore/protein interaction. A transient blue-shifted intermediate (BSI) cannot be trapped at low temperatures. Time-resolved UV−vis measurements revealed the existence of additional transient forms of Lumi (Lumi II),[570,571] and Meta I (Meta I_{380};[572,573] Meta Ib).[574] The $RSBH^+$ remains protonated up through Meta I, probably due to the low pK_a of the stabilizing counterion Glu113. Larger protein conformational changes lead to Meta II (comprising substates Meta IIa and Meta IIb) which is in equilibrium with its predecessor Meta I. Meta II is the agonist-bound active receptor state capable of catalyzing GDP/GTP nucleotide exchange in the G protein transducin. Meta II is characterized by a deprotonated RSB resulting in a large blue-shifted value for λ_{max} (380 nm). As a result of RSB hydrolysis Meta II decays to the apoprotein opsin and all-*trans*-retinal. Meta I can also form Meta III, involving thermal isomerization of the $RSBH^+$ (λ_{max} = 465 nm) from all-*trans*,15-*anti* to all-*trans*,15-*syn*. Meta III decays to opsin and all-*trans*-retinal, but can also be photoconverted to Meta I and Meta II.[575] Unlike in invertebrates, bovine rhodopsin cannot be regenerated *in situ* by reisomerization of retinal with a second photon. All-*trans*-retinal is reduced to retinol by retinol dehydrogenase and transported out of the photoreceptor cell to adjacent retinal pigment epithelial cells, where 11-*cis*-retinal is regenerated (for details, see ref 551). Adapted with permission from ref 576. Copyright 2002 John Wiley & Sons, Inc.

aromatic rings of Tyr306 on TM7 and Phe313 on H8. Asn302 of the $NPxxY(x)_{5,6}F$ motif is linked to the most conserved residues on TM1 (Asn55) and TM2 (Asp83) forming the TM1/2/7 network. The model of rhodopsin in Figure 20 also reflects results from GPCR sequence analyses,[463] with the ribbon thickness coding for amino acid conservation, and results from GPCR structure analyses, where structurally bound waters are observed in "homologous" positions. This homology of water positions couples to the high degree of conservation seen in residues interacting with these waters, suggesting a functional role for water in the activation process.[464,465]

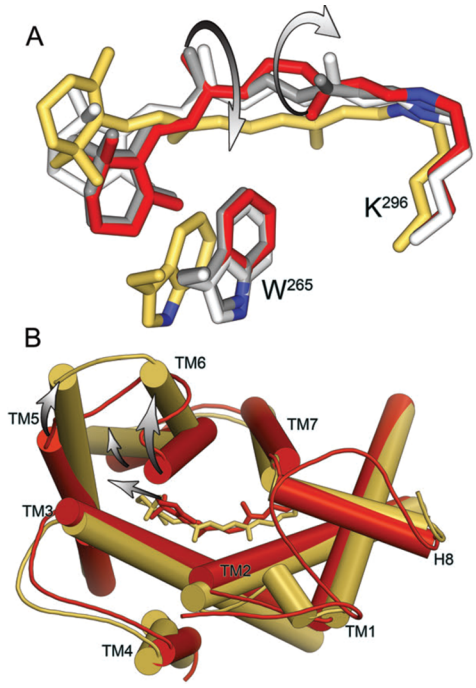

Figure 23. Isomerization, elongation, and rotation of retinal upon light activation of rhodopsin. (A) Superposition of retinal and the Lys296 and Trp265 side chains in bovine Rho (11-*cis*-retinal, PDB ID: 1U19, red sticks), Batho (twisted all-*trans*-retinal, PDB ID: 2G87, gray sticks), Lumi (partially relaxed all-*trans*-retinal, PDB ID: 2HPY, white sticks), and Meta II (relaxed all-*trans*-retinal, PDB ID: 3PXO, yellow sticks) structures. Note that from Lumi to Meta II retinal undergoes a large rotation along its long axis. (B) Overlay of rhodopsin and Meta II structures showing differences in the positions of the TM helices. Note that retinal movement induces TM5 motion and rotational tilt of TM6.[426,435] View from cytoplasmic side.

4.2.1. Photochemical Core and GPCR Conformations in Equilibrium. Rhodopsin differs from diffusible ligand-activated GPCRs by its covalently linked retinal and photochemical core enabling photosensory function. 11-*cis*-retinal serves together with the constraints described above in highly efficient stabilization of the inactive dark state of rhodopsin. As a consequence, thermal activation of a single bovine rhodopsin molecule occurs only after 420 years on average,[466] which is a prerequisite for rhodopsin's high photosensitivity and the ability of rod photoreceptor cells to function as a single photon detector. Thermal rhodopsin activation causes discrete electrical signals in the dark (dark events) and is thought to occur from retinal isomerization.[399,467,468] The measured thermal activation barrier of 80−110 kJ/mol is lower than the barrier for light-dependent activation of bovine Rho (≥180 kJ/mol, Figure 7 and section 2).[469−471] For a value of >180 kJ/mol, thermal isomerization of a rhodopsin molecule once every 10^{10} years would be expected, implying that thermal and light-dependent processes follow different pathways. A more recent theoretical study proposed a pathway of thermal isomerization in rhodopsin with a transition state displaying the same charge-transfer character as the electronically excited state of Rho.[472] From a quantitative relation between rhodopsin's photoactivation energy and its peak absorption, λ_{max}, it was proposed that dark noise arises from thermal retinal isomerization which needs to overcome the same energy barrier as in the photoisomerization process.[399] On the basis of the slow hydrogen/deuterium exchange of Thr118 in bovine Rho, it

dx.doi.org/10.1021/cr4003769 | Chem. Rev. 2014, 114, 126−163

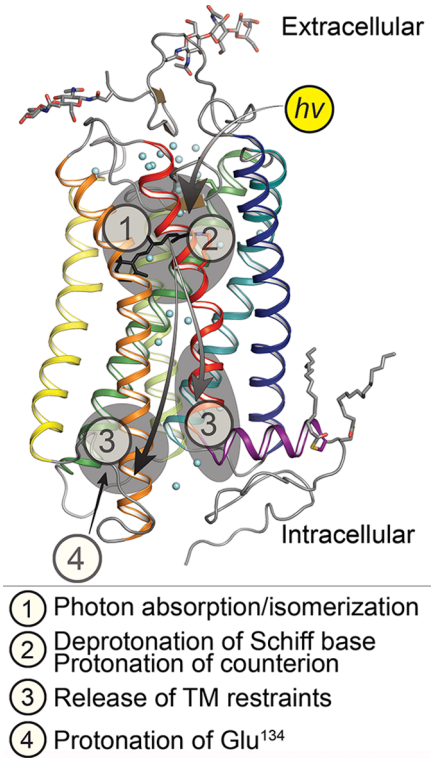

Figure 24. Conformational changes upon rhodopsin activation leading to the Meta II activated state. ① Photon absorption causes retinal *cis* → *trans* isomerization and small scale changes in structure in the immediate vicinity of the retinal, driving all subsequent activation steps. ② Deprotonation of the $RSBH^+$ along with further small-scale changes within the TM region. ③ Signal propagation to two regions almost universally conserved in class A GPCRs, the (D/E)RY and $NPxxY(x)_{5,6}F$ motifs. Changes in the (D/E)RY motif (in TM3; Glu134, Arg135, Tyr136 of bovine Rho), resulting in disruption of the "ionic lock" between Arg135 and Glu247 (on TM6), and changes in the $NPxxY(x)_{5,6}F$ region (TM7/H8) which rearranges. ④ Proton uptake from the cytoplasm onto Glu134. The TM helices are depicted in the following colors: TM1, blue; TM2, teal; TM3, green; TM4, lime green; TM5, yellow; TM6, orange; TM7, red; and H8, purple.

was suggested that local protein structural fluctuations transiently widen the retinal binding pocket for thermal retinal isomerization.[473] It is interesting to note that *Drosophila* rhodopsin also has a light-independent role in temperature discrimination in larvae which may be related to thermal retinal isomerization.[474]

To effectively release the structural constraints that stabilize the inactive rhodopsin state, photon energy is absorbed and used for retinal isomerization (cf. section 2), driving subsequent protein conformational changes. About 150 kJ/mol of the initially absorbed photon energy are stored in the "distorted" all-*trans*-retinal of the Batho photointermediate and gradually dissipated via a transient blue-shifted intermediate (BSI)[475] and the Lumi intermediate, concomitantly with a release of strain in retinal (Figures 21−23), eventually yielding Meta I after a few microseconds. The "early" photointermediates Batho and Lumi can be trapped by low temperature and have been studied structurally,[120,146] as well as spectroscopically.[476−478] The distinct absorption maxima of each intermediate reflect the gradual changes in chromophore−protein interaction. It is not until the formation of Meta I that significant backbone structural changes occur.[479,480] In Batho and to a lesser extent in Lumi intermediates, protein conformational adjustments to retinal relaxation are limited to a few amino acid side chains within the retinal binding pocket.[120,146]

When the Meta I state is attained, an equilibrium between Meta I and Meta II states develops (Figure 21), which is dependent upon pH and temperature, with lower pH and higher temperature favoring Meta II.[481,482] Deprotonation of the $RSBH^+$ upon Meta II formation results in the characteristic 100 nm blue-shift of the absorption maximum to the near UV region (λ_{max} = 380 nm).[481,483] Meta II, as defined by its 380 nm absorption, comprises both the isochromic Meta IIa and Meta IIb substates which develop sequentially from Meta I.[484] In Meta IIb, proton uptake occurs to Glu134 of the (D/E)RY motif in TM3,[485,486] explaining why low pH favors Meta II despite the loss of a proton from the $RSBH^+$.[487] Time-resolved EPR studies with bovine Rho in dodecylmaltoside detergent revealed that the large TM6 movement occurs during transition from Meta IIa to Meta IIb and led to the reaction scheme for the Meta states shown in Figure 21.[488] FTIR studies confirmed this reaction scheme for bovine Rho in its native membrane environment.[489,490] Electron crystallography on bovine Rho 2-D crystals that were illuminated and trapped in the Meta I photointermediate by the crystal lattice demonstrated that up until Meta I the protein backbone remains in a conformation similar to that of the rhodopsin dark state.[491] Illumination of 3-D bovine Rho crystals yielded the spectral shift characteristic to Meta II, but only revealed a small TM6 movement and some rearrangement of the cytoplasmic surface.[492,493] On the basis of absorption maximum and the extent of TM6 movement, the structure of this photoactivated Rho most likely represents the Meta IIa state. The Meta IIb state with fully opened cytoplasmic domain is represented in the bovine Meta II structures obtained by reconstitution of Ops* crystals with all-*trans*-retinal or by illumination of the constitutively active M257Y rhodopsin mutant before crystallization.[426,433]

Examination of agonist-bound GPCR structures reveals that GPCRs exist in conformations with differing extents of TM6 movement, with no or little TM6 movement for inverse agonists and larger TM6 movement for partial agonists and full agonists.[418] However, stabilizing mutations, truncations of loops, and in many cases insertion of T4 lysozyme or apocytochrome b_{562} fusion partners into cytoplasmic loop 3 (connecting TMs 5 and 6) or at the N-terminus have been necessary for the crystallization of all nonrhodopsin GPCRs to have their structures determined to date.[419,494,495] This affects affinity for agonist or antagonist binding and likely exerts some influence upon the degree of movement of TM6.[496−498] NMR and hydrogen/deuterium exchange studies on β_2AR lacking fusion partners provide evidence for substantial conformational heterogeneity of agonist- and inverse agonist-bound β_2-AR preparations.[499−502] The heterogeneity supports the view of conformational equilibria of GPCRs that can be shifted to either side depending on the type of ligand and are comparable to the Meta I/Meta II equilibrium of rhodopsin (Figures 21 and 22).[503,504] A difference between diffusible ligand-activated GPCRs and the activation of rhodopsin by light is reflected in the mode by which the ligand acts in the activation process. It was proposed that diffusible ligands might select the suitable conformation from the equilibrium of inactive and active GPCR conformations, whereas in an induced-fit scenario the ligand would bind an inactive conformation and induce a conformational change toward the active conformation.[503] Rhodopsin with its activation by retinal photoisomerization is

dx.doi.org/10.1021/cr4003769 | *Chem. Rev.* 2014, 114, 126−163

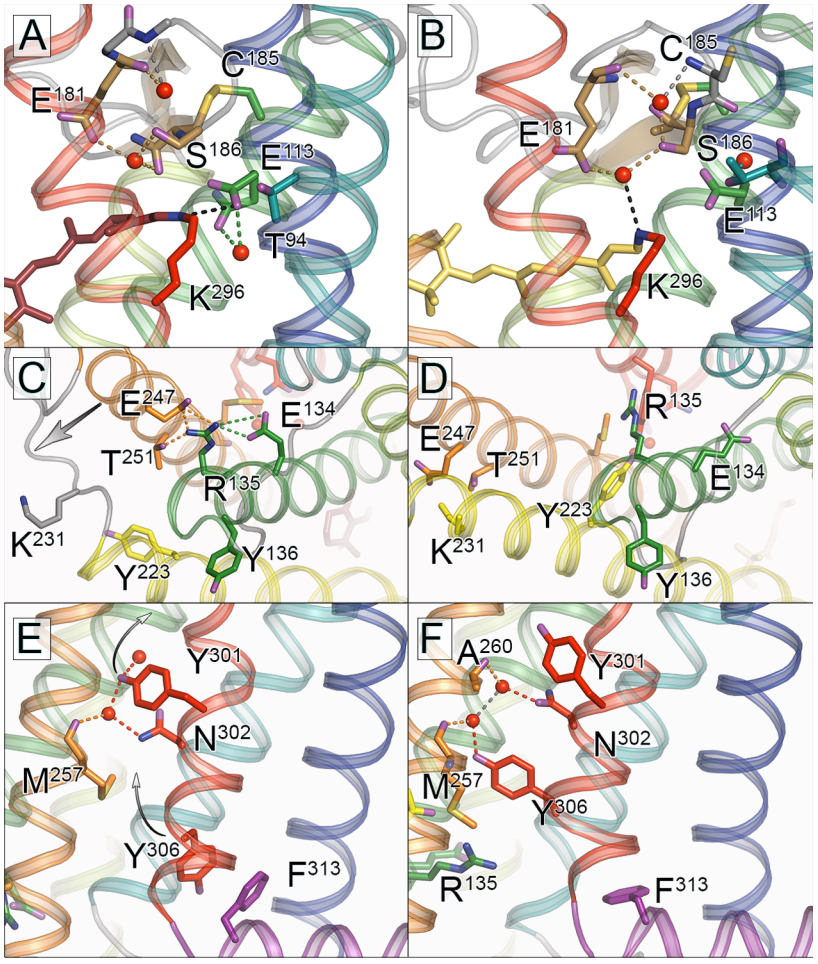

Figure 25. Structural changes in the chromophore binding site and conserved motifs that accompany bovine Rho activation. Upon light-induced activation of Rho a series of small scale structural changes result in the release of restraints enabling attainment of the fully active Meta II state. (A, B) Glu181 is found hydrogen bonded to a water molecule in both the dark state and Meta II structures, and it appears that this water functions as a noncovalently bound cofactor which moves along with Glu181 to stabilize the deprotonated RSB in Meta II. (C, D) TM3/TM6 restraints in the dark state due to the "ionic lock" formed by Arg135, Glu134, Glu247, and Thr251 are released upon Rho activation. In Meta II new interactions are formed between TM3−TM5 (Arg135−Tyr223) and TM6−TM5 (Glu247−Lys231). (E, F) Structural changes within the NPxxY(x)$_{5,6}$F motif upon activation of Rho entail a remodeling of solvent-mediated hydrogen bonding of two water molecules as well as a 180° change of rotamer for Tyr306 and a concomitant shift of the conserved Phe313 residue. For ease of interpretation, helices are depicted in the following colors: TM1, blue; TM2, teal; TM3, green; TM4, lime green; TM5, yellow; TM6, orange; TM7, red; and H8, purple. For all comparisons, PDB ID: 1U19 was used for dark state and PDB ID: 3PQR was used for Meta II state.

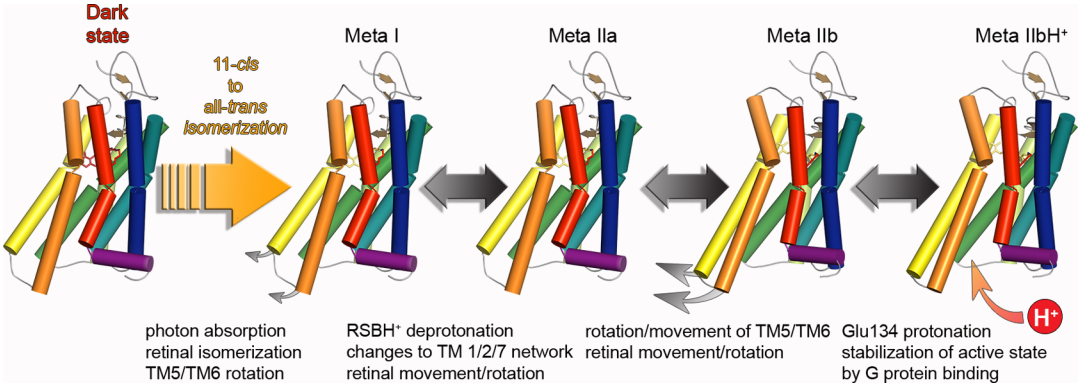

Figure 26. Structural and functional changes in the activation pathway of bovine Rho based on structural and complementary biophysical data discussed in the text and ref 490 and described in Figures 23 and 24.

likely to correspond to an induced-fit scenario for initial events, whereas both scenarios are conceivable for later activation phases as well as for GPCRs activated by diffusible ligands.

4.2.2. Rhodopsin Activation. The steps involved in rhodopsin activation are illustrated in Figures 24−26. In the rhodopsin dark state, 11-*cis*-retinal is tightly bound as an inverse

dx.doi.org/10.1021/cr4003769 | *Chem. Rev.* 2014, 114, 126−163

agonist in its binding pocket and covalently fixed by the $RSBH^+$ to Lys296 on TM7. The positively charged $RSBH^+$ is stabilized by a complex counterion comprising negatively charged residues Glu113 on TM3 and Glu181 on extracellular loop 2,[505,506] with the former functioning as the primary counterion (Figure 25A). The β-ionone ring at the other end of the retinal is ensconced in a hydrophobic pocket formed by aromatic side chains, and the conjugated double-bond system linking the two is tightly engaged by a constriction in the retinal binding site which forces a negative 6-s-*cis* twist of the β-ionone ring about the C6—C7 single bond and a twist about the C11═C12 double bond.[46,420,421] A twist about the C12—C13 single bond results from a steric interaction between a proton at C10 and the methyl group at C20. In addition to the pretwist of the C11═C12 double bond, the proximity of the negatively charged Glu181, which was predicted from modeling,[507] reduces the bond order further to enable selective isomerization around the C11═C12 double bond in the direction shown in Figure 23. Following the gradual release of the potential energy stored in the distorted retinal−protein complex via Batho and the transient BSI, it is not until Lumi that a displacement of the β-ionone ring is observed as a result of the elongation of the retinal. The local perturbations of amino acid side chains in Lumi increase slightly when compared with Batho, but the protein structural changes are still limited to the residues making up the retinal binding site and do not propagate to the cytoplasmic surface.[146] FTIR studies using site-directed infrared labels suggest that the first global movement of the protein backbone is a small rotation of TM5 and TM6 which occurs upon Meta I formation.[479] Solid-state NMR experiments on Meta I and changes in electron density in TM6 on the side facing retinal in the Meta I electron crystallography structure are consistent with a slight motion of TM6[491] which can be described as rotation, but not outward movement.[480] Also consistent with this, another rhodopsin-specific constraint, the TM3/TM5 hydrogen bonding network including Glu122 and Trp126 on TM3 and His211 on TM5, changes upon formation of Meta I as concluded from FTIR data.[508] Straightening of the retinal due to isomerization is thought to move the β-ionone ring toward the region of Met207 to Phe212 on TM5 and thus driving TM rearrangement.[480,509,510]

Until formation of Meta I, the $RSBH^+$ remains protonated, but structural changes in the RSB region occur. In the rhodopsin dark state, $RSBH^+$ interacts with the negatively charged Glu113 counterion (Figure 25A)[511−513] from which a hydrogen bonding network extends to Glu181 on extracellular loop 2.[46] On the basis of both UV−vis and Raman spectroscopy it was hypothesized that in Meta I Glu181 transfers a proton to Glu113 and the $RSBH^+$ switches counterions from Glu113 to Glu181.[514] This view was later modified on the basis of FTIR,[505,515] NMR,[516] and molecular dynamics simulations[517] whose data argue for a complex-counterion made up by Glu113 and Glu181, with both residues being deprotonated and giving the retinal binding pocket a net negative charge.[505,516] In the complex-counterion switch model, Glu113 functions as the primary counterion in the photo-intermediates up to Lumi; in Meta I, the conformational changes in retinal lead to a shift of the counterion from Glu113 to Glu181.[505,515,517]

With the deprotonation of the RSB, an equilibrium of Meta II states is reached, in which the RSB nitrogen is deprotonated prior to the occurrence of TM movements.[488,490] As a result of retinal isomerization, the $RSBH^+$ reorients (Figure 23), and its high pK_a (determined experimentally to be above 16 in the dark state[518] and suggested to have contributions from the negatively charged Glu181[505,506]) drops so that the proton dissociates for the formation of the first Meta II state, Meta IIa. Concomitantly, Glu113 becomes protonated, and a direct internal proton transfer from the $RSBH^+$ is likely to be the source of this proton.[519] According to FTIR studies,[490] $RSBH^+$ deprotonation upon transition to Meta IIa leads to a rearrangement of the TM1/2/7 network as seen by changes of infrared bands assigned to Asp83 on TM2. In this water-mediated hydrogen-bonding network, Asp83 (on TM2) links Asn55 (on TM1) with the $NPxxY(x)_{5,6}F$ motif (TM7), and extends to Trp265 (on TM6) adjacent to retinal's β-ionone ring. Activating conformational changes in the TM3/TM5 network occur in the Meta IIa → Meta IIb transition, as seen by changes of infrared bands assigned to Glu122.[490] This hydrogen bonding network links Glu122 and Trp126 (both on TM3) with His211 (on TM5) which is in contact with the β-ionone ring of retinal. Retinal movement toward TM5 exerts its full effect upon transition to Meta IIb, reflected in a weakening of the hydrogen bond to Glu122.[508,520] In the Meta IIa → Meta IIb transition, changes in infrared amide I marker bands indicate structural changes in the protein backbone.[490] According to Meta II structures, these structural alterations include an elongation of TM5 by 1.5 to 2.5 helix turns depending on the dark state reference structure (PDB ID: 1GZM/3C9L or 1U19, respectively) and a rotational tilt of the kinked TM6 where the TM rotation results in the 6−7 Å outward movement of the cytoplasmic end of TM6 (Figure 23).[426,429,433,435] Time-resolved EPR studies with a spin label sensor at position 227 on TM5, designed to detect TM6 movement, probed the Meta IIa → Meta IIb transition for this event, although the sensor might have detected movements of both TM5 and TM6.[488]

TM6 rotation is facilitated by the breakage of the (D/E)RY ionic lock between TM3 and TM6 consisting of Glu134 and Arg135 (on TM3) and Glu247 and Thr251 (on TM6). The cytoplasmic end of TM5 contains two residues, Tyr223 and Lys231, which function as microswitches.[521] These residues face the lipid environment in the dark state, but stabilize the Meta IIb state when the Arg135-Glu247 ionic lock has been disrupted and TM5 and TM6 rearrangements have occurred (Figure 25C,D). By swiveling inward, Tyr223 can hydrogen bond to Arg135 of the ionic lock, thereby linking TM3 and TM5. Glu247 (on TM6) is freed in Meta IIb from Arg135 and can form a salt bridge to Lys231 on TM5, thus stabilizing TM6 in the outward position. Also in the transition to Meta II when TM6 moves, the electrostatic interaction between Tyr306 and Phe313 becomes disrupted allowing Tyr306 to swivel into the vacated space below Arg135 where it becomes part of an extended water-mediated hydrogen bonding network reaching from the retinal binding site via Ser298, Asp83, Asn302, Met257, Tyr306, and Tyr223 to Arg135.[435] Studies with mutants of the $NPxxY(x)_{5,6}F$ motif suggested dual roles for the NP and the $Y(x)_{5,6}F$ submotifs.[522] Whereas the first has a structural role related to the hydrogen bonding network, the latter is involved in the interaction with G protein. The crystal structure revealed how Tyr306 stabilizes Arg135 and thus the cytoplasmic cleft for binding of the Gt_α C-terminus.

In the structure of the Meta II·GαCT2 peptide complex the backbone carbonyls of Cys347 and Lys345 (on GαCT2) form hydrogen bonds to Arg135 and Gln312, respectively. The presence of the GαCT2 peptide in the cytoplasmic G protein

dx.doi.org/10.1021/cr4003769 | Chem. Rev. 2014, 114, 126−163

binding cleft moves the cytoplasmic end of TM7 slightly toward the center, leading to a somewhat narrower binding cleft. The proposed water-mediated hydrogen bonding network provides an answer regarding how the retinal binding site and the G protein binding site 30 Å apart are connected.[426,435,464,465]

4.2.3. Retinal Channeling in Rhodopsin. The structure of bovine Ops* revealed that the retinal binding pocket has two openings toward the lipid bilayer, one opening between TM1 and 7, the other between TM5 and 6, which form the two halves of the channel leading to the retinal binding pocket (Figure 27). Using molecular docking of retinal, a 3−12 Å wide

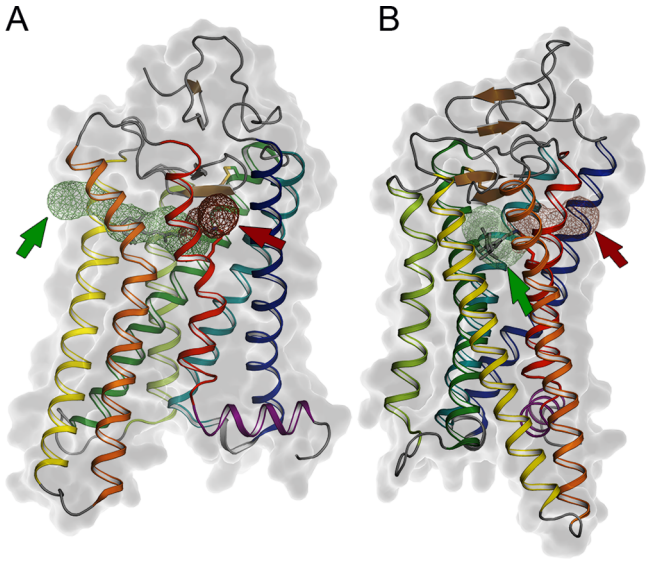

Figure 27. Retinal channel in the Ops*/Meta II conformation. (A) Meta II structure (PDB ID: 3PXO) with the putative retinal channel indicated, rotated to face opening one (red arrow and half channel indicated in red mesh) which is located between TM1 and TM7, and (B) rotated to face opening two (green arrow and half channel indicated in green mesh) which is located between TM5 and TM6. Channels were determined using MOLE[577] on the Ops* structure (PDB ID: 3CAP). The Meta II structure was used for the figure so that the retinal could be shown as it is absent in the Ops* structure.

continuous channel through opsin with the retinal binding pocket as the central part was found.[523,524] The openings to these channels are lined with aromatic residues while the central part is more polar. A major constriction of the channel is around Lys296 which enforces a 90° elbow-like kink in the channel. Passage of that restriction would be easier for the kinked 11-*cis*-retinal, whereas the more elongated and rigid all-*trans*-retinal would require global conformational changes. A study with rhodopsins containing mutations throughout the channel failed to correlate specific opening(s) with retinal entry and exit.[525] However, the study suggested that the ease of retinal passage through constrictions in the channel is not rate-limiting for rhodopsin reconstitution or Meta II decay, but for RSB formation and hydrolysis, respectively. Upon rhodopsin activation, when the helix bundle opens up, bulk solvent molecules obtain access to the RSB,[526−528] most likely from the cytoplasmic side of rhodopsin for RSB hydrolysis and retinal release.[526] This hypothetical solvent channel appears to be quite narrow because only small nucleophiles such as water and hydroxylamine have access to the RSB for retinal hydrolysis.[526,529]

The size of the opening of the retinal channel varies in different Ops*, Meta II, and Meta II-like structures due to variations in side chain rotamers. In the rhodopsin dark state with its compact helix bundle, and presumably in the conformation of inactive opsin, which is similar to dark state rhodopsin,[530] no opening is observed and the 11-*cis*-retinal appears to reside in a hermetically sealed retinal binding pocket (Figure 28A).[46,420,421] Opsin crystals in the Ops* conformation

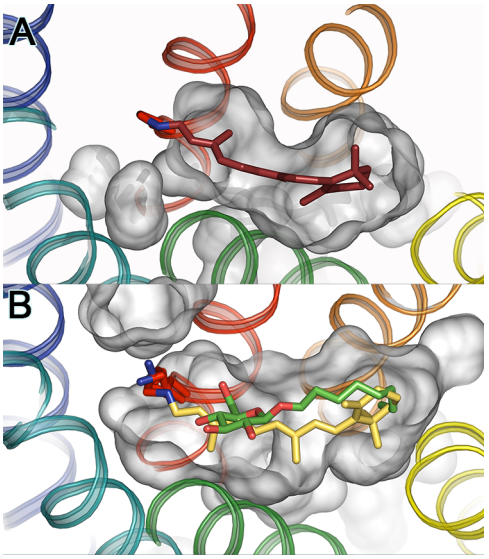

Figure 28. Retinal binding site of bovine rhodopsin. (A) Crystal structure of inactive dark state (PDB ID: 1U19) where 11-*cis*-retinal is tightly bound deep in the protein with no openings of the retinal binding site toward the lipidic environment. (B) In the active Ops* (or Meta II) conformation the retinal channel allows all-*trans*-retinal access and egress, and some detergents like *β*-D-octylglucoside, mimicking the all-*trans*-retinal chromophore, to enter the retinal binding site. Shown is an overlay of the two ligands in the retinal binding pocket as observed in the crystal structures of Meta II (all-*trans*-retinal depicted in yellow; PDB ID: 3PXO) and Ops* in complex with *β*-D-octylglucoside (depicted in green/red; two rotamers of Lys296 are shown in red; PDB ID: 4J4Q). Note that the ring moieties of chromophore and detergent are oriented in opposite directions. Whereas all-*trans*-retinal is covalently linked by the RSB to Lys296, *β*-D-octylglucoside is fixed in the ligand binding site by hydrogen bonding of its hydroxyl groups to the opsin environment.

with an open channel therefore allowed reconstitution of Meta II in soaking experiments with all-*trans*-retinal.[426] All-*trans*-retinal can bind tightly in its binding pocket in Meta II with only slight adjustment of the surrounding amino acid side chains. The binding pocket, however, is flexible enough to allow retinal rotation along its long axis upon rhodopsin activation as concluded from the Meta II crystal structures.[426,433] A limited data set of intramolecular distances obtained by solid-state NMR experiments on Meta II is mostly consistent with the crystal structure. A different degree of retinal rotation in the NMR experiment, however, cannot be ruled out, but could be explained by the equilibrium of Meta II substates.[174,426,509,510,531]

After uptake of 11-*cis*- or 9-*cis*-retinal by opsin (likely by the Ops* conformation when openings to the retinal channel are present) and RSB formation, a conformational change yields inactive rhodopsin or isorhodopsin, respectively, both of which generate the same photoproducts after photon absorption.[46,420,421,532] For the formation of artifical rhodopsin

dx.doi.org/10.1021/cr4003769 | *Chem. Rev.* 2014, 114, 126−163

pigments, the retinal channel in opsin is flexible enough to take up a wide variety of bulkier retinal analogues, e.g., featuring larger or additional alkyl groups or alkyl rings which prevent isomerization around the C11=C12 double bond.[533] Recently, crystallographic evidence was provided that the detergent, β-D-octylglucoside, can bind within rhodopsin's retinal binding pocket thus stabilizing the Ops* conformation (Figure 28B).[432] A study on rhodopsin reconstitution from bovine opsin and 11-*cis*-retinal in the presence of various glucose- or maltose-containing detergents suggested that even some maltoside detergents can enter the retinal channel, while the affinity of various detergents for opsin was dependent on the alkyl chain length.[432] The varied hydrogen-bonding possibilities of the glucose hydroxyl groups to opsin within the retinal binding pocket is reminiscent of the proposed dynamic binding of odorants within olfactory receptors.[534] With its lateral ligand entry and its active GPCR conformation, Ops* was suggested to be ideal for homology modeling of olfactory receptors binding olfactant agonists.[432]

4.3. Mechanistic Variations in Other Rhodopsins

4.3.1. Color Pigments. Rod and cone cells are responsible for scotopic and photopic vision, i.e., vision under low light and daylight conditions, respectively. Rods are characterized by high sensitivity, slow response, slow dark adaptation, and a single type of rhodopsin, whereas cones have low sensitivity, fast response, fast dark adaptation, and several types of cone rhodopsins.[3,535] Some of the features of cone cells can be attributed to the cone visual pigments, which absorb at different wavelengths [red (λ_{max} = 560 nm), green (λ_{max} = 530 nm), and blue (λ_{max} = 420 nm) rhodopsins in humans] necessary to discriminate colors for color vision. The vertebrate cone opsins and rod rhodopsins (λ_{max} = 500 nm) form a single family of homologous proteins,[26] where rod rhodopsins have evolved from cone visual pigments, being closer to the short-wavelength cone opsins.[536,537] The extinction coefficient and quantum yield and thus photosensitivity of bovine Rho and chicken green pigment are comparable.[538] Cone rhodopsins are also thought to undergo a photoactivation process similar to rod rhodopsin, with some variation for the long wavelength pigments.[539,540] A difference, however, is a shorter lifetime of the Meta II state, with parallel formation of Meta III (a late nonproductive photointermediate involved in the decay of the photoactivated state to the apoprotein opsin and retinal) from Meta I (which is in equilibrium with Meta II, Figure 22).[538,541,542] Additionally, regeneration of cone opsins with 11-*cis*-retinal is faster than that of rod rhodopsins.[538,543] The faster kinetics of cone opsins (by 1−2 orders of magnitude) of the active state decay and rhodopsin regeneration are optimal and necessary for the high light levels present during the daytime.

Site-directed mutagenesis studies identified amino acids at position 122 and 189 (Glu122 and Ile189 in bovine Rho, replaced by Gln/Ile and Pro in cone opsins) to be responsible for this functional difference.[544,545] In bovine Rho, Glu122 is a part of a hydrogen bonding network with His211 (TM3/5 network).[546] Glu122 and Ile189, present in rhodopsin but not in cone pigments, also potentiate a more efficient G protein activation compared with cone pigments.[542] The lower Gt activation capacity of cone pigments and faster Meta II decay contribute to the lower photosensitivity of cones compared with rods. Formation and decay of Meta II are related to TM6 movements as outlined above, and EPR experiments could potentially give insights into structural dynamics and conformational changes of color pigments. Unfortunately, because of the difficulties in the sample isolation and preparation of cone pigments, structural studies on these pigments have lagged significantly behind those of bovine Rho. From resonance Raman spectroscopy it is known that the chromophore structure is similar between human green and red sensitive pigments, with both being similar to that of rhodopsin.[547] From FTIR spectroscopy it was concluded that the protein structure of monkey green and red pigments is clearly different from that of rhodopsin, and that hydrogen-bonding networks differ between green and red pigments.[145] It should be noted that in human red and green color vision pigments Glu181 (in bovine Rho) is replaced by a His residue that functions as a chloride binding site,[548,549] suggesting that participation of an anion is a prerequisite for seeing red light. Future structural and modeling studies will be needed to further elucidate the molecular mechanism(s) of color tuning and structural dynamics in cone pigments.[550]

4.3.2. Bistable Rhodopsins and Photoisomerases. The rhodopsins we have discussed so far are stable in the dark, but once retinal isomerization has occurred and metarhodopsin states are reached, the eventual decay into opsin and all-*trans*-retinal takes place. These rhodopsins are also called monostable rhodopsins, and their opsins must be regenerated with new 11-*cis*-retinal produced in the adjacent retinal pigment epithelium cells.[551] Vertebrates and invertebrates possess in addition to these monostable rhodopsins, a second type of rhodopsins, the bistable rhodopsins,[552] which mostly couple to the G protein, Gq, to initiate phosphoinositol signaling cascades. While this Gq signaling is typical for the majority of bistable rhodopsins including those of squid and octopus, other bistable rhodopsins have been shown to couple to other G proteins such as Go.[3,552] A characteristic of bistable rhodopsins is that the dark state and the active states are both thermally stable; i.e., RSB hydrolysis does not occur.[553] Furthermore, a secondary absorption of a photon is utilized to photoregenerate the dark state.[554] These opsins lack the conserved $RSBH^+$ stabilizing counterion found in monostable rhodopsins (Glu113 on TM3 in bovine Rho). Instead, in squid rhodopsin the $RSBH^+$ forms a hydrogen bond to Asn87 or Tyr111 side chains (the equivalent positions in bovine Rho are Gly89 on TM2 and Glu113 on TM3).[422] In other bistable opsins, position 113 is occupied by neutral amino acid residues such as Tyr, Phe, or Met, which can explain why in contrast to bovine Rho, $RSBH^+$ deprotonation of the active state is not required.[555] The conserved Glu181 (bovine Rho numbering) may serve as the sole negatively charged residue near the $RSBH^+$, which is, however, not close enough for direct interaction with the $RSBH^+$.[422] Molecular evolutionary analysis implies that the counterion has been switched from Glu181 to Glu113 during the evolution of vertebrate opsins and that Glu181 serves as a counterion in bistable pigments.[3,552,556,557] Another distinctive feature of bistable pigments is that their opsins can bind all-*trans*-retinal to form the pigment.[3,552]

Rhodopsin from the Japanese flying squid, *T. pacificus* is the only invertebrate opsin (and incidentally the only other GPCR purified from native source apart from bovine rhodopsin) to have its structure determined. This structural information has been instrumental in understanding its chromophore−protein interactions in the dark and bathorhodopsin states as well as in the artificial isorhodopsin pigment (containing 9-*cis*-retinal).[422,423,558] The crystal structures of dark state bovine Rho and squid rhodopsin exhibit similar features including the

dx.doi.org/10.1021/cr4003769 | *Chem. Rev.* 2014, 114, 126−163

presence of the disulfide bridge at the extracellular side of the retinal pocket, a hydrophobic aromatic cage surrounding the retinal and the presence of the (D/E)RY (ionic lock) and NPxxY(x)$_{5,6}$F motifs.[422,423] As in bovine Rho, the retinal is attached through a RSBH$^+$ linkage to the conserved Lys residue on TM7, but retinal itself takes a more relaxed configuration in squid rhodopsin as opposed to the distortions observed in bovine Rho.[422] The structure for squid bathorhodopsin indicates that just as in the bovine Rho early intermediate states, there is little structural change except for a change in the twist of the retinal.[558] It has been postulated from protein structure and sequence analysis that the extended TM5 and TM6 observed in the squid rhodopsin structure may explain the selectivity of coupling to Gq proteins.[422,559] Squid rhodopsin contains an additional C-terminal domain that might be involved in G protein binding, but it was not structurally characterized as it was necessary to proteolytically remove this domain comprising the last 90 amino acids for crystallization.[422,423] Another reason for the functional difference may be the extent of TM6 movement upon photoactivation of bistable rhodopsins as proposed from site-directed fluorescence labeling measurements. A comparison of bovine Rho and parapinopsin, a bistable nonvisual Gt-coupled rhodopsin, revealed much smaller light-induced TM5 and TM6 movement for parapinopsin which correlates with its reduced capability to activate G protein.[560] Of further interest among Gq-coupled bistable rhodopsins is melanopsin, which has been identified in various vertebrates.[552,561] In mammals, melanopsin is localized in intrinsically photosensitive retinal ganglion cells and is involved in nonvisual functions, including photoentrainment of the circadian clock, pupillary light reflex, and sleep.[4]

Another, more divergent grouping of opsins are the photoisomerases, which function to bind all-*trans* retinoids and photoisomerize them to their 11-*cis*-forms.[410] Structural information remains elusive for these opsins. The best characterized of these photoisomerases are retinochrome from molluscan species and the mammalian retinal G-protein-coupled receptor (RGR).[97,562,563] In mollusks, retinochrome functions to provide the 11-*cis*-retinal to newly synthesized apoprotein opsin, whereas in mammals, RGR appears to play more of a regulatory role in the mobilization of all-*trans*-retinyl esters into the retinoid cycle.[562,564] These photoisomerases lack the NPxxY(x)$_{5,6}$Y motif and thus may be deficient in G protein coupling.[3] A close relative is peropsin from mammalian retinal pigment epithelium (RPE) cells. Peropsin shows photoisomerase activity, but contains the (D/E)RY and NPxxY(x)$_{5,6}$Y motifs and therefore may couple to G protein and be involved in activation of signaling cascades.[565]

5. CONCLUSIONS AND PERSPECTIVE

In the past, the impact of research on both microbial and animal rhodopsins propagated far beyond the boundaries of the retinal-binding protein field. It will suffice to give just a few of the most striking examples. Structural work on BR and Rho has greatly contributed to our understanding of the structural principles of membrane proteins in general. The detailed understanding of the proton transport mechanism by BR has been extremely useful to the bioenergetics community, who extended these principles to important systems such as cytochrome oxidases and ATPases. The great structural and mechanistic advances in the understanding of visual signal transduction significantly enriched the GPCR field, and for many years bovine Rho served (and continues to serve) as a model GPCR. More recently, the discovery of proteorhodopsins gave a strong push to the field of metagenomics, while the discovery of channelrhodopsins gave birth to optogenetics. Finally, rhodopsins have been serving as testing grounds for many cutting-edge biophysical techniques, aiding, for example, in the development of time-resolved and low-temperature FTIR spectroscopy, ultrafast spectroscopy, advanced Raman techniques, new methods for 2-D and 3-D crystallization of membrane proteins, protein solid-state NMR, and high-field EPR, including site-directed spin-labeling techniques.

But what are the next exciting steps in rhodopsin research? Expanding on these recent trends, we can predict many more interesting developments without being too speculative. Judging from the large number of new rhodopsin variants unearthed by genomic and metagenomic sequencing, new interesting functions of retinal proteins will continue to be discovered. This applies to both microbial and animal rhodopsins, and will lead to new breakthroughs in understanding microbial, invertebrate, and vertebrate physiology and evolution. These new functional variants of rhodopsins may also find use in optogenetics, enriching its arsenal of tools. New advanced techniques of structural biology and biophysics will be applied to these new rhodopsins leading to new insights, capitalizing on such emerging methods as, for example, high-speed AFM, ultrafast time-resolved crystallography, structural mass spectroscopy, and dynamic nuclear polarization NMR.

From the point of view of structural biology, the next challenging frontier in the field will be to understand the mechanisms of rhodopsin−protein interactions. While structural methods have enjoyed great success in determining structures of isolated rhodopsins and their binding partners, structures of inactive and activated protein complexes, especially those of membrane and soluble proteins, remain elusive. This is especially important for visual rhodopsins with their multiple interacting partners, and bears on the entirety of the GPCR field, contributing to a better understanding of GPCR signaling cascade, activation, and regulation.

ASSOCIATED CONTENT

Supporting Information

Figures S1 and S2 containing information on sequence identities for microbial rhodopsins. Figure S3 illustrating functional conversion between light-driven proton and chloride pumps. Figure S4 illustrating sequence conservation in GPCRs. This material is available free of charge via the Internet at http://pubs.acs.org.

AUTHOR INFORMATION

Corresponding Author

*E-mail: oliver.ernst@utoronto.ca. Phone: (416) 978-3849. Fax: (416) 978-8548.

Notes

The authors declare no competing financial interest.

Biographies

Oliver P. Ernst studied chemistry with a focus on biochemistry at the University of Freiburg, Germany, where he received his doctoral degree (Dr. rer. nat.) in 1994. After research training at Rockefeller University, he started in 1995 with a position as a scientific assistant at the Charité—Universitätsmedizin Berlin, Germany, where he became a group leader and made his Habilitation in biophysics in 2003. Since 2011, he has been a full professor in the Departments of Biochemistry and Molecular Genetics at the University of Toronto. He holds the Canada Excellence Research Chair in Structural Neurobiology and the Max and Anne Tanenbaum Chair in Neuroscience at University of Toronto. His research focuses on rhodopsin and visual signal transduction as well as other GPCRs.

David T. Lodowski graduated in 1998 from Tulane University with a B.S. in cellular and molecular biology. This was followed by graduate studies at the University of Texas at Austin, where, under supervision of Dr. John Tesmer, he obtained his Ph.D. (Structural Basis for the Regulation of GRK2 by G$\beta\gamma$) in 2005. He followed this work with a postdoctoral fellowship in the laboratory of Dr. Krzysztof Palczewski at Case Western Reserve University examining the structural changes in bovine rhodopsin that accompany photoactivation and GPCR activation from 2005 to 2011. Currently he is an assistant professor in the Case Center for Proteomics and Bioinformatics where his laboratory focuses on the interactions of GPCRs with their downstream partners via the combination of X-ray crystallography, electron microscopy, and structural mass spectrometry.

Marcus Elstner studied physics and graduated in 1998 from University of Paderborn (Germany). From 1999 to 2000 he was a postdoctoral fellow in the group of Professor Kaxiras, in the Physics Department at Harvard University, Cambridge, Massachusetts. From 2000 to 2002 he was a scientific assistant, and from 2003 to 2006 he was a junior professor of theoretical physics at the University of Paderborn. In 2006, he became professor at the TU Braunschweig and, in 2009, professor at the Kalsruhe Institute of Technology (KIT). His research focuses on the development of quantum chemical and combined quantum chemical/molecular mechanics (QM/MM) methods and their application to proton/electron transfer processes and the optical properties of proteins.

Peter Hegemann studied chemistry and finished his dissertation (Dr. rer. nat.) at the Max Planck Institute for Biochemistry in Munich, Germany, in 1984. After postgraduate training at Syracuse University, New York, with K. W. Foster, he headed in 1986 a research group at the Max Planck Institute for Biochemistry in Munich, Germany, before he became in 1993 a professor at the University of Regensburg, Germany. Since 2005 he has been a professor at Humboldt University Berlin, Germany. His research focuses on the photobiology of green algae, which led to the discovery of channelrhodopsin and the birth of optogenetics.

dx.doi.org/10.1021/cr4003769 | *Chem. Rev.* 2014, 114, 126−163

Leonid S. Brown is a full professor in the Department of Physics, University of Guelph, Ontario. He received his Ph.D. in biophysics from Lomonosov Moscow State University, in Russia, in 1991, and received postgraduate training at the University of California, Irvine. His early research focused on spectrocopic studies of bacteriorhodopsin, and currently he is working on new microbial rhodopsins of eucaryotic and eubacterial origin.

Hideki Kandori received a Ph.D. from the Department of Biophysics, Kyoto University, Japan, in 1989. After postdoctoral research at the Institute for Molecular Science (Okazaki, Japan) and RIKEN (Wako, Japan), he joined the faculty of the Biophysics Deparment, Kyoto Univeristy, as a research associate in 1993. He then moved to Nagoya Institute of Technology in 2001, and has been a full professor in the Department of Frontier Materials, Nagoya Institute of Technology, since 2003. His research interest is "light and life", performing spectroscopic studies of photoreceptive proteins such as animal and microbial rhodopsins and flavoproteins. One of his recent research highlights is the detection of protein-bound water molecules by FTIR spectroscopy, and he attempts to find new functions and engineer conversion of function in rhodopsins and flavoproteins.

ACKNOWLEDGMENTS

We thank Dr. Keiichi Inoue, Dr. Rei Yoshizumi, Dr. Susumu Yoshizawa, Mr. Yoshitaka Kato, and Mr. Yuya Ozaki for help with preparation of figures and alignments and Dr. Philip Johnson for discussions. This research was supported by the Canada Excellence Research Chair program (O.P.E.). O.P.E. is Anne and Max Tanenbaum Chair in Neuroscience at University of Toronto. This work was also supported by Grant EY019718 (D.T.L.) from the National Institutes of Health, by the DFG Cluster of Excellence Unifying Concepts of Catalysis (P.H.), and grants from the Japanese Ministry of Education, Culture, Sports, Science and Technology (H.K.), and the Natural Sciences and Engineering Research Council of Canada (L.S.B.).

ABBREVIATIONS

ASR	*Anabaena* sensory rhodopsin
ASRT	ASR soluble transducer protein
β_2AR	β_2-adrenergic receptor
BPR	blue-absorbing proteorhodopsin
BR	bacteriorhodopsin
ChR	channelrhodopsin
GPCR	G-protein-coupled receptor
GPR	green-absorbing proteorhodopsin
GR	*Gloeobacter* rhodopsin
HR	halorhodopsin
MD	molecular dynamics
MM	molecular mechanics
NR	*Neurospora* rhodopsin
PR	proteorhodopsin
QM	quantum mechanical
Rho	bovine visual rhodopsin
RSB	retinal Schiff base
$RSBH^+$	protonated retinal Schiff base
SR	sensory rhodopsin
TM	transmembrane helix
XR	xanthorhodopsin

REFERENCES

(1) Spudich, J. L.; Yang, C. S.; Jung, K. H.; Spudich, E. N. *Annu. Rev. Cell Dev. Biol.* **2000**, *16*, 365.
(2) Palczewski, K. *Annu. Rev. Biochem.* **2006**, *75*, 743.
(3) Shichida, Y.; Matsuyama, T. *Philos. Trans. R. Soc., B* **2009**, *364*, 2881.
(4) Schmidt, T. M.; Chen, S. K.; Hattar, S. *Trends Neurosci.* **2011**, *34*, 572.
(5) Soppa, J. *FEBS Lett.* **1994**, *342*, 7.
(6) Nakanishi, K. *Am. Zool.* **1991**, *31*, 479.
(7) Klare, J. P.; Chizhov, I.; Engelhard, M. *Results Probl. Cell Differ.* **2008**, *45*, 73.
(8) Oesterhelt, D.; Stoeckenius, W. *Nature (London), New Biol.* **1971**, *233*, 149.
(9) Matsuno-Yagi, A.; Mukohata, Y. *Biochem. Biophys. Res. Commun.* **1977**, *78*, 237.
(10) Spudich, J. L.; Bogomolni, R. A. *Nature* **1984**, *312*, 509.
(11) Jung, K. H.; Trivedi, V. D.; Spudich, J. L. *Mol. Microbiol.* **2003**, *47*, 1513.
(12) Nagel, G.; Ollig, D.; Fuhrmann, M.; Kateriya, S.; Musti, A. M.; Bamberg, E.; Hegemann, P. *Science* **2002**, *296*, 2395.
(13) Nagel, G.; Szellas, T.; Huhn, W.; Kateriya, S.; Adeishvili, N.; Berthold, P.; Ollig, D.; Hegemann, P.; Bamberg, E. *Proc. Natl. Acad. Sci. U.S.A.* **2003**, *100*, 13940.
(14) Miesenbock, G. *Annu. Rev. Cell Dev. Biol.* **2011**, *27*, 731.
(15) Zarbin, M. A.; Montemagno, C.; Leary, J. F.; Ritch, R. *Curr. Opin. Pharmacol.* **2013**, *13*, 134.
(16) Deisseroth, K. *Nat. Methods* **2011**, *8*, 26.
(17) Diester, I.; Kaufman, M. T.; Mogri, M.; Pashaie, R.; Goo, W.; Yizhar, O.; Ramakrishnan, C.; Deisseroth, K.; Shenoy, K. V. *Nat. Neurosci.* **2011**, *14*, 387.
(18) Pierce, K. L.; Premont, R. T.; Lefkowitz, R. J. *Nat. Rev. Mol. Cell. Biol.* **2002**, *3*, 639.
(19) Rosenbaum, D. M.; Rasmussen, S. G.; Kobilka, B. K. *Nature* **2009**, *459*, 356.
(20) Lefkowitz, R. J.; Shenoy, S. K. *Science* **2005**, *308*, 512.
(21) Rieke, F.; Baylor, D. A. *Biophys. J.* **1998**, *75*, 1836.
(22) Kühne, W. *On the Photochemistry of the Retina and on Visual Purple*; Macmillan and Co.: London, 1878.
(23) Stoeckenius, W. *Acc. Chem. Res.* **1980**, *13*, 337.

(24) Wald, G. *Nature* **1968**, *219*, 800.
(25) Kakitani, H.; Kakitani, T.; Rodman, H.; Honig, B. *Photochem. Photobiol.* **1985**, *41*, 471.
(26) Nathans, J.; Thomas, D.; Hogness, D. S. *Science* **1986**, *232*, 193.
(27) Oprian, D. D.; Asenjo, A. B.; Lee, N.; Pelletier, S. L. *Biochemistry* **1991**, *30*, 11367.
(28) Cronin, T. W.; Caldwell, R. L.; Marshall, J. *Nature* **2001**, *411*, 547.
(29) Liu, R. S.; Krogh, E.; Li, X. Y.; Mead, D.; Colmenares, L. U.; Thiel, J. R.; Ellis, J.; Wong, D.; Asato, A. E. *Photochem. Photobiol.* **1993**, *58*, 701.
(30) Motto, M. G.; Sheves, M.; Tsujimoto, K.; Baloghnair, V.; Nakanishi, K. *J. Am. Chem. Soc.* **1980**, *102*, 7947.
(31) Ottolenghi, M.; Sheves, M. *J. Membr. Biol.* **1989**, *112*, 193.
(32) Yan, B.; Spudich, J. L.; Mazur, P.; Vunnam, S.; Derguini, F.; Nakanishi, K. *J. Biol. Chem.* **1995**, *270*, 29668.
(33) Krebs, M. P.; Mollaaghababa, R.; Khorana, H. G. *Proc. Natl. Acad. Sci. U.S.A.* **1993**, *90*, 1987.
(34) Sakmar, T. P.; Menon, S. T.; Marin, E. P.; Awad, E. S. *Annu. Rev. Biophys. Biomol. Struct.* **2002**, *31*, 443.
(35) Soppa, J.; Otomo, J.; Straub, J.; Tittor, J.; Meessen, S.; Oesterhelt, D. *J. Biol. Chem.* **1989**, *264*, 13049.
(36) Wang, W.; Nossoni, Z.; Berbasova, T.; Watson, C. T.; Yapici, I.; Lee, K. S.; Vasileiou, C.; Geiger, J. H.; Borhan, B. *Science* **2012**, *338*, 1340.
(37) Song, L.; El-Sayed, M. A.; Lanyi, J. K. *Science* **1993**, *261*, 891.
(38) Schenkl, S.; van Mourik, F.; van der Zwan, G.; Haacke, S.; Chergui, M. *Science* **2005**, *309*, 917.
(39) Blatz, P. E.; Mohler, J. H.; Navangul, H. V. *Biochemistry* **1972**, *11*, 848.
(40) Andersen, L. H.; Nielsen, I. B.; Kristensen, M. B.; El Ghazaly, M. O.; Haacke, S.; Nielsen, M. B.; Petersen, M. A. *J. Am. Chem. Soc.* **2005**, *127*, 12347.
(41) Nakanishi, K.; Baloghnair, V.; Arnaboldi, M.; Tsujimoto, K.; Honig, B. *J. Am. Chem. Soc.* **1980**, *102*, 7945.
(42) Kochendoerfer, G. G.; Lin, S. W.; Sakmar, T. P.; Mathies, R. A. *Trends Biochem. Sci.* **1999**, *24*, 300.
(43) Rangarajan, R.; Galan, J. F.; Whited, G.; Birge, R. R. *Biochemistry* **2007**, *46*, 12679.
(44) Sekharan, S.; Sugihara, M.; Buss, V. *Angew. Chem., Int. Ed.* **2007**, *46*, 269.
(45) Yokoyama, S. *Annu. Rev. Genomics Hum. Genet.* **2008**, *9*, 259.
(46) Okada, T.; Sugihara, M.; Bondar, A. N.; Elstner, M.; Entel, P.; Buss, V. *J. Mol. Biol.* **2004**, *342*, 571.
(47) Ahuja, S.; Eilers, M.; Hirshfeld, A.; Yan, E. C.; Ziliox, M.; Sakmar, T. P.; Sheves, M.; Smith, S. O. *J. Am. Chem. Soc.* **2009**, *131*, 15160.
(48) Childs, R. F.; Shaw, G. S.; Wasylishen, R. E. *J. Am. Chem. Soc.* **1987**, *109*, 5362.
(49) Becker, R. S.; Freedman, K. *J. Am. Chem. Soc.* **1985**, *107*, 1477.
(50) Yokoyama, S.; Tada, T.; Zhang, H.; Britt, L. *Proc. Natl. Acad. Sci. U.S.A.* **2008**, *105*, 13480.
(51) Kato, H. E.; Zhang, F.; Yizhar, O.; Ramakrishnan, C.; Nishizawa, T.; Hirata, K.; Ito, J.; Aita, Y.; Tsukazaki, T.; Hayashi, S.; Hegemann, P.; Maturana, A. D.; Ishitani, R.; Deisseroth, K.; Nureki, O. *Nature* **2012**, *482*, 369.
(52) Luecke, H.; Schobert, B.; Lanyi, J. K.; Spudich, E. N.; Spudich, J. L. *Science* **2001**, *293*, 1499.
(53) Royant, A.; Nollert, P.; Edman, K.; Neutze, R.; Landau, E. M.; Pebay-Peyroula, E.; Navarro, J. *Proc. Natl. Acad. Sci. U.S.A.* **2001**, *98*, 10131.
(54) Birge, R. R.; Murray, L. P.; Pierce, B. M.; Akita, H.; Balogh-Nair, V.; Findsen, L. A.; Nakanishi, K. *Proc. Natl. Acad. Sci. U.S.A.* **1985**, *82*, 4117.
(55) Tavan, P.; Schulten, K.; Oesterhelt, D. *Biophys. J.* **1985**, *47*, 415.
(56) Warshel, A. *Proc. Natl. Acad. Sci. U.S.A.* **1978**, *75*, 2558.
(57) Wanko, M.; Hoffmann, M.; Frauenheim, T.; Elstner, M. *J. Comput.-Aided Mol. Des.* **2006**, *20*, 511.
(58) Sakurai, M.; Sakata, K.; Saito, S.; Nakajima, S.; Inoue, Y. *J. Am. Chem. Soc.* **2003**, *125*, 3108.
(59) Soderhjelm, P.; Husberg, C.; Strambi, A.; Olivucci, M.; Ryde, U. *J. Chem. Theory Comput.* **2009**, *5*, 649.
(60) Wanko, M.; Hoffmann, M.; Frahmcke, J.; Frauenheim, T.; Elstner, M. *J. Phys. Chem. B* **2008**, *112*, 11468.
(61) Fujimoto, K. J.; Asai, K.; Hasegawa, J. Y. *Phys. Chem. Chem. Phys.* **2010**, *12*, 13107.
(62) Kloppmann, E.; Becker, T.; Ullmann, G. M. *Proteins* **2005**, *61*, 953.
(63) Rajamani, R.; Gao, J. *J. Comput. Chem.* **2002**, *23*, 96.
(64) Wanko, M.; Hoffmann, M.; Strodel, P.; Koslowski, A.; Thiel, W.; Neese, F.; Frauenheim, T.; Elstner, M. *J. Phys. Chem. B* **2005**, *109*, 3606.
(65) Ryazantsev, M. N.; Altun, A.; Morokuma, K. *J. Am. Chem. Soc.* **2012**, *134*, 5520.
(66) Hoffmann, M.; Wanko, M.; Strodel, P.; Konig, P. H.; Frauenheim, T.; Schulten, K.; Thiel, W.; Tajkhorshid, E.; Elstner, M. *J. Am. Chem. Soc.* **2006**, *128*, 10808.
(67) Wanko, M.; Hoffmann, M.; Frauenheim, T.; Elstner, M. *J. Phys. Chem. B* **2008**, *112*, 11462.
(68) Melaccio, F.; Ferre, N.; Olivucci, M. *Phys. Chem. Chem. Phys.* **2012**, *14*, 12485.
(69) Coto, P. B.; Strambi, A.; Ferre, N.; Olivucci, M. *Proc. Natl. Acad. Sci. U.S.A.* **2006**, *103*, 17154.
(70) Frahmcke, J. S.; Wanko, M.; Phatak, P.; Mroginski, M. A.; Elstner, M. *J. Phys. Chem. B* **2010**, *114*, 11338.
(71) Sekharan, S. *Photochem. Photobiol.* **2009**, *85*, 517.
(72) Sugihara, M.; Buss, V.; Entel, P.; Elstner, M.; Frauenheim, T. *Biochemistry* **2002**, *41*, 15259.
(73) Tomasello, G.; Olaso-Gonzalez, G.; Altoe, P.; Stenta, M.; Serrano-Andres, L.; Merchan, M.; Orlandi, G.; Bottoni, A.; Garavelli, M. *J. Am. Chem. Soc.* **2009**, *131*, 5172.
(74) Sekharan, S.; Morokuma, K. *J. Phys. Chem. Lett.* **2010**, *1*, 668.
(75) Amora, T. L.; Ramos, L. S.; Galan, J. F.; Birge, R. R. *Biochemistry* **2008**, *47*, 4614.
(76) Sekharan, S.; Wei, J. N.; Batista, V. S. *J. Am. Chem. Soc.* **2012**, *134*, 19536.
(77) Frahmcke, J. S.; Wanko, M.; Elstner, M. *J. Phys. Chem. B* **2012**, *116*, 3313.
(78) Hillebrecht, J. R.; Galan, J.; Rangarajan, R.; Ramos, L.; McCleary, K.; Ward, D. E.; Stuart, J. A.; Birge, R. R. *Biochemistry* **2006**, *45*, 1579.
(79) Liu, R. S.; Asato, A. E. *Proc. Natl. Acad. Sci. U.S.A.* **1985**, *82*, 259.
(80) Salem, L.; Bruckmann, P. *Nature* **1975**, *258*, 526.
(81) Salem, L. *Science* **1976**, *191*, 822.
(82) Warshel, A. *Nature* **1976**, *260*, 679.
(83) Hurley, J. B.; Ebrey, T. G.; Honig, B.; Ottolenghi, M. *Nature* **1977**, *270*, 540.
(84) Kandori, H.; Shichida, Y.; Yoshizawa, T. *Biochemistry (Moscow)* **2001**, *66*, 1197.
(85) Kochendoerfer, G. G.; Mathies, R. A. *Isr. J. Chem.* **1995**, *35*, 211.
(86) Kochendoerfer, G. G.; Mathies, R. A. *J. Phys. Chem.* **1996**, *100*, 14526.
(87) Strickler, S. J.; Berg, R. A. *J. Chem. Phys.* **1962**, *37*, 814.
(88) Doukas, A. G.; Junnarkar, M. R.; Alfano, R. R.; Callender, R. H.; Kakitani, T.; Honig, B. *Proc. Natl. Acad. Sci. U.S.A.* **1984**, *81*, 4790.
(89) Yoshizawa, T.; Kito, Y. *Nature* **1958**, *182*, 1604.
(90) Yoshizawa, T.; Wald, G. *Nature* **1963**, *197*, 1279.
(91) Busch, G. E.; Applebury, M. L.; Lamola, A. A.; Rentzepis, P. M. *Proc. Natl. Acad. Sci. U.S.A.* **1972**, *69*, 2802.
(92) Peters, K.; Applebury, M. L.; Rentzepis, P. M. *Proc. Natl. Acad. Sci. U.S.A.* **1977**, *74*, 3119.
(93) Tittor, J.; Oesterhelt, D. *FEBS Lett.* **1990**, *263*, 269.
(94) Govindjee, R.; Balashov, S. P.; Ebrey, T. G. *Biophys. J.* **1990**, *58*, 597.
(95) Dartnall, H. J. *Vision Res.* **1968**, *8*, 339.
(96) Furutani, Y.; Terakita, A.; Shichida, Y.; Kandori, H. *Biochemistry* **2005**, *44*, 7988.

(97) Hara, T.; Hara, R. *Nature* **1967**, *214*, 573.
(98) Matsuyama, T.; Yamashita, T.; Imamoto, Y.; Shichida, Y. *Biochemistry* **2012**, *51*, 5454.
(99) Mizukami, T.; Kandori, H.; Shichida, Y.; Chen, A. H.; Derguini, F.; Caldwell, C. G.; Biffe, C. F.; Nakanishi, K.; Yoshizawa, T. *Proc. Natl. Acad. Sci. U.S.A.* **1993**, *90*, 4072.
(100) Schoenlein, R. W.; Peteanu, L. A.; Mathies, R. A.; Shank, C. V. *Science* **1991**, *254*, 412.
(101) Wang, Q.; Schoenlein, R. W.; Peteanu, L. A.; Mathies, R. A.; Shank, C. V. *Science* **1994**, *266*, 422.
(102) Chosrowjan, H.; Mataga, N.; Shibata, Y.; Tachibanaki, S.; Kandori, H.; Shichida, Y.; Okada, T.; Kouyama, T. *J. Am. Chem. Soc.* **1998**, *120*, 9706.
(103) Kukura, P.; McCamant, D. W.; Yoon, S.; Wandschneider, D. B.; Mathies, R. A. *Science* **2005**, *310*, 1006.
(104) Sharkov, A. V.; Pakulev, A. V.; Chekalin, S. V.; Matveetz, Y. A. *Biochim. Biophys. Acta* **1985**, *808*, 94.
(105) Dobler, J.; Zinth, W.; Kaiser, W.; Oesterhelt, D. *Chem. Phys. Lett.* **1988**, *144*, 215.
(106) Mathies, R. A.; Brito Cruz, C. H.; Pollard, W. T.; Shank, C. V. *Science* **1988**, *240*, 777.
(107) Zhong, Q.; Ruhman, S.; Ottolenghi, M.; Sheves, M.; Friedman, N.; Atkinson, G. H.; Delaney, J. K. *J. Am. Chem. Soc.* **1996**, *118*, 12828.
(108) Atkinson, G. H.; Ujj, L.; Zhou, Y. D. *J. Phys. Chem. A* **2000**, *104*, 4130.
(109) Herbst, J.; Heyne, K.; Diller, R. *Science* **2002**, *297*, 822.
(110) Kobayashi, T.; Saito, T.; Ohtani, H. *Nature* **2001**, *414*, 531.
(111) Yabushita, A.; Kobayashi, T. *Biophys. J.* **2009**, *96*, 1447.
(112) Doig, S. J.; Reid, P. J.; Mathies, R. A. *J. Phys. Chem.* **1991**, *95*, 6372.
(113) Prokhorenko, V. I.; Nagy, A. M.; Waschuk, S. A.; Brown, L. S.; Birge, R. R.; Miller, R. J. *Science* **2006**, *313*, 1257.
(114) Du, M.; Fleming, G. R. *Biophys. Chem.* **1993**, *48*, 101.
(115) Gai, F.; Hasson, K. C.; McDonald, J. C.; Anfinrud, P. A. *Science* **1998**, *279*, 1886.
(116) Ruhman, S.; Hou, B.; Friedman, N.; Ottolenghi, M.; Sheves, M. *J. Am. Chem. Soc.* **2002**, *124*, 8854.
(117) Wand, A.; Rozin, R.; Eliash, T.; Jung, K. H.; Sheves, M.; Ruhman, S. *J. Am. Chem. Soc.* **2011**, *133*, 20922.
(118) Kochendoerfer, G. G.; Verdegem, P. J.; van der Hoef, I.; Lugtenburg, J.; Mathies, R. A. *Biochemistry* **1996**, *35*, 16230.
(119) Sugihara, M.; Hufen, J.; Buss, V. *Biochemistry* **2006**, *45*, 801.
(120) Nakamichi, H.; Okada, T. *Angew. Chem., Int. Ed.* **2006**, *45*, 4270.
(121) Ganter, U. M.; Schmid, E. D.; Perez-Sala, D.; Rando, R. R.; Siebert, F. *Biochemistry* **1989**, *28*, 5954.
(122) Meyer, C. K.; Böhme, M.; Ockenfels, A.; Gärtner, W.; Hofmann, K. P.; Ernst, O. P. *J. Biol. Chem.* **2000**, *275*, 19713.
(123) Garavelli, M.; Celani, P.; Bernardi, F.; Robb, M. A.; Olivucci, M. *J. Am. Chem. Soc.* **1997**, *119*, 6891.
(124) Garavelli, M. *Theor. Chem. Acc.* **2006**, *116*, 87.
(125) Schapiro, I.; Melaccio, F.; Laricheva, E. N.; Olivucci, M. *Photochem. Photobiol. Sci.* **2011**, *10*, 867.
(126) Cembran, A.; Bernardi, F.; Olivucci, M.; Garavelli, M. *J. Am. Chem. Soc.* **2004**, *126*, 16018.
(127) Cembran, A.; Bernardi, F.; Olivucci, M.; Garavelli, M. *Proc. Natl. Acad. Sci. U.S.A.* **2005**, *102*, 6255.
(128) Frutos, L. M.; Andruniow, T.; Santoro, F.; Ferre, N.; Olivucci, M. *Proc. Natl. Acad. Sci. U.S.A.* **2007**, *104*, 7764.
(129) Hayashi, S.; Tajkhorshid, E.; Schulten, K. *Biophys. J.* **2003**, *85*, 1440.
(130) Hayashi, S.; Tajkhorshid, E.; Schulten, K. *Biophys. J.* **2009**, *96*, 403.
(131) Li, X.; Chung, L. W.; Morokuma, K. *J. Chem. Theory Comput.* **2011**, *7*, 2694.
(132) Polli, D.; Altoe, P.; Weingart, O.; Spillane, K. M.; Manzoni, C.; Brida, D.; Tomasello, G.; Orlandi, G.; Kukura, P.; Mathies, R. A.; Garavelli, M.; Cerullo, G. *Nature* **2010**, *467*, 440.
(133) Schapiro, I.; Ryazantsev, M. N.; Frutos, L. M.; Ferre, N.; Lindh, R.; Olivucci, M. *J. Am. Chem. Soc.* **2011**, *133*, 3354.
(134) Strambi, A.; Coto, P. B.; Frutos, L. M.; Ferre, N.; Olivucci, M. *J. Am. Chem. Soc.* **2008**, *130*, 3382.
(135) Warshel, A.; Chu, Z. T. *J. Phys. Chem. B* **2001**, *105*, 9857.
(136) Weingart, O.; Garavelli, M. *J. Chem. Phys.* **2012**, *137*, 22A523.
(137) Sekharan, S.; Morokuma, K. *J. Am. Chem. Soc.* **2011**, *133*, 19052.
(138) Schenkl, S.; van Mourik, F.; Friedman, N.; Sheves, M.; Schlesinger, R.; Haacke, S.; Chergui, M. *Proc. Natl. Acad. Sci. U.S.A.* **2006**, *103*, 4101.
(139) Neumann-Verhoefen, M. K.; Neumann, K.; Bamann, C.; Radu, I.; Heberle, J.; Bamberg, E.; Wachtveitl, J. *J. Am. Chem. Soc.* **2013**, *135*, 6968.
(140) Eyring, G.; Mathies, R. *Proc. Natl. Acad. Sci. U.S.A.* **1979**, *76*, 33.
(141) Cooper, A. *Nature* **1979**, *282*, 531.
(142) Nishioku, Y.; Nakagawa, M.; Tsuda, M.; Terazima, M. *Biophys. J.* **2002**, *83*, 1136.
(143) Palings, I.; van den Berg, E. M.; Lugtenburg, J.; Mathies, R. A. *Biochemistry* **1989**, *28*, 1498.
(144) Ota, T.; Furutani, Y.; Terakita, A.; Shichida, Y.; Kandori, H. *Biochemistry* **2006**, *45*, 2845.
(145) Katayama, K.; Furutani, Y.; Imai, H.; Kandori, H. *Angew. Chem., Int. Ed.* **2010**, *49*, 891.
(146) Nakamichi, H.; Okada, T. *Proc. Natl. Acad. Sci. U.S.A.* **2006**, *103*, 12729.
(147) Birge, R. R.; Cooper, T. M. *Biophys. J.* **1983**, *42*, 61.
(148) Birge, R. R. *Biochim. Biophys. Acta* **1990**, *1016*, 293.
(149) Losi, A.; Wegener, A. A.; Engelhard, M.; Gartner, W.; Braslavsky, S. E. *Biophys. J.* **1999**, *77*, 3277.
(150) Edman, K.; Nollert, P.; Royant, A.; Belrhali, H.; Pebay-Peyroula, E.; Hajdu, J.; Neutze, R.; Landau, E. M. *Nature* **1999**, *401*, 822.
(151) Matsui, Y.; Sakai, K.; Murakami, M.; Shiro, Y.; Adachi, S.; Okumura, H.; Kouyama, T. *J. Mol. Biol.* **2002**, *324*, 469.
(152) Schobert, B.; Cupp-Vickery, J.; Hornak, V.; Smith, S.; Lanyi, J. *J. Mol. Biol.* **2002**, *321*, 715.
(153) Kandori, H. In *Supramolecular Photochemistry: Controlling Photochemical Processes*, 1st ed.; Ramamurthy, V., Inoue, Y., Eds.; John Wiley & Sons, Inc.: Hoboken, NJ, 2011.
(154) Kandori, H.; Belenky, M.; Herzfeld, J. *Biochemistry* **2002**, *41*, 6026.
(155) Shibata, M.; Kandori, H. *Biochemistry* **2005**, *44*, 7406.
(156) Kandori, H.; Shichida, Y. *J. Am. Chem. Soc.* **2000**, *122*, 11745.
(157) Hayashi, S.; Tajkhorshid, E.; Schulten, K. *Biophys. J.* **2002**, *83*, 1281.
(158) Hayashi, S.; Tajkhorshid, E.; Kandori, H.; Schulten, K. *J. Am. Chem. Soc.* **2004**, *126*, 10516.
(159) Bondar, A. N.; Fischer, S.; Suhai, S.; Smith, J. C. *J. Phys. Chem. B* **2005**, *109*, 14786.
(160) Muroda, K.; Nakashima, K.; Shibata, M.; Demura, M.; Kandori, H. *Biochemistry* **2012**, *51*, 4677.
(161) Kiser, P. D.; Golczak, M.; Maeda, A.; Palczewski, K. *Biochim. Biophys. Acta* **2012**, *1821*, 137.
(162) Palczewski, K. *J. Biol. Chem.* **2012**, *287*, 1612.
(163) Hara, R.; Hara, T. *Vision Res.* **1984**, *24*, 1629.
(164) Brown, L. S.; Jung, K. H. *Photochem. Photobiol. Sci.* **2006**, *5*, 538.
(165) Kouyama, T.; Murakami, M. *Photochem. Photobiol. Sci.* **2010**, *9*, 1458.
(166) Sharma, A. K.; Spudich, J. L.; Doolittle, W. F. *Trends Microbiol.* **2006**, *14*, 463.
(167) Hegemann, P. *Annu. Rev. Plant Biol.* **2008**, *59*, 167.
(168) Inoue, K.; Ono, H.; Abe-Yoshizumi, R.; Yoshizawa, S.; Ito, H.; Kogure, K.; Kandori, H. *Nat. Commun.* **2013**, *4*, 1678.
(169) Jung, K. H. *Photochem. Photobiol.* **2007**, *83*, 63.

(170) Zhang, F.; Vierock, J.; Yizhar, O.; Fenno, L. E.; Tsunoda, S.; Kianianmomeni, A.; Prigge, M.; Berndt, A.; Cushman, J.; Polle, J.; Magnuson, J.; Hegemann, P.; Deisseroth, K. *Cell* **2011**, *147*, 1446.
(171) Brown, L. S. *Biochim. Biophys. Acta* **2013**, DOI: http://dx.doi.org/10.1016/j.bbabio.2013.05.006.
(172) Lanyi, J. K.; Balashov, S. P. In *Halophiles and Hypersaline Environments*; Ventosa, A., Oren, A., Ma, Y., Eds.; Springer: Berlin, 2011.
(173) Luecke, H.; Schobert, B.; Cartailler, J. P.; Richter, H. T.; Rosengarth, A.; Needleman, R.; Lanyi, J. K. *J. Mol. Biol.* **2000**, *300*, 1237.
(174) Crocker, E.; Eilers, M.; Ahuja, S.; Hornak, V.; Hirshfeld, A.; Sheves, M.; Smith, S. O. *J. Mol. Biol.* **2006**, *357*, 163.
(175) Ihara, K.; Umemura, T.; Katagiri, I.; Kitajima-Ihara, T.; Sugiyama, Y.; Kimura, Y.; Mukohata, Y. *J. Mol. Biol.* **1999**, *285*, 163.
(176) Bergo, V. B.; Ntefidou, M.; Trivedi, V. D.; Amsden, J. J.; Kralj, J. M.; Rothschild, K. J.; Spudich, J. L. *J. Biol. Chem.* **2006**, *281*, 15208.
(177) Shi, L. C.; Yoon, S. R.; Bezerra, A. G.; Jung, K. H.; Brown, L. S. *J. Mol. Biol.* **2006**, *358*, 686.
(178) Aton, B.; Doukas, A. G.; Callender, R. H.; Becher, B.; Ebrey, T. G. *Biochim. Biophys. Acta* **1979**, *576*, 424.
(179) Harbison, G. S.; Smith, S. O.; Pardoen, J. A.; Winkel, C.; Lugtenburg, J.; Herzfeld, J.; Mathies, R.; Griffin, R. G. *Proc. Natl. Acad. Sci. U.S.A.* **1984**, *81*, 1706.
(180) Maeda, A.; Iwasa, T.; Yoshizawa, T. *J. Biochem.* **1977**, *82*, 1599.
(181) Scherrer, P.; Mathew, M. K.; Sperling, W.; Stoeckenius, W. *Biochemistry* **1989**, *28*, 829.
(182) Kalisky, O.; Goldschmidt, C. R.; Ottolenghi, M. *Biophys. J.* **1977**, *19*, 185.
(183) Kawanabe, A.; Furutani, Y.; Jung, K. H.; Kandori, H. *J. Am. Chem. Soc.* **2007**, *129*, 8644.
(184) Vogeley, L.; Sineshchekov, O. A.; Trivedi, V. D.; Sasaki, J.; Spudich, J. L.; Luecke, H. *Science* **2004**, *306*, 1390.
(185) Balashov, S. P.; Ebrey, T. G. *Photochem. Photobiol.* **2001**, *73*, 453.
(186) Haupts, U.; Tittor, J.; Oesterhelt, D. *Annu. Rev. Biophys. Biomol. Struct.* **1999**, *28*, 367.
(187) Herzfeld, J.; Lansing, J. C. *Annu. Rev. Biophys. Biomol. Struct.* **2002**, *31*, 73.
(188) Lanyi, J. K. *Annu. Rev. Physiol.* **2004**, *66*, 665.
(189) Mathies, R. A.; Lin, S. W.; Ames, J. B.; Pollard, W. T. *Annu. Rev. Biophys. Biophys. Chem.* **1991**, *20*, 491.
(190) Lozier, R. H.; Bogomolni, R. A.; Stoeckenius, W. *Biophys. J.* **1975**, *15*, 955.
(191) Braiman, M.; Mathies, R. *Biochemistry* **1980**, *19*, 5421.
(192) Varo, G.; Brown, L. S.; Sasaki, J.; Kandori, H.; Maeda, A.; Needleman, R.; Lanyi, J. K. *Biochemistry* **1995**, *34*, 14490.
(193) Klare, J. P.; Bordignon, E.; Engelhard, M.; Steinhoff, H. J. *Photochem. Photobiol. Sci.* **2004**, *3*, 543.
(194) Oesterhelt, D.; Stoeckenius, W. *Proc. Natl. Acad. Sci. U.S.A.* **1973**, *70*, 2853.
(195) Henderson, R.; Unwin, P. N. *Nature* **1975**, *257*, 28.
(196) Khorana, H. G.; Gerber, G. E.; Herlihy, W. C.; Gray, C. P.; Anderegg, R. J.; Nihei, K.; Biemann, K. *Proc. Natl. Acad. Sci. U.S.A.* **1979**, *76*, 5046.
(197) Alshuth, T.; Stockburger, M. *Ber. Bunsen-Ges.* **1981**, *85*, 484.
(198) Maeda, A. *Isr. J. Chem.* **1995**, *35*, 387.
(199) Rothschild, K. J. *J. Bioenerg. Biomembr.* **1992**, *24*, 147.
(200) Braiman, M. S.; Bousche, O.; Rothschild, K. J. *Proc. Natl. Acad. Sci. U.S.A.* **1991**, *88*, 2388.
(201) Engelhard, M.; Gerwert, K.; Hess, B.; Kreutz, W.; Siebert, F. *Biochemistry* **1985**, *24*, 400.
(202) Pfefferle, J. M.; Maeda, A.; Sasaki, J.; Yoshizawa, T. *Biochemistry* **1991**, *30*, 6548.
(203) Drachev, L. A.; Kaulen, A. D.; Skulachev, V. P. *FEBS Lett.* **1984**, *178*, 331.
(204) Butt, H. J.; Fendler, K.; Bamberg, E.; Tittor, J.; Oesterhelt, D. *EMBO J.* **1989**, *8*, 1657.
(205) Otto, H.; Marti, T.; Holz, M.; Mogi, T.; Lindau, M.; Khorana, H. G.; Heyn, M. P. *Proc. Natl. Acad. Sci. U.S.A.* **1989**, *86*, 9228.
(206) Brown, L. S.; Dioumaev, A. K.; Needleman, R.; Lanyi, J. K. *Biochemistry* **1998**, *37*, 3982.
(207) Haupts, U.; Tittor, J.; Bamberg, E.; Oesterhelt, D. *Biochemistry* **1997**, *36*, 2.
(208) Honig, B.; Ebrey, T.; Callender, R. H.; Dinur, U.; Ottolenghi, M. *Proc. Natl. Acad. Sci. U.S.A.* **1979**, *76*, 2503.
(209) Schulten, K.; Tavan, P. *Nature* **1978**, *272*, 85.
(210) Subramaniam, S.; Henderson, R. *Nature* **2000**, *406*, 653.
(211) Han, B. G.; Vonck, J.; Glaeser, R. M. *Biophys. J.* **1994**, *67*, 1179.
(212) Hessling, B.; Herbst, J.; Rammelsberg, R.; Gerwert, K. *Biophys. J.* **1997**, *73*, 2071.
(213) Hu, J. G.; Sun, B. Q.; Bizounok, M.; Hatcher, M. E.; Lansing, J. C.; Raap, J.; Verdegem, P. J. E.; Lugtenburg, J.; Griffin, R. G.; Herzfeld, J. *Biochemistry* **1998**, *37*, 8088.
(214) Lanyi, J. K.; Schobert, B. *J. Mol. Biol.* **2002**, *321*, 727.
(215) Nagel, G.; Kelety, B.; Mockel, B.; Buldt, G.; Bamberg, E. *Biophys. J.* **1998**, *74*, 403.
(216) Sass, H. J.; Schachowa, I. W.; Rapp, G.; Koch, M. H.; Oesterhelt, D.; Dencher, N. A.; Buldt, G. *EMBO J.* **1997**, *16*, 1484.
(217) Varo, G.; Lanyi, J. K. *Biochemistry* **1991**, *30*, 5008.
(218) Lorenz-Fonfria, V. A.; Kandori, H. *J. Am. Chem. Soc.* **2009**, *131*, 5891.
(219) Gerwert, K. *Biol. Chem.* **1999**, *380*, 931.
(220) Heberle, J. *Biochim. Biophys. Acta* **2000**, *1458*, 135.
(221) Kandori, H. *Biochim. Biophys. Acta* **2000**, *1460*, 177.
(222) Siebert, F. *Methods Enzymol.* **1995**, *246*, 501.
(223) Gerwert, K.; Souvignier, G.; Hess, B. *Proc. Natl. Acad. Sci. U.S.A.* **1990**, *87*, 9774.
(224) Souvignier, G.; Gerwert, K. *Biophys. J.* **1992**, *63*, 1393.
(225) Balashov, S. P.; Imasheva, E. S.; Ebrey, T. G.; Chen, N.; Menick, D. R.; Crouch, R. K. *Biochemistry* **1997**, *36*, 8671.
(226) Brown, L. S.; Sasaki, J.; Kandori, H.; Maeda, A.; Needleman, R.; Lanyi, J. K. *J. Biol. Chem.* **1995**, *270*, 27122.
(227) Govindjee, R.; Kono, M.; Balashov, S. P.; Imasheva, E.; Sheves, M.; Ebrey, T. G. *Biochemistry* **1995**, *34*, 4828.
(228) Hutson, M. S.; Alexiev, U.; Shilov, S. V.; Wise, K. J.; Braiman, M. S. *Biochemistry* **2000**, *39*, 13189.
(229) Zscherp, C.; Heberle, J. *J. Phys. Chem. B* **1997**, *101*, 10542.
(230) Rammelsberg, R.; Huhn, G.; Lubben, M.; Gerwert, K. *Biochemistry* **1998**, *37*, 5001.
(231) Lorenz-Fonfria, V. A.; Furutani, Y.; Kandori, H. *Biochemistry* **2008**, *47*, 4071.
(232) Garczarek, F.; Brown, L. S.; Lanyi, J. K.; Gerwert, K. *Proc. Natl. Acad. Sci. U.S.A.* **2005**, *102*, 3633.
(233) Phatak, P.; Ghosh, N.; Yu, H.; Cui, Q.; Elstner, M. *Proc. Natl. Acad. Sci. U.S.A.* **2008**, *105*, 19672.
(234) Balashov, S. P. *Biochim. Biophys. Acta* **2000**, *1460*, 75.
(235) Balashov, S. P.; Imasheva, E. S.; Govindjee, R.; Ebrey, T. G. *Biophys. J.* **1996**, *70*, 473.
(236) Dioumaev, A. K.; Richter, H. T.; Brown, L. S.; Tanio, M.; Tuzi, S.; Saito, H.; Kimura, Y.; Needleman, R.; Lanyi, J. K. *Biochemistry* **1998**, *37*, 2496.
(237) Kandori, H. *Biochim. Biophys. Acta* **2004**, *1658*, 72.
(238) Garczarek, F.; Gerwert, K. *Nature* **2006**, *439*, 109.
(239) Luecke, H.; Schobert, B.; Richter, H. T.; Cartailler, J. P.; Lanyi, J. K. *Science* **1999**, *286*, 255.
(240) Luecke, H.; Schobert, B.; Richter, H. T.; Cartailler, J. P.; Lanyi, J. K. *J. Mol. Biol.* **1999**, *291*, 899.
(241) Kamikubo, H.; Kataoka, M.; Varo, G.; Oka, T.; Tokunaga, F.; Needleman, R.; Lanyi, J. K. *Proc. Natl. Acad. Sci. U.S.A.* **1996**, *93*, 1386.
(242) Oka, T.; Kamikubo, H.; Tokunaga, F.; Lanyi, J. K.; Needleman, R.; Kataoka, M. *Biophys. J.* **1999**, *76*, 1018.
(243) Rink, T.; Pfeiffer, M.; Oesterhelt, D.; Gerwert, K.; Steinhoff, H. J. *Biophys. J.* **2000**, *78*, 1519.
(244) Shibata, M.; Yamashita, H.; Uchihashi, T.; Kandori, H.; Ando, T. *Nat. Nanotechnol.* **2010**, *5*, 208.

(245) Subramaniam, S.; Lindahl, I.; Bullough, P.; Faruqi, A. R.; Tittor, J.; Oesterhelt, D.; Brown, L.; Lanyi, J.; Henderson, R. *J. Mol. Biol.* **1999**, *287*, 145.
(246) Vonck, J. *Biochemistry* **1996**, *35*, 5870.
(247) Brown, L. S.; Kamikubo, H.; Zimanyi, L.; Kataoka, M.; Tokunaga, F.; Verdegem, P.; Lugtenburg, J.; Lanyi, J. K. *Proc. Natl. Acad. Sci. U.S.A.* **1997**, *94*, 5040.
(248) Tittor, J.; Paula, S.; Subramaniam, S.; Heberle, J.; Henderson, R.; Oesterhelt, D. *J. Mol. Biol.* **2002**, *319*, 555.
(249) Dioumaev, A. K.; Brown, L. S.; Needleman, R.; Lanyi, J. K. *Biochemistry* **1998**, *37*, 9889.
(250) Lanyi, J. K.; Schobert, B. *Biochemistry* **2004**, *43*, 3.
(251) Lanyi, J. K. *J. Mol. Microbiol. Biotechnol.* **2007**, *12*, 210.
(252) Hirai, T.; Subramaniam, S.; Lanyi, J. K. *Curr. Opin. Struct. Biol.* **2009**, *19*, 433.
(253) Luecke, H.; Lanyi, J. K. *Membrane Proteins* **2003**, *63*, 111.
(254) Neutze, R.; Pebay-Peyroula, E.; Edman, K.; Royant, A.; Navarro, J.; Landau, E. M. *Biochim. Biophys. Acta* **2002**, *1565*, 144.
(255) Betancourt, F. M.; Glaeser, R. M. *Biochim. Biophys. Acta* **2000**, *1460*, 106.
(256) Facciotti, M. T.; Rouhani, S.; Glaeser, R. M. *FEBS Lett.* **2004**, *564*, 301.
(257) Luecke, H.; Lanyi, J. K. *J. Gen. Physiol.* **2000**, *116*, 3A.
(258) Beja, O.; Aravind, L.; Koonin, E. V.; Suzuki, M. T.; Hadd, A.; Nguyen, L. P.; Jovanovich, S.; Gates, C. M.; Feldman, R. A.; Spudich, J. L.; Spudich, E. N.; DeLong, E. F. *Science* **2000**, *289*, 1902.
(259) Atamna-Ismaeel, N.; Sabehi, G.; Sharon, I.; Witzel, K. P.; Labrenz, M.; Jurgens, K.; Barkay, T.; Stomp, M.; Huisman, J.; Beja, O. *ISME J.* **2008**, *2*, 656.
(260) de la Torre, J. R.; Christianson, L. M.; Beja, O.; Suzuki, M. T.; Karl, D. M.; Heidelberg, J.; DeLong, E. F. *Proc. Natl. Acad. Sci. U.S.A.* **2003**, *100*, 12830.
(261) Martinez-Garcia, M.; Swan, B. K.; Poulton, N. J.; Gomez, M. L.; Masland, D.; Sieracki, M. E.; Stepanauskas, R. *ISME J.* **2012**, *6*, 113.
(262) McCarren, J.; DeLong, E. F. *Environ. Microbiol.* **2007**, *9*, 846.
(263) Venter, J. C.; Remington, K.; Heidelberg, J. F.; Halpern, A. L.; Rusch, D.; Eisen, J. A.; Wu, D.; Paulsen, I.; Nelson, K. E.; Nelson, W.; Fouts, D. E.; Levy, S.; Knap, A. H.; Lomas, M. W.; Nealson, K.; White, O.; Peterson, J.; Hoffman, J.; Parsons, R.; Baden-Tillson, H.; Pfannkoch, C.; Rogers, Y. H.; Smith, H. O. *Science* **2004**, *304*, 66.
(264) Beja, O.; Spudich, E. N.; Spudich, J. L.; Leclerc, M.; DeLong, E. F. *Nature* **2001**, *411*, 786.
(265) Bielawski, J. P.; Dunn, K. A.; Sabehi, G.; Beja, O. *Proc. Natl. Acad. Sci. U.S.A.* **2004**, *101*, 14824.
(266) Sineshchekov, O. A.; Spudich, J. L. *Photochem. Photobiol. Sci.* **2004**, *3*, 548.
(267) Walter, J. M.; Greenfield, D.; Bustamante, C.; Liphardt, J. *Proc. Natl. Acad. Sci. U.S.A.* **2007**, *104*, 2408.
(268) DeLong, E. F.; Beja, O. *PLoS Biol.* **2010**, *8*, e1000359.
(269) Gomez-Consarnau, L.; Akram, N.; Lindell, K.; Pedersen, A.; Neutze, R.; Milton, D. L.; Gonzalez, J. M.; Pinhassi, J. *PLoS Biol.* **2010**, *8*, e1000358.
(270) Steindler, L.; Schwalbach, M. S.; Smith, D. P.; Chan, F.; Giovannoni, S. J. *PLoS One* **2011**, *6*, e19725.
(271) Stingl, U.; Desiderio, R. A.; Cho, J. C.; Vergin, K. L.; Giovannoni, S. J. *Appl. Environ. Microbiol.* **2007**, *73*, 2290.
(272) Fuhrman, J. A.; Schwalbach, M. S.; Stingl, U. *Nat. Rev. Microbiol.* **2008**, *6*, 488.
(273) Kralj, J. M.; Bergo, V. B.; Amsden, J. J.; Spudich, E. N.; Spudich, J. L.; Rothschild, K. J. *Biochemistry* **2008**, *47*, 3447.
(274) Spudich, J. L. *Trends Microbiol.* **2006**, *14*, 480.
(275) Miranda, M. R.; Choi, A. R.; Shi, L.; Bezerra, A. G., Jr.; Jung, K. H.; Brown, L. S. *Biophys. J.* **2009**, *96*, 1471.
(276) Sharma, A. K.; Zhaxybayeva, O.; Papke, R. T.; Doolittle, W. F. *Environ. Microbiol.* **2008**, *10*, 1039.
(277) Sharma, A. K.; Sommerfeld, K.; Bullerjahn, G. S.; Matteson, A. R.; Wilhelm, S. W.; Jezbera, J.; Brandt, U.; Doolittle, W. F.; Hahn, M. W. *ISME J.* **2009**, *3*, 726.
(278) Balashov, S. P.; Imasheva, E. S.; Boichenko, V. A.; Anton, J.; Wang, J. M.; Lanyi, J. K. *Science* **2005**, *309*, 2061.
(279) Luecke, H.; Schobert, B.; Stagno, J.; Imasheva, E. S.; Wang, J. M.; Balashov, S. P.; Lanyi, J. K. *Proc. Natl. Acad. Sci. U.S.A.* **2008**, *105*, 16561.
(280) Imasheva, E. S.; Balashov, S. P.; Choi, A. R.; Jung, K. H.; Lanyi, J. K. *Biochemistry* **2009**, *48*, 10948.
(281) Balashov, S. P.; Petrovskaya, L. E.; Lukashev, E. P.; Imasheva, E. S.; Dioumaev, A. K.; Wang, J. M.; Sychev, S. V.; Dolgikh, D. A.; Rubin, A. B.; Kirpichnikov, M. P.; Lanyi, J. K. *Biochemistry* **2012**, *51*, 5748.
(282) Bergo, V. B.; Sineshchekov, O. A.; Kralj, J. M.; Partha, R.; Spudich, E. N.; Rothschild, K. J.; Spudich, J. L. *J. Biol. Chem.* **2009**, *284*, 2836.
(283) Hempelmann, F.; Holper, S.; Verhoefen, M. K.; Woerner, A. C.; Kohler, T.; Fiedler, S. A.; Pfleger, N.; Wachtveitl, J.; Glaubitz, C. *J. Am. Chem. Soc.* **2011**, *133*, 4645.
(284) Partha, R.; Krebs, R.; Caterino, T. L.; Braiman, M. S. *Biochim. Biophys. Acta, Bioenerg.* **2005**, *1708*, 6.
(285) Dioumaev, A. K.; Brown, L. S.; Shih, J.; Spudich, E. N.; Spudich, J. L.; Lanyi, J. K. *Biochemistry* **2002**, *41*, 5348.
(286) Friedrich, T.; Geibel, S.; Kalmbach, R.; Chizhov, I.; Ataka, K.; Heberle, J.; Engelhard, M.; Bamberg, E. *J. Mol. Biol.* **2002**, *321*, 821.
(287) Imasheva, E. S.; Balashov, S. P.; Wang, J. M.; Lanyi, J. K. *Photochem. Photobiol.* **2006**, *82*, 1406.
(288) Tamogami, J.; Kikukawa, T.; Nara, T.; Shimono, K.; Demura, M.; Kamo, N. *Biochemistry* **2012**, *51*, 9290.
(289) Hashimoto, K.; Choi, A. R.; Furutani, Y.; Jung, K. H.; Kandori, H. *Biochemistry* **2010**, *49*, 3343.
(290) Petrovskaya, L. E.; Lukashev, E. P.; Chupin, V. V.; Sychev, S. V.; Lyukmanova, E. N.; Kryukova, E. A.; Ziganshin, R. H.; Spirina, E. V.; Rivkina, E. M.; Khatypov, R. A.; Erokhina, L. G.; Gilichinsky, D. A.; Shuvalov, V. A.; Kirpichnikov, M. P. *FEBS Lett.* **2010**, *584*, 4193.
(291) Slamovits, C. H.; Okamoto, N.; Burri, L.; James, E. R.; Keeling, P. J. *Nat. Commun.* **2011**, *2*, 183.
(292) Brown, L. S. *Photochem. Photobiol. Sci.* **2004**, *3*, 555.
(293) Fan, Y.; Solomon, P.; Oliver, R. P.; Brown, L. S. *Biochim. Biophys. Acta* **2011**, *1807*, 1457.
(294) Waschuk, S. A.; Bezerra, A. G., Jr.; Shi, L.; Brown, L. S. *Proc. Natl. Acad. Sci. U.S.A.* **2005**, *102*, 6879.
(295) Idnurm, A.; Verma, S.; Corrochano, L. M. *Fungal Genet. Biol.* **2010**, *47*, 881.
(296) Tsunoda, S. P.; Ewers, D.; Gazzarrini, S.; Moroni, A.; Gradmann, D.; Hegemann, P. *Biophys. J.* **2006**, *91*, 1471.
(297) Wada, T.; Shimono, K.; Kikukawa, T.; Hato, M.; Shinya, N.; Kim, S. Y.; Kimura-Someya, T.; Shirouzu, M.; Tamogami, J.; Miyauchi, S.; Jung, K. H.; Kamo, N.; Yokoyama, S. *J. Mol. Biol.* **2011**, *411*, 986.
(298) Ito, H.; Sumii, M.; Kawanabe, A.; Fan, Y.; Furutani, Y.; Brown, L. S.; Kandori, H. *J. Phys. Chem. B* **2012**, *116*, 11881.
(299) Furutani, Y.; Ikeda, D.; Shibata, M.; Kandori, H. *Chem. Phys.* **2006**, *324*, 705.
(300) Schobert, B.; Lanyi, J. K. *J. Biol. Chem.* **1982**, *257*, 10306.
(301) Sasaki, J.; Brown, L. S.; Chon, Y. S.; Kandori, H.; Maeda, A.; Needleman, R.; Lanyi, J. K. *Science* **1995**, *269*, 73.
(302) Tittor, J.; Haupts, U.; Haupts, C.; Oesterhelt, D.; Becker, A.; Bamberg, E. *J. Mol. Biol.* **1997**, *271*, 405.
(303) Kolbe, M.; Besir, H.; Essen, L. O.; Oesterhelt, D. *Science* **2000**, *288*, 1390.
(304) Kouyama, T.; Kanada, S.; Takeguchi, Y.; Narusawa, A.; Murakami, M.; Ihara, K. *J. Mol. Biol.* **2010**, *396*, 564.
(305) Nakashima, K.; Nakamura, T.; Takeuchi, S.; Shibata, M.; Demura, M.; Tahara, T.; Kandori, H. *J. Phys. Chem. B* **2009**, *113*, 8429.
(306) Shibata, M.; Muneda, N.; Sasaki, T.; Shimono, K.; Kamo, N.; Demura, M.; Kandori, H. *Biochemistry* **2005**, *44*, 12279.
(307) Hegemann, P.; Oesterbelt, D.; Steiner, M. *EMBO J.* **1985**, *4*, 2347.
(308) Lanyi, J. K. *Biochemistry* **1986**, *25*, 6706.
(309) Chizhov, I.; Engelhard, M. *Biophys. J.* **2001**, *81*, 1600.

(310) Chon, Y. S.; Kandori, H.; Sasaki, J.; Lanyi, J. K.; Needleman, R.; Maeda, A. *Biochemistry* **1999**, *38*, 9449.
(311) Hackmann, C.; Guijarro, J.; Chizhov, I.; Engelhard, M.; Rodig, C.; Siebert, F. *Biophys. J.* **2001**, *81*, 394.
(312) Gerscher, S.; Mylrajan, M.; Hildebrandt, P.; Baron, M. H.; Muller, R.; Engelhard, M. *Biochemistry* **1997**, *36*, 11012.
(313) Gruia, A. D.; Bondar, A. N.; Smith, J. C.; Fischer, S. *Structure* **2005**, *13*, 617.
(314) Kanada, S.; Takeguchi, Y.; Murakami, M.; Ihara, K.; Kouyama, T. *J. Mol. Biol.* **2011**, *413*, 162.
(315) Havelka, W. A.; Henderson, R.; Oesterhelt, D. *J. Mol. Biol.* **1995**, *247*, 726.
(316) Varo, G.; Brown, L. S.; Needleman, R.; Lanyi, J. K. *Biochemistry* **1996**, *35*, 6604.
(317) Muneda, N.; Shibata, M.; Demura, M.; Kandori, H. *J. Am. Chem. Soc.* **2006**, *128*, 6294.
(318) Kwon, S. K.; Kim, B. K.; Song, J. Y.; Kwak, M. J.; Lee, C. H.; Yoon, J. H.; Oh, T. K.; Kim, J. F. *Genome Biol. Evol.* **2013**, *5*, 187.
(319) Hoff, W. D.; Jung, K. H.; Spudich, J. L. *Annu. Rev. Biophys. Biomol. Struct.* **1997**, *26*, 223.
(320) Bogomolni, R. A.; Spudich, J. L. *Proc. Natl. Acad. Sci. U.S.A.* **1982**, *79*, 6250.
(321) Takahashi, T.; Yan, B.; Nakanishi, K.; Spudich, J. L. *Biol. Chem. Hoppe-Seyler* **1990**, *371*, 901.
(322) Mongodin, E. F.; Nelson, K. E.; Daugherty, S.; Deboy, R. T.; Wister, J.; Khouri, H.; Weidman, J.; Walsh, D. A.; Papke, R. T.; Sanchez Perez, G.; Sharma, A. K.; Nesbo, C. L.; MacLeod, D.; Bapteste, E.; Doolittle, W. F.; Charlebois, R. L.; Legault, B.; Rodriguez-Valera, F. *Proc. Natl. Acad. Sci. U.S.A.* **2005**, *102*, 18147.
(323) Klare, J. P.; Gordeliy, V. I.; Labahn, J.; Buldt, G.; Steinhoff, H. J.; Engelhard, M. *FEBS Lett.* **2004**, *564*, 219.
(324) Bogomolni, R. A.; Stoeckenius, W.; Szundi, I.; Perozo, E.; Olson, K. D.; Spudich, J. L. *Proc. Natl. Acad. Sci. U.S.A.* **1994**, *91*, 10188.
(325) Sasaki, J.; Spudich, J. L. *Biochim. Biophys. Acta* **2000**, *1460*, 230.
(326) Sudo, Y.; Iwamoto, M.; Shimono, K.; Sumi, M.; Kamo, N. *Biophys. J.* **2001**, *80*, 916.
(327) Takahashi, T.; Mochizuki, Y.; Kamo, N.; Kobatake, Y. *Biochem. Biophys. Res. Commun.* **1985**, *127*, 99.
(328) Sineshchekov, O. A.; Sasaki, J.; Wang, J.; Spudich, J. L. *Biochemistry* **2010**, *49*, 6696.
(329) Gordeliy, V. I.; Labahn, J.; Moukhametzianov, R.; Efremov, R.; Granzin, J.; Schlesinger, R.; Buldt, G.; Savopol, T.; Scheidig, A. J.; Klare, J. P.; Engelhard, M. *Nature* **2002**, *419*, 484.
(330) Inoue, K.; Sasaki, J.; Morisaki, M.; Tokunaga, F.; Terazima, M. *Biophys. J.* **2004**, *87*, 2587.
(331) Moukhametzianov, R.; Klare, J. P.; Efremov, R.; Baeken, C.; Goppner, A.; Labahn, J.; Engelhard, M.; Buldt, G.; Gordeliy, V. I. *Nature* **2006**, *440*, 115.
(332) Wegener, A. A.; Chizhov, I.; Engelhard, M.; Steinhoff, H. J. *J. Mol. Biol.* **2000**, *301*, 881.
(333) Wegener, A. A.; Klare, J. P.; Engelhard, M.; Steinhoff, H. J. *EMBO J.* **2001**, *20*, 5312.
(334) Ito, M.; Sudo, Y.; Furutani, Y.; Okitsu, T.; Wada, A.; Homma, M.; Spudich, J. L.; Kandori, H. *Biochemistry* **2008**, *47*, 6208.
(335) Sudo, Y.; Furutani, Y.; Wada, A.; Ito, M.; Kamo, N.; Kandori, H. *J. Am. Chem. Soc.* **2005**, *127*, 16036.
(336) Sudo, Y.; Spudich, J. L. *Proc. Natl. Acad. Sci. U.S.A.* **2006**, *103*, 16129.
(337) Wang, S.; Kim, S. Y.; Jung, K. H.; Ladizhansky, V.; Brown, L. S. *J. Mol. Biol.* **2011**, *411*, 449.
(338) Ugalde, J. A.; Podell, S.; Narasingarao, P.; Allen, E. E. *Biol. Direct* **2011**, *6*, 52.
(339) Irieda, H.; Morita, T.; Maki, K.; Homma, M.; Aiba, H.; Sudo, Y. *J. Biol. Chem.* **2012**, *287*, 32485.
(340) Furutani, Y.; Kawanabe, A.; Jung, K. H.; Kandori, H. *Biochemistry* **2005**, *44*, 12287.
(341) Sineshchekov, O. A.; Trivedi, V. D.; Sasaki, J.; Spudich, J. L. *J. Biol. Chem.* **2005**, *280*, 14663.
(342) Kondoh, M.; Inoue, K.; Sasaki, J.; Spudich, J. L.; Terazima, M. *J. Am. Chem. Soc.* **2011**, *133*, 13406.
(343) Kateriya, S.; Nagel, G.; Bamberg, E.; Hegemann, P. *News Physiol. Sci.* **2004**, *19*, 133.
(344) Luck, M.; Mathes, T.; Bruun, S.; Fudim, R.; Hagedorn, R.; Tran Nguyen, T. M.; Kateriya, S.; Kennis, J. T.; Hildebrandt, P.; Hegemann, P. *J. Biol. Chem.* **2012**, *287*, 40083.
(345) Engelmann, T. W. *Bot. Ztg.* **1882**, *40*, 419.
(346) Mast, S. O. *J. Exp. Zool.* **1916**, *20*, 1.
(347) Halldal, P. *Nature* **1957**, *179*, 215.
(348) Schmidt, J. A.; Eckert, R. *Nature* **1976**, *262*, 713.
(349) Foster, K. W.; Smyth, R. D. *Microbiol. Rev.* **1980**, *44*, 572.
(350) Foster, K. W.; Saranak, J.; Patel, N.; Zarilli, G.; Okabe, M.; Kline, T.; Nakanishi, K. *Nature* **1984**, *311*, 756.
(351) Derguini, F.; Mazur, P.; Nakanishi, K.; Starace, D. M.; Saranak, J.; Foster, K. W. *Photochem. Photobiol.* **1991**, *54*, 1017.
(352) Beckmann, M.; Hegemann, P. *Biochemistry* **1991**, *30*, 3692.
(353) Harz, H.; Hegemann, P. *Nature* **1991**, *351*, 489.
(354) Braun, F. J.; Hegemann, P. *Biophys. J.* **1999**, *76*, 1668.
(355) Hegemann, P.; Fuhrmann, M.; Kateriya, S. *J. Phycol.* **2001**, *37*, 668.
(356) Sineshchekov, O. A.; Jung, K. H.; Spudich, J. L. *Proc. Natl. Acad. Sci. U.S.A.* **2002**, *99*, 8689.
(357) Suzuki, T.; Yamasaki, K.; Fujita, S.; Oda, K.; Iseki, M.; Yoshida, K.; Watanabe, M.; Daiyasu, H.; Toh, H.; Asamizu, E.; Tabata, S.; Miura, K.; Fukuzawa, H.; Nakamura, S.; Takahashi, T. *Biochem. Biophys. Res. Commun.* **2003**, *301*, 711.
(358) Govorunova, E. G.; Jung, K. H.; Sineshchekov, O. A.; Spudich, J. L. *Biophys. J.* **2004**, *86*, 2342.
(359) Berthold, P.; Tsunoda, S. P.; Ernst, O. P.; Mages, W.; Gradmann, D.; Hegemann, P. *Plant Cell* **2008**, *20*, 1665.
(360) Bi, A.; Cui, J.; Ma, Y. P.; Olshevskaya, E.; Pu, M.; Dizhoor, A. M.; Pan, Z. H. *Neuron* **2006**, *50*, 23.
(361) Boyden, E. S.; Zhang, F.; Bamberg, E.; Nagel, G.; Deisseroth, K. *Nat. Neurosci.* **2005**, *8*, 1263.
(362) Ishizuka, T.; Kakuda, M.; Araki, R.; Yawo, H. *Neurosci. Res.* **2006**, *54*, 85.
(363) Li, X.; Gutierrez, D. V.; Hanson, M. G.; Han, J.; Mark, M. D.; Chiel, H.; Hegemann, P.; Landmesser, L. T.; Herlitze, S. *Proc. Natl. Acad. Sci. U.S.A.* **2005**, *102*, 17816.
(364) Nagel, G.; Brauner, M.; Liewald, J. F.; Adeishvili, N.; Bamberg, E.; Gottschalk, A. *Curr. Biol.* **2005**, *15*, 2279.
(365) Ullrich, S.; Gueta, R.; Nagel, G. *Biol. Chem.* **2013**, *394*, 271.
(366) Govorunova, E. G.; Spudich, E. N.; Lane, C. E.; Sineshchekov, O. A.; Spudich, J. L. *mBio* **2011**, *2*, e00115.
(367) Kleinlogel, S.; Terpitz, U.; Legrum, B.; Gokbuget, D.; Boyden, E. S.; Bamann, C.; Wood, P. G.; Bamberg, E. *Nat. Methods* **2011**, *8*, 1083.
(368) Ernst, O. P.; Sanchez Murcia, P. A.; Daldrop, P.; Tsunoda, S. P.; Kateriya, S.; Hegemann, P. *J. Biol. Chem.* **2008**, *283*, 1637.
(369) Bamann, C.; Kirsch, T.; Nagel, G.; Bamberg, E. *J. Mol. Biol.* **2008**, *375*, 686.
(370) Ritter, E.; Stehfest, K.; Berndt, A.; Hegemann, P.; Bartl, F. J. *J. Biol. Chem.* **2008**, *283*, 35033.
(371) Muller, M.; Bamann, C.; Bamberg, E.; Kuhlbrandt, W. *J. Mol. Biol.* **2011**, *414*, 86.
(372) Tsunoda, S. P.; Hegemann, P. *Photochem. Photobiol.* **2009**, *85*, 564.
(373) Wen, L.; Wang, H.; Tanimoto, S.; Egawa, R.; Matsuzaka, Y.; Mushiake, H.; Ishizuka, T.; Yawo, H. *PLoS One* **2010**, *5*, e12893.
(374) Lin, J. Y.; Lin, M. Z.; Steinbach, P.; Tsien, R. Y. *Biophys. J.* **2009**, *96*, 1803.
(375) Watanabe, H. C.; Welke, K.; Schneider, F.; Tsunoda, S.; Zhang, F.; Deisseroth, K.; Hegemann, P.; Elstner, M. *J. Biol. Chem.* **2012**, *287*, 7456.
(376) Watanabe, H. C.; Welke, K.; Sindhikara, D. J.; Hegemann, P.; Elstner, M. *J. Mol. Biol.* **2013**, *425*, 1795.

(377) Eisenhauer, K.; Kuhne, J.; Ritter, E.; Berndt, A.; Wolf, S.; Freier, E.; Bartl, F.; Hegemann, P.; Gerwert, K. *J. Biol. Chem.* **2012**, *287*, 6904.
(378) Lorenz-Fonfria, V. A.; Resler, T.; Krause, N.; Nack, M.; Gossing, M.; Fischer von Mollard, G.; Bamann, C.; Bamberg, E.; Schlesinger, R.; Heberle, J. *Proc. Natl. Acad. Sci. U.S.A.* **2013**, *110*, E1273.
(379) Verhoefen, M. K.; Bamann, C.; Blocher, R.; Forster, U.; Bamberg, E.; Wachtveitl, J. *ChemPhysChem* **2010**, *11*, 3113.
(380) Kamiya, M.; Kato, H. E.; Ishitani, R.; Nureki, O.; Hayashi, S. *Chem. Phys. Lett.* **2013**, *556*, 266.
(381) Sineshchekov, O. A.; Govorunova, E. G.; Wang, J.; Li, H.; Spudich, J. L. *Biophys. J.* **2013**, *104*, 807.
(382) Gunaydin, L. A.; Yizhar, O.; Berndt, A.; Sohal, V. S.; Deisseroth, K.; Hegemann, P. *Nat. Neurosci.* **2010**, *13*, 387.
(383) Gradmann, D.; Berndt, A.; Schneider, F.; Hegemann, P. *Biophys. J.* **2011**, *101*, 1057.
(384) Sattig, T.; Rickert, C.; Bamberg, E.; Steinhoff, H. J.; Bamann, C. *Angew. Chem., Int. Ed.* **2013**, *52*, 9705.
(385) Krause, N.; Engelhard, C.; Heberle, J.; Schlesinger, R.; Bittl, R. *FEBS Lett.* **2013**, *587*, 3309.
(386) Berndt, A.; Yizhar, O.; Gunaydin, L. A.; Hegemann, P.; Deisseroth, K. *Nat. Neurosci.* **2009**, *12*, 229.
(387) Bamann, C.; Gueta, R.; Kleinlogel, S.; Nagel, G.; Bamberg, E. *Biochemistry* **2010**, *49*, 267.
(388) Yizhar, O.; Fenno, L.; Zhang, F.; Hegemann, P.; Diesseroth, K. *Cold Spring Harbor Protoc.* **2011**, *2011*, top102.
(389) Nack, M.; Radu, I.; Bamann, C.; Bamberg, E.; Heberle, J. *FEBS Lett.* **2009**, *583*, 3676.
(390) Nack, M.; Radu, I.; Schultz, B. J.; Resler, T.; Schlesinger, R.; Bondar, A. N.; del Val, C.; Abbruzzetti, S.; Viappiani, C.; Bamann, C.; Bamberg, E.; Heberle, J. *FEBS Lett.* **2012**, *586*, 1344.
(391) Radu, I.; Bamann, C.; Nack, M.; Nagel, G.; Bamberg, E.; Heberle, J. *J. Am. Chem. Soc.* **2009**, *131*, 7313.
(392) Gaiko, O.; Dempski, R. E. *Biophys. J.* **2013**, *104*, 1230.
(393) Plazzo, A. P.; De Franceschi, N.; Da Broi, F.; Zonta, F.; Sanasi, M. F.; Filippini, F.; Mongillo, M. *J. Biol. Chem.* **2012**, *287*, 4818.
(394) Harz, H.; Nonnengasser, C.; Hegemann, P. *Philos. Trans. R. Soc., B* **1992**, *338*, 39.
(395) Feldbauer, K.; Zimmermann, D.; Pintschovius, V.; Spitz, J.; Bamann, C.; Bamberg, E. *Proc. Natl. Acad. Sci. U.S.A.* **2009**, *106*, 12317.
(396) Sugiyama, Y.; Wang, H.; Hikima, T.; Sato, M.; Kuroda, J.; Takahashi, T.; Ishizuka, T.; Yawo, H. *Photochem. Photobiol. Sci.* **2009**, *8*, 328.
(397) Ruffert, K.; Himmel, B.; Lall, D.; Bamann, C.; Bamberg, E.; Betz, H.; Eulenburg, V. *Biochem. Biophys. Res. Commun.* **2011**, *410*, 737.
(398) Tanimoto, S.; Sugiyama, Y.; Takahashi, T.; Ishizuka, T.; Yawo, H. *Neurosci. Res.* **2013**, *75*, 13.
(399) Luo, D. G.; Yue, W. W.; Ala-Laurila, P.; Yau, K. W. *Science* **2011**, *332*, 1307.
(400) Hou, S. Y.; Govorunova, E. G.; Ntefidou, M.; Lane, C. E.; Spudich, E. N.; Sineshchekov, O. A.; Spudich, J. L. *Photochem. Photobiol.* **2012**, *88*, 119.
(401) Govorunova, E. G.; Sineshchekov, O. A.; Li, H.; Janz, R.; Spudich, J. L. *J. Biol. Chem.* **2013**, *288*, 29911.
(402) Lin, J. Y.; Knutsen, P. M.; Muller, A.; Kleinfeld, D.; Tsien, R. Y. *Nat. Neurosci.* **2013**, *16*, 1499.
(403) Papagiakoumou, E.; Anselmi, F.; Begue, A.; de Sars, V.; Gluckstad, J.; Isacoff, E. Y.; Emiliani, V. *Nat. Methods* **2010**, *7*, 848.
(404) Zhang, F.; Gradinaru, V.; Adamantidis, A. R.; Durand, R.; Airan, R. D.; de Lecea, L.; Deisseroth, K. *Nat. Protoc.* **2010**, *5*, 439.
(405) Burguiere, E.; Monteiro, P.; Feng, G.; Graybiel, A. M. *Science* **2013**, *340*, 1243.
(406) Sahel, J. A.; Roska, B. *Annu. Rev. Neurosci.* **2013**, *36*, 467.
(407) Kleinlogel, S.; Feldbauer, K.; Dempski, R. E.; Fotis, H.; Wood, P. G.; Bamann, C.; Bamberg, E. *Nat. Neurosci.* **2011**, *14*, 513.
(408) Caro, L. N.; Moreau, C. J.; Estrada-Mondragon, A.; Ernst, O. P.; Vivaudou, M. *PLoS One* **2012**, *7*, e43766.
(409) Yau, K. W.; Hardie, R. C. *Cell* **2009**, *139*, 246.
(410) Terakita, A. *Genome Biol.* **2005**, *6*, 213.
(411) Kojima, D.; Fukada, Y. *Novartis Found. Symp.* **1999**, *224*, 265.
(412) Ohuchi, H.; Yamashita, T.; Tomonari, S.; Fujita-Yanagibayashi, S.; Sakai, K.; Noji, S.; Shichida, Y. *PLoS One* **2012**, *7*, e31534.
(413) Fredriksson, R.; Lagerstrom, M. C.; Lundin, L. G.; Schioth, H. B. *Mol. Pharmacol.* **2003**, *63*, 1256.
(414) Porter, M. L.; Blasic, J. R.; Bok, M. J.; Cameron, E. G.; Pringle, T.; Cronin, T. W.; Robinson, P. R. *Proc. R. Soc. B* **2012**, *279*, 3.
(415) Gehring, W. J. *WIREs Dev. Biol.* **2012**, 1759.
(416) Wicks, N. L.; Chan, J. W.; Najera, J. A.; Ciriello, J. M.; Oancea, E. *Curr. Biol.* **2011**, *21*, 1906.
(417) Katritch, V.; Cherezov, V.; Stevens, R. C. *Trends Pharmacol. Sci.* **2012**, *33*, 17.
(418) Katritch, V.; Cherezov, V.; Stevens, R. C. *Annu. Rev. Pharmacol. Toxicol.* **2013**, *53*, 531.
(419) Venkatakrishnan, A. J.; Deupi, X.; Lebon, G.; Tate, C. G.; Schertler, G. F.; Babu, M. M. *Nature* **2013**, *494*, 185.
(420) Li, J.; Edwards, P. C.; Burghammer, M.; Villa, C.; Schertler, G. F. *J. Mol. Biol.* **2004**, *343*, 1409.
(421) Palczewski, K.; Kumasaka, T.; Hori, T.; Behnke, C. A.; Motoshima, H.; Fox, B. A.; Le Trong, I.; Teller, D. C.; Okada, T.; Stenkamp, R. E.; Yamamoto, M.; Miyano, M. *Science* **2000**, *289*, 739.
(422) Murakami, M.; Kouyama, T. *Nature* **2008**, *453*, 363.
(423) Shimamura, T.; Hiraki, K.; Takahashi, N.; Hori, T.; Ago, H.; Masuda, K.; Takio, K.; Ishiguro, M.; Miyano, M. *J. Biol. Chem.* **2008**, *283*, 17753.
(424) Filipek, S.; Stenkamp, R. E.; Teller, D. C.; Palczewski, K. *Annu. Rev. Physiol.* **2003**, *65*, 851.
(425) Janz, J. M.; Fay, J. F.; Farrens, D. L. *J. Biol. Chem.* **2003**, *278*, 16982.
(426) Choe, H.-W.; Kim, Y. J.; Park, J. H.; Morizumi, T.; Pai, E. F.; Krauss, N.; Hofmann, K. P.; Scheerer, P.; Ernst, O. P. *Nature* **2011**, *471*, 651.
(427) Park, J. H.; Scheerer, P.; Hofmann, K. P.; Choe, H. W.; Ernst, O. P. *Nature* **2008**, *454*, 183.
(428) Scheerer, P.; Park, J. H.; Hildebrand, P. W.; Kim, Y. J.; Krauss, N.; Choe, H.-W.; Hofmann, K. P.; Ernst, O. P. *Nature* **2008**, *455*, 497.
(429) Altenbach, C.; Kusnetzow, A. K.; Ernst, O. P.; Hofmann, K. P.; Hubbell, W. L. *Proc. Natl. Acad. Sci. U.S.A.* **2008**, *105*, 7439.
(430) Farrens, D. L.; Altenbach, C.; Yang, K.; Hubbell, W. L.; Khorana, H. G. *Science* **1996**, *274*, 768.
(431) Sheikh, S. P.; Zvyaga, T. A.; Lichtarge, O.; Sakmar, T. P.; Bourne, H. R. *Nature* **1996**, *383*, 347.
(432) Park, J. H.; Morizumi, T.; Li, Y.; Hong, J. E.; Pai, E. F.; Hofmann, K. P.; Choe, H. W.; Ernst, O. P. *Angew. Chem., Int. Ed.* **2013**, *52*, 11021.
(433) Deupi, X.; Edwards, P.; Singhal, A.; Nickle, B.; Oprian, D.; Schertler, G.; Standfuss, J. *Proc. Natl. Acad. Sci. U.S.A.* **2012**, *109*, 119.
(434) Singhal, A.; Ostermaier, M. K.; Vishnivetskiy, S. A.; Panneels, V.; Homan, K. T.; Tesmer, J. J.; Veprintsev, D.; Deupi, X.; Gurevich, V. V.; Schertler, G. F.; Standfuss, J. *EMBO Rep.* **2013**, *14*, 520.
(435) Standfuss, J.; Edwards, P. C.; D'Antona, A.; Fransen, M.; Xie, G.; Oprian, D. D.; Schertler, G. F. *Nature* **2011**, *471*, 656.
(436) Rasmussen, S. G.; Choi, H. J.; Fung, J. J.; Pardon, E.; Casarosa, P.; Chae, P. S.; Devree, B. T.; Rosenbaum, D. M.; Thian, F. S.; Kobilka, T. S.; Schnapp, A.; Konetzki, I.; Sunahara, R. K.; Gellman, S. H.; Pautsch, A.; Steyaert, J.; Weis, W. I.; Kobilka, B. K. *Nature* **2011**, *469*, 175.
(437) Steyaert, J.; Kobilka, B. K. *Curr. Opin. Struct. Biol.* **2011**, *21*, 567.
(438) Rasmussen, S. G.; DeVree, B. T.; Zou, Y.; Kruse, A. C.; Chung, K. Y.; Kobilka, T. S.; Thian, F. S.; Chae, P. S.; Pardon, E.; Calinski, D.; Mathiesen, J. M.; Shah, S. T.; Lyons, J. A.; Caffrey, M.; Gellman, S. H.; Steyaert, J.; Skiniotis, G.; Weis, W. I.; Sunahara, R. K.; Kobilka, B. K. *Nature* **2011**, *477*, 549.
(439) Oldham, W. M.; Hamm, H. E. *Adv. Protein Chem.* **2007**, *74*, 67.

(440) Oldham, W. M.; Hamm, H. E. *Nat. Rev. Mol. Cell Biol.* **2008**, *9*, 60.
(441) Van Eps, N.; Preininger, A. M.; Alexander, N.; Kaya, A. I.; Meier, S.; Meiler, J.; Hamm, H. E.; Hubbell, W. L. *Proc. Natl. Acad. Sci. U.S.A.* **2011**, *108*, 9420.
(442) Jastrzebska, B.; Ringler, P.; Lodowski, D. T.; Moiseenkova-Bell, V.; Golczak, M.; Muller, S. A.; Palczewski, K.; Engel, A. *J. Struct. Biol.* **2011**, *176*, 387.
(443) Jastrzebska, B.; Orban, T.; Golczak, M.; Engel, A.; Palczewski, K. *FASEB J.* **2013**, *27*, 1572.
(444) Jastrzebska, B.; Ringler, P.; Palczewski, K.; Engel, A. *J. Struct. Biol.* **2013**, *182*, 164.
(445) Cottet, M.; Faklaris, O.; Maurel, D.; Scholler, P.; Doumazane, E.; Trinquet, E.; Pin, J. P.; Durroux, T. *Front. Endocrinol.* **2012**, *3*, 92.
(446) Fotiadis, D.; Liang, Y.; Filipek, S.; Saperstein, D. A.; Engel, A.; Palczewski, K. *Nature* **2003**, *421*, 127.
(447) Liang, Y.; Fotiadis, D.; Filipek, S.; Saperstein, D. A.; Palczewski, K.; Engel, A. *J. Biol. Chem.* **2003**, *278*, 21655.
(448) Park, P. S.; Palczewski, K. *Proc. Natl. Acad. Sci. U.S.A.* **2005**, *102*, 8793.
(449) Heck, M.; Hofmann, K. P. *J. Biol. Chem.* **2001**, *276*, 10000.
(450) Hein, P.; Rochais, F.; Hoffmann, C.; Dorsch, S.; Nikolaev, V. O.; Engelhardt, S.; Berlot, C. H.; Lohse, M. J.; Bunemann, M. *J. Biol. Chem.* **2006**, *281*, 33345.
(451) Fein, A.; Szuts, E. Z. *Photoreceptors: Their Role in Vision*; Cambridge University Press: Cambridge, 1982.
(452) Audet, M.; Bouvier, M. *Cell* **2012**, *151*, 14.
(453) Burns, M. E.; Pugh, E. N., Jr. *Physiology* **2010**, *25*, 72.
(454) Hargrave, P. A.; McDowell, J. H.; Curtis, D. R.; Wang, J. K.; Juszczak, E.; Fong, S. L.; Rao, J. K.; Argos, P. *Biophys. Struct. Mech.* **1983**, *9*, 235.
(455) Ovchinnikov, Yu. A. *FEBS Lett.* **1982**, *148*, 179.
(456) Nathans, J.; Hogness, D. S. *Cell* **1983**, *34*, 807.
(457) Dixon, R. A.; Kobilka, B. K.; Strader, D. J.; Benovic, J. L.; Dohlman, H. G.; Frielle, T.; Bolanowski, M. A.; Bennett, C. D.; Rands, E.; Diehl, R. E.; Mumford, R. A.; Slater, E. E.; Sigal, I. S.; Caron, M. G.; Lefkowitz, R. J.; Strader, C. D. *Nature* **1986**, *321*, 75.
(458) Ferretti, L.; Karnik, S. S.; Khorana, H. G.; Nassal, M.; Oprian, D. D. *Proc. Natl. Acad. Sci. U.S.A.* **1986**, *83*, 599.
(459) Hubbell, W. L.; Altenbach, C.; Hubbell, C. M.; Khorana, H. G. *Adv. Protein Chem.* **2003**, *63*, 243.
(460) Khorana, H. G. *J. Biol. Chem.* **1992**, *267*, 1.
(461) Oprian, D. D.; Molday, R. S.; Kaufman, R. J.; Khorana, H. G. *Proc. Natl. Acad. Sci. U.S.A.* **1987**, *84*, 8874.
(462) Ballesteros, J. A.; Jensen, A. D.; Liapakis, G.; Rasmussen, S. G.; Shi, L.; Gether, U.; Javitch, J. A. *J. Biol. Chem.* **2001**, *276*, 29171.
(463) Mirzadegan, T.; Benkö, G.; Filipek, S.; Palczewski, K. *Biochemistry* **2003**, *42*, 2759.
(464) Angel, T. E.; Chance, M. R.; Palczewski, K. *Proc. Natl. Acad. Sci. U.S.A.* **2009**, *106*, 8555.
(465) Angel, T. E.; Gupta, S.; Jastrzebska, B.; Palczewski, K.; Chance, M. R. *Proc. Natl. Acad. Sci. U.S.A.* **2009**, *106*, 14367.
(466) Baylor, D. A.; Nunn, B. J.; Schnapf, J. L. *J. Physiol.* **1984**, *357*, 575.
(467) Yau, K. W.; Matthews, G.; Baylor, D. A. *Nature* **1979**, *279*, 806.
(468) Baylor, D. *Proc. Natl. Acad. Sci. U.S.A.* **1996**, *93*, 560.
(469) Baylor, D. A.; Matthews, G.; Yau, K. W. *J. Physiol.* **1980**, *309*, 591.
(470) Matthews, G. *J. Physiol.* **1984**, *349*, 607.
(471) Birge, R. R.; Barlow, R. B. *Biophys. Chem.* **1995**, *55*, 115.
(472) Gozem, S.; Schapiro, I.; Ferre, N.; Olivucci, M. *Science* **2012**, *337*, 1225.
(473) Lorenz-Fonfria, V. A.; Furutani, Y.; Ota, T.; Ido, K.; Kandori, H. *J. Am. Chem. Soc.* **2010**, *132*, 5693.
(474) Shen, W. L.; Kwon, Y.; Adegbola, A. A.; Luo, J.; Chess, A.; Montell, C. *Science* **2011**, *331*, 1333.
(475) Hug, S. J.; Lewis, J. W.; Einterz, C. M.; Thorgeirsson, T. E.; Kliger, D. S. *Biochemistry* **1990**, *29*, 1475.
(476) Yoshizawa, T.; Shichida, Y. *Methods Enzymol.* **1982**, *81*, 333.
(477) Ganter, U. M.; Gärtner, W.; Siebert, F. *Biochemistry* **1988**, *27*, 7480.
(478) Furutani, Y.; Shichida, Y.; Kandori, H. *Biochemistry* **2003**, *42*, 9619.
(479) Ye, S.; Zaitseva, E.; Caltabiano, G.; Schertler, G. F.; Sakmar, T. P.; Deupi, X.; Vogel, R. *Nature* **2010**, *464*, 1386.
(480) Eilers, M.; Goncalves, J. A.; Ahuja, S.; Kirkup, C.; Hirshfeld, A.; Simmerling, C.; Reeves, P. J.; Sheves, M.; Smith, S. O. *J. Phys. Chem. B* **2012**, *116*, 10477.
(481) Matthews, R. G.; Hubbard, R.; Brown, P. K.; Wald, G. *J. Gen. Physiol.* **1963**, *47*, 215.
(482) Parkes, J. H.; Liebman, P. A. *Biochemistry* **1984**, *23*, 5054.
(483) Doukas, A. G.; Aton, B.; Callender, R. H.; Ebrey, T. G. *Biochemistry* **1978**, *17*, 2430.
(484) Arnis, S.; Hofmann, K. P. *Proc. Natl. Acad. Sci. U.S.A.* **1993**, *90*, 7849.
(485) Arnis, S.; Fahmy, K.; Hofmann, K. P.; Sakmar, T. P. *J. Biol. Chem.* **1994**, *269*, 23879.
(486) Vogel, R.; Mahalingam, M.; Ludeke, S.; Huber, T.; Siebert, F.; Sakmar, T. P. *J. Mol. Biol.* **2008**, *380*, 648.
(487) Lüdeke, S.; Mahalingam, M.; Vogel, R. *Photochem. Photobiol.* **2009**, *85*, 437.
(488) Knierim, B.; Hofmann, K. P.; Ernst, O. P.; Hubbell, W. L. *Proc. Natl. Acad. Sci. U.S.A.* **2007**, *104*, 20290.
(489) Mahalingam, M.; Martinez-Mayorga, K.; Brown, M. F.; Vogel, R. *Proc. Natl. Acad. Sci. U.S.A.* **2008**, *105*, 17795.
(490) Zaitseva, E.; Brown, M. F.; Vogel, R. *J. Am. Chem. Soc.* **2010**, *132*, 4815.
(491) Ruprecht, J. J.; Mielke, T.; Vogel, R.; Villa, C.; Schertler, G. F. *EMBO J.* **2004**, *23*, 3609.
(492) Salom, D.; Lodowski, D. T.; Stenkamp, R. E.; Le Trong, I.; Golczak, M.; Jastrzebska, B.; Harris, T.; Ballesteros, J. A.; Palczewski, K. *Proc. Natl. Acad. Sci. U.S.A.* **2006**, *103*, 16123.
(493) Salom, D.; Le Trong, I.; Pohl, E.; Ballesteros, J. A.; Stenkamp, R. E.; Palczewski, K.; Lodowski, D. T. *J. Struct. Biol.* **2006**, *156*, 497.
(494) Chun, E.; Thompson, A. A.; Liu, W.; Roth, C. B.; Griffith, M. T.; Katritch, V.; Kunken, J.; Xu, F.; Cherezov, V.; Hanson, M. A.; Stevens, R. C. *Structure* **2012**, *20*, 967.
(495) Rosenbaum, D. M.; Cherezov, V.; Hanson, M. A.; Rasmussen, S. G.; Thian, F. S.; Kobilka, T. S.; Choi, H. J.; Yao, X. J.; Weis, W. I.; Stevens, R. C.; Kobilka, B. K. *Science* **2007**, *318*, 1266.
(496) Dore, A. S.; Robertson, N.; Errey, J. C.; Ng, I.; Hollenstein, K.; Tehan, B.; Hurrell, E.; Bennett, K.; Congreve, M.; Magnani, F.; Tate, C. G.; Weir, M.; Marshall, F. H. *Structure* **2011**, *19*, 1283.
(497) Robertson, N.; Jazayeri, A.; Errey, J.; Baig, A.; Hurrell, E.; Zhukov, A.; Langmead, C. J.; Weir, M.; Marshall, F. H. *Neuropharmacology* **2011**, *60*, 36.
(498) Rosenbaum, D. M.; Zhang, C.; Lyons, J. A.; Holl, R.; Aragao, D.; Arlow, D. H.; Rasmussen, S. G.; Choi, H. J.; Devree, B. T.; Sunahara, R. K.; Chae, P. S.; Gellman, S. H.; Dror, R. O.; Shaw, D. E.; Weis, W. I.; Caffrey, M.; Gmeiner, P.; Kobilka, B. K. *Nature* **2011**, *469*, 236.
(499) Bokoch, M. P.; Zou, Y.; Rasmussen, S. G.; Liu, C. W.; Nygaard, R.; Rosenbaum, D. M.; Fung, J. J.; Choi, H. J.; Thian, F. S.; Kobilka, T. S.; Puglisi, J. D.; Weis, W. I.; Pardo, L.; Prosser, R. S.; Mueller, L.; Kobilka, B. K. *Nature* **2010**, *463*, 108.
(500) Kim, T. H.; Chung, K. Y.; Manglik, A.; Hansen, A. L.; Dror, R. O.; Mildorf, T. J.; Shaw, D. E.; Kobilka, B. K.; Prosser, R. S. *J. Am. Chem. Soc.* **2013**, *135*, 9465.
(501) Nygaard, R.; Zou, Y.; Dror, R. O.; Mildorf, T. J.; Arlow, D. H.; Manglik, A.; Pan, A. C.; Liu, C. W.; Fung, J. J.; Bokoch, M. P.; Thian, F. S.; Kobilka, T. S.; Shaw, D. E.; Mueller, L.; Prosser, R. S.; Kobilka, B. K. *Cell* **2013**, *152*, 532.
(502) West, G. M.; Chien, E. Y.; Katritch, V.; Gatchalian, J.; Chalmers, M. J.; Stevens, R. C.; Griffin, P. R. *Structure* **2011**, *19*, 1424.
(503) Deupi, X.; Kobilka, B. K. *Physiology* **2010**, *25*, 293.
(504) Okada, T.; Ernst, O. P.; Palczewski, K.; Hofmann, K. P. *Trends Biochem. Sci.* **2001**, *26*, 318.

(505) Lüdeke, S.; Beck, M.; Yan, E. C.; Sakmar, T. P.; Siebert, F.; Vogel, R. *J. Mol. Biol.* **2005**, *353*, 345.
(506) Sandberg, M. N.; Amora, T. L.; Ramos, L. S.; Chen, M. H.; Knox, B. E.; Birge, R. R. *J. Am. Chem. Soc.* **2011**, *133*, 2808.
(507) Honig, B.; Dinur, U.; Nakanishi, K.; Balogh-Nair, V.; Gawinowicz, M. A.; Arnaboldi, M.; Motto, M. G. *J. Am. Chem. Soc.* **1979**, *101*, 7084.
(508) Beck, M.; Sakmar, T. P.; Siebert, F. *Biochemistry* **1998**, *37*, 7630.
(509) Ahuja, S.; Crocker, E.; Eilers, M.; Hornak, V.; Hirshfeld, A.; Ziliox, M.; Syrett, N.; Reeves, P. J.; Khorana, H. G.; Sheves, M.; Smith, S. O. *J. Biol. Chem.* **2009**, *284*, 10190.
(510) Ahuja, S.; Hornak, V.; Yan, E. C.; Syrett, N.; Goncalves, J. A.; Hirshfeld, A.; Ziliox, M.; Sakmar, T. P.; Sheves, M.; Reeves, P. J.; Smith, S. O.; Eilers, M. *Nat. Struct. Mol. Biol.* **2009**, *16*, 168.
(511) Sakmar, T. P.; Franke, R. R.; Khorana, H. G. *Proc. Natl. Acad. Sci. U.S.A.* **1989**, *86*, 8309.
(512) Zhukovsky, E. A.; Oprian, D. D. *Science* **1989**, *246*, 928.
(513) Nathans, J. *Biochemistry* **1990**, *29*, 9746.
(514) Yan, E. C.; Kazmi, M. A.; Ganim, Z.; Hou, J. M.; Pan, D.; Chang, B. S.; Sakmar, T. P.; Mathies, R. A. *Proc. Natl. Acad. Sci. U.S.A.* **2003**, *100*, 9262.
(515) Vogel, R.; Siebert, F.; Yan, E. C.; Sakmar, T. P.; Hirshfeld, A.; Sheves, M. *J. Am. Chem. Soc.* **2006**, *128*, 10503.
(516) Salgado, G. F.; Struts, A. V.; Tanaka, K.; Krane, S.; Nakanishi, K.; Brown, M. F. *J. Am. Chem. Soc.* **2006**, *128*, 11067.
(517) Martinez-Mayorga, K.; Pitman, M. C.; Grossfield, A.; Feller, S. E.; Brown, M. F. *J. Am. Chem. Soc.* **2006**, *128*, 16502.
(518) Steinberg, G.; Ottolenghi, M.; Sheves, M. *Biophys. J.* **1993**, *64*, 1499.
(519) Jager, F.; Fahmy, K.; Sakmar, T. P.; Siebert, F. *Biochemistry* **1994**, *33*, 10878.
(520) Patel, A. B.; Crocker, E.; Reeves, P. J.; Getmanova, E. V.; Eilers, M.; Khorana, H. G.; Smith, S. O. *J. Mol. Biol.* **2005**, *347*, 803.
(521) Hofmann, K. P.; Scheerer, P.; Hildebrand, P. W.; Choe, H. W.; Park, J. H.; Heck, M.; Ernst, O. P. *Trends Biochem. Sci.* **2009**, *34*, 540.
(522) Fritze, O.; Filipek, S.; Kuksa, V.; Palczewski, K.; Hofmann, K. P.; Ernst, O. P. *Proc. Natl. Acad. Sci. U.S.A.* **2003**, *100*, 2290.
(523) Schädel, S. A.; Heck, M.; Maretzki, D.; Filipek, S.; Teller, D. C.; Palczewski, K.; Hofmann, K. P. *J. Biol. Chem.* **2003**, *278*, 24896.
(524) Hildebrand, P. W.; Scheerer, P.; Park, J. H.; Choe, H. W.; Piechnick, R.; Ernst, O. P.; Hofmann, K. P.; Heck, M. *PLoS One* **2009**, *4*, e4382.
(525) Piechnick, R.; Ritter, E.; Hildebrand, P. W.; Ernst, O. P.; Scheerer, P.; Hofmann, K. P.; Heck, M. *Proc. Natl. Acad. Sci. U.S.A.* **2012**, *109*, 5247.
(526) Jastrzebska, B.; Palczewski, K.; Golczak, M. *J. Biol. Chem.* **2011**, *286*, 18930.
(527) Janz, J. M.; Farrens, D. L. *J. Biol. Chem.* **2004**, *279*, 55886.
(528) Grossfield, A.; Pitman, M. C.; Feller, S. E.; Soubias, O.; Gawrisch, K. *J. Mol. Biol.* **2008**, *381*, 478.
(529) Piechnick, R.; Heck, M.; Sommer, M. E. *Biochemistry* **2011**, *50*, 7168.
(530) Vogel, R.; Siebert, F. *J. Biol. Chem.* **2001**, *276*, 38487.
(531) Patel, A. B.; Crocker, E.; Eilers, M.; Hirshfeld, A.; Sheves, M.; Smith, S. O. *Proc. Natl. Acad. Sci. U.S.A.* **2004**, *101*, 10048.
(532) Nakamichi, H.; Buss, V.; Okada, T. *Biophys. J.* **2007**, *92*, L106.
(533) Nakanishi, K.; Crouch, R. K. *Isr. J. Chem.* **1995**, *35*, 253.
(534) Gelis, L.; Wolf, S.; Hatt, H.; Neuhaus, E. M.; Gerwert, K. *Angew. Chem., Int. Ed.* **2012**, *51*, 1274.
(535) Kefalov, V. J. *J. Biol. Chem.* **2012**, *287*, 1635.
(536) Okano, T.; Kojima, D.; Fukada, Y.; Shichida, Y.; Yoshizawa, T. *Proc. Natl. Acad. Sci. U.S.A.* **1992**, *89*, 5932.
(537) Ebrey, T.; Koutalos, Y. *Prog. Retinal Eye Res.* **2001**, *20*, 49.
(538) Shichida, Y.; Imai, H.; Imamoto, Y.; Fukada, Y.; Yoshizawa, T. *Biochemistry* **1994**, *33*, 9040.
(539) Kandori, H.; Mizukami, T.; Okada, T.; Imamoto, Y.; Fukada, Y.; Shichida, Y.; Yoshizawa, T. *Proc. Natl. Acad. Sci. U.S.A.* **1990**, *87*, 8908.
(540) Sato, K.; Morizumi, T.; Yamashita, T.; Shichida, Y. *Biochemistry* **2010**, *49*, 736.
(541) Chen, M. H.; Kuemmel, C.; Birge, R. R.; Knox, B. E. *Biochemistry* **2012**, *51*, 4117.
(542) Imamoto, Y.; Seki, I.; Yamashita, T.; Shichida, Y. *Biochemistry* **2013**, *52*, 3010.
(543) Kefalov, V. J.; Crouch, R. K.; Cornwall, M. C. *Neuron* **2001**, *29*, 749.
(544) Imai, H.; Kojima, D.; Oura, T.; Tachibanaki, S.; Terakita, A.; Shichida, Y. *Proc. Natl. Acad. Sci. U.S.A.* **1997**, *94*, 2322.
(545) Kuwayama, S.; Imai, H.; Hirano, T.; Terakita, A.; Shichida, Y. *Biochemistry* **2002**, *41*, 15245.
(546) Vogel, R.; Sakmar, T. P.; Sheves, M.; Siebert, F. *Photochem. Photobiol.* **2007**, *83*, 286.
(547) Kochendoerfer, G. G.; Wang, Z.; Oprian, D. D.; Mathies, R. A. *Biochemistry* **1997**, *36*, 6577.
(548) Wang, Z.; Asenjo, A. B.; Oprian, D. D. *Biochemistry* **1993**, *32*, 2125.
(549) Morizumi, T.; Sato, K.; Shichida, Y. *Biochemistry* **2012**, *51*, 10017.
(550) Stenkamp, R. E.; Filipek, S.; Driessen, C. A.; Teller, D. C.; Palczewski, K. *Biochim. Biophys. Acta* **2002**, *1565*, 168.
(551) Kiser, P. D.; Golczak, M.; Palczewski, K. *Chem. Rev.* **2014**.
(552) Tsukamoto, H.; Terakita, A. *Photochem. Photobiol. Sci.* **2010**, *9*, 1435.
(553) Hillman, P.; Hochstein, S.; Minke, B. *Physiol. Rev.* **1983**, *63*, 668.
(554) Tsuda, M. *Biochim. Biophys. Acta* **1978**, *502*, 495.
(555) Nakagawa, M.; Iwasa, T.; Kikkawa, S.; Tsuda, M.; Ebrey, T. G. *Proc. Natl. Acad. Sci. U.S.A.* **1999**, *96*, 6189.
(556) Terakita, A.; Yamashita, T.; Shichida, Y. *Proc. Natl. Acad. Sci. U.S.A.* **2000**, *97*, 14263.
(557) Terakita, A.; Koyanagi, M.; Tsukamoto, H.; Yamashita, T.; Miyata, T.; Shichida, Y. *Nat. Struct. Mol. Biol.* **2004**, *11*, 284.
(558) Murakami, M.; Kouyama, T. *J. Mol. Biol.* **2011**, *413*, 615.
(559) Nobes, C.; Baverstock, J.; Saibil, H. *Biochem. J.* **1992**, *287* (Pt 2), 545.
(560) Tsukamoto, H.; Farrens, D. L.; Koyanagi, M.; Terakita, A. *J. Biol. Chem.* **2009**, *284*, 20676.
(561) Provencio, I.; Jiang, G.; De Grip, W. J.; Hayes, W. P.; Rollag, M. D. *Proc. Natl. Acad. Sci. U.S.A.* **1998**, *95*, 340.
(562) Radu, R. A.; Hu, J.; Peng, J.; Bok, D.; Mata, N. L.; Travis, G. H. *J. Biol. Chem.* **2008**, *283*, 19730.
(563) Shen, D.; Jiang, M.; Hao, W.; Tao, L.; Salazar, M.; Fong, H. K. *Biochemistry* **1994**, *33*, 13117.
(564) Wenzel, A.; Oberhauser, V.; Pugh, E. N., Jr.; Lamb, T. D.; Grimm, C.; Samardzija, M.; Fahl, E.; Seeliger, M. W.; Reme, C. E.; von Lintig, J. *J. Biol. Chem.* **2005**, *280*, 29874.
(565) Koyanagi, M.; Terakita, A.; Kubokawa, K.; Shichida, Y. *FEBS Lett.* **2002**, *531*, 525.
(566) Tanimoto, T.; Furutani, Y.; Kandori, H. *Biochemistry* **2003**, *42*, 2300.
(567) Kobilka, B. K.; Deupi, X. *Trends Pharmacol. Sci.* **2007**, *28*, 397.
(568) Vaidehi, N.; Kenakin, T. *Curr. Opin. Pharmacol.* **2010**, *10*, 775.
(569) Kliger, D. S.; Lewis, J. W. *Isr. J. Chem.* **1995**, *35*, 289.
(570) Epps, J.; Lewis, J. W.; Szundi, I.; Kliger, D. S. *Photochem. Photobiol.* **2006**, *82*, 1436.
(571) Szundi, I.; Lewis, J. W.; Kliger, D. S. *Biochemistry* **2003**, *42*, 5091.
(572) Szundi, I.; Lewis, J. W.; Kliger, D. S. *Biophys. J.* **1997**, *73*, 688.
(573) Szundi, I.; Mah, T. L.; Lewis, J. W.; Jager, S.; Ernst, O. P.; Hofmann, K. P.; Kliger, D. S. *Biochemistry* **1998**, *37*, 14237.
(574) Tachibanaki, S.; Imai, H.; Terakita, A.; Shichida, Y. *FEBS Lett.* **1998**, *425*, 126.
(575) Bartl, F. J.; Vogel, R. *Phys. Chem. Chem. Phys.* **2007**, *9*, 1648.
(576) Ernst, O. P.; Bartl, F. J. *ChemBioChem* **2002**, *3*, 968.
(577) Petrek, M.; Kosinova, P.; Koca, J.; Otyepka, M. *Structure* **2007**, *15*, 1357.